Supporting Information

AIEE Active Perylene Bisimide Supported Mercury Nanoparticles for Synthesis of Amides via Aldoximes/Ketoximes Rearrangement

Sandeep Kaur, Manoj Kumar and Vandana Bhalla*

Department of Chemistry, UGC Sponsored-Centre for Advanced Studies-I, Guru Nanak Dev University, Amritsar-143005, Punjab, India

Email Address: vanmanan@yahoo.co.in

General Experimental Procedures:

Materials and reagents: All reagents were purchased from Aldrich and were used without further purification. THF was dried over sodium and benzophenone as an indicator. UV–vis studies were performed in THF, distilled water and HEPES buffer (0.05 M) (pH = 7.05).

Instrumentation:

All reagents were purchased from Aldrich and were used without further purification. The UV/vis and fluorescence spectra were recorded with Shimdzu UV-2450 spectrophotometer and Shimadzu RF-5301(PC) spectrofluorophotometer, respectively. The SEM images were recorded from Scanning Electron Microscope (SEM)-Zeiss EV040. The TEM mages was recorded from Transmission Electron Microscope (TEM) - JEOL 2100F. The FT-IR spectra were recorded with VARIAN 660 IR Spectrometer. The dynamic light scattering (DLS) data were recorded with MALVERN Instruments (Nano-ZS). The Time resolved fluorescence spectra were recorded with a HORIBA Time Resolved Fluorescence Spectrometer. Elemental analysis was done using a Flash EA 1112 CHNS/O analyzer from Thermo Electron Corporation. ^{1}H and ^{13}C NMR was recorded on a JOEL-FT NMR-AL 300 and Bruker-AVANCE-II FT NMR-AL 500 MHz spectrophotometer using $CDCl_3$ as solvent and tetramethylsilane $SiMe_4$ as internal standards. Data are reported as follows: chemical shifts in ppm (δ), multiplicity (s = singlet, d = doublet, br s = broad singlet m = multiplet), coupling constants *J* (Hz), integration, and interpretation. Silica gel 60 (60-120 mesh) was used for column chromatography.

Calculations for quantum yield[1]:

Fluorescence quantum yield was determined using optically matching solutions of rhodamine B (Φ_{fr} = 0.65 in ethanol) as standard at an excitation wavelength of 530 nm and quantum yield is calculated using the equation:

$$\Phi_{fs} = \Phi_{fr} \times \frac{1-10^{-ArLr}}{1-10^{-AsLs}} \times \frac{N_s^2}{N_r^2} \times \frac{D_s}{D_r}$$

Φ_{fs} and Φ_{fr} are the radiative quantum yields of sample and the reference respectively, A_s and A_r are the absorbance of the sample and the reference respectively, D_s and D_r the respective areas of emission for sample and reference. L_s and L_r are the lengths of the absorption cells of

[1]J. N. Deams, G. A. Grosby, *J. Phys. Chem.*, 1971, **75**, 991.

sample and reference respectively. N_s and N_r are the refractive indices of the sample and reference solutions (pure solvents were assumed respectively).

UV–vis and fluorescence titrations:

The concentration of HEPES buffer (pH = 7.05) is 0.05 M. For each experiment we have taken 3 ml solution which contains solution of derivative **3** in THF and 1.5 ml HEPES buffer (0.05 M, pH = 7.05) or double distilled water. UV-vis and fluorescence titrations were performed with 5.0 μM solutions of ligand in H_2O/THF (1:1, v/v). Typically, aliquots of freshly prepared standard solutions (10^{-1}M to 10^{-3}M) of metal ions such as Zn^{2+}, Hg^{2+}, Cu^{2+}, Fe^{2+}, Fe^{3+}, Co^{2+}, Pb^{2+}, Ni^{2+}, Cd^{2+}, Ag^{+}, Ba^{2+}, Al^{3+}, Mg^{2+}, K^{+} and Na^{+} ions as their perchlorate [$M(ClO_4)_x$; X = 1-3]/chloride [$M(Cl)_x$; X = 1-3] in THF were added to record the UV-vis and fluorescence spectra.

Synthetic scheme of compound 3:

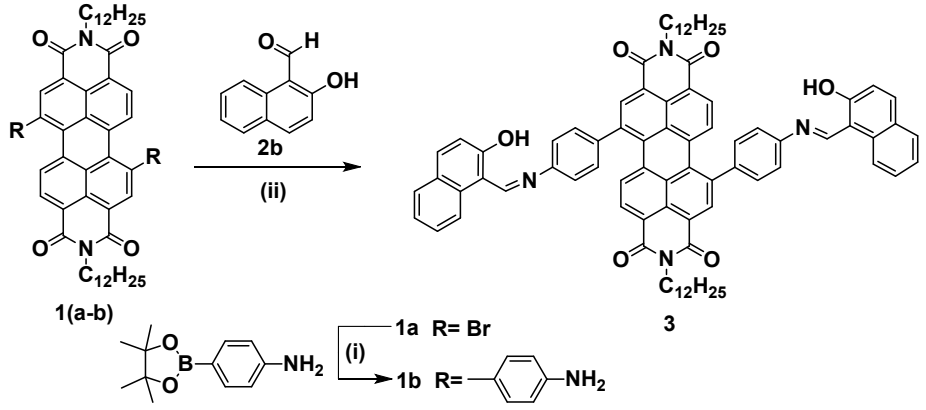

Scheme 1: Synthesis of PBIs derivative **3**: (i) K_2CO_3 (aq.), $PdCl_2(PPh_3)_2$, THF, 80 ^{0}C; (ii) dry THF : methanol (4 : 6), 80 ^{0}C.

Synthesis of derivative 1b:

To a solution of **1a** (0.5 g, 0.567 mmol) and **2** (0.322 g, 0.884 mmol) in 20 ml of dry THF were added K_2CO_3 (0.203 g, 0.884 mmol), distilled H_2O (1.3 mL) and $Pd(Cl)_2(PPh_3)_2$ (0.238 g, 0.204 mmol) under N_2, and the reaction mixture was then refluxed overnight. After completion of the reaction (TLC), the mixture was cooled to room temperature. Dry THF was then removed under vacuum, and the residue so obtained was treated with water, extracted with CH_2Cl_2 and dried over anhydrous Na_2SO_4.The organic layer was evaporated, and the compound was purified by column chromatography using $CHCl_3$/MeOH (9.5:0.5, v/v) as an eluent to give 0.40 g (78%) of compound **1b** as a red solid. Mp: >260 °C. IR (KBr) ν_{max} = (-NH_2) 3368.13, (C=O) 1694.2119, 1655.27. ^{1}H NMR (300MHz, $CDCl_3$, ppm): 0.84 [(t, *J* = 6Hz, 6H, N-CH_2-CH_2-$(CH_2)_9$-CH_3], 1.11-1.24 [(m, 36H, N-CH_2-CH_2-$(CH_2)_9$-CH_3], 1.45-1.79 [(m, *J* = 9Hz, 4H, N-CH_2-CH_2-$(CH_2)_9$-CH_3], 3.91(s, 4H, NH_2), 4.19 (t, *J* = 6Hz, 4 H, N-CH_2-CH_2-$(CH_2)_9$-CH_3, 6.75 (d, *J* = 9Hz, 4H, ArH), 7.32 (d, *J* = 9Hz, 4H, ArH), 7.91 (d, *J* = 12Hz, 2H, ArH), 8.13 (d, *J* = 6Hz, 2H, ArH), 8.54 (s, 2H, ArH). ^{13}C NMR ($CDCl_3$, 75 MHz): δ = 14.12, 22.69, 29.35, 29.56, 29.63, 29.65, 29.70, 31.92, 39.13, 40.57, 116.37, 121.48, 128.47, 128.57, 129.46, 130.33, 130.96, 132.06, 132.14, 134.34, 138.43, 150.52, 164.00. ESI-MS mass spectrum of compound **3** showed a parent ion peak, m/z = 908.3805. Elemental analysis: Calc. for C, 79.26; H, 7.54; N, 6.16. Found: C, 79.24; H, 7.52; N, 6.17.

Synthesis of compound 3:

A mixture of compound **3** (0.05 g, 0.055 mmol) and β-hydroxy naphthaldehyde (0.02 g, 0.116 mmol) in THF-methanol was refluxed for 24 hrs. After the completion of the reaction, the solvent was evaporated and the residue left was crystallized from methanol to give compound **3** in 86% (0.058 g) yield; mp: > 280ºC. IR (KBr) ν_{max} = (-OH) 3339.28, (C=O) 1696.17, 1657.24, (C=N) 1620.55 cm^{-1}. ^1H NMR ($CDCl_3$, 300 MHz): δ = 0.85 [(t, 6H, CH_2-$(CH_2)_{18}$-$\underline{(CH_3)_2}$], 1.01-1.39 [(m, 36H, CH_2-$\underline{(CH_2)_{18}}$ $(CH_3)_2$], 1.61-1.71 (m, 4H, $\underline{[(CH_2)}$-$(CH_2)_{18}$-$(CH_3)_2$]), 4.19 (t, *J* = 4.5 Hz, 4H, N-$\underline{(CH_2)_2}$, 7.12 (d, *J* = 9Hz, 4H, ArH), 7.37 (t, *J* = 7.5Hz, 4H, ArH), 7.50-7.56 (m, 6H, ArH), 7.66 (d, *J* = 6Hz, 2H, ArH), 7.75 (d, *J* = 6Hz, 2H, ArH), 7.84 (d, *J* = 9 Hz, 2H, ArH), 7.93 (d, *J* = 6Hz, 2H, ArH), 8.18 (d, *J* = 9 Hz, 2H, ArH), 8.63 (s, 2H, ArH), 9.47 (s, 2H, HC=N), 13.31 (s, 2H, OH). ^{13}C NMR ($CDCl_3$, 75 MHz): δ = 14.12, 22.68, 27.13, 27.21, 29.35, 29.41, 29.56, 29.58, 29.63, 31.92, 35.15, 38.04, 109.19, 120.24, 121.87, 122.21, 123.82, 129.52, 130.72, 133.17, 134.24, 135.21, 137.34, 139.35, 140.09, 141.92, 154.88, 155.37, 159.91, 170.55 ppm. ESI-MS mass spectrum of compound **3** showed a parent ion peak, m/z = 1216.23 $[M+H]^+$. Elemental analysis: Calc. for C, 80.89; H, 6.62; N, 4.60. Found: C, 80.88; H, 6.61; N, 4.62.

Synthesis of aldoximes/ ketoximes derivatives 4a-g/6a-6h:

In a 25 ml round-bottom flask, aldehyde/ketone was dissolved in 10 ml ethanol followed by the addition of triethylamine and hydroxylamine-HCl. The reaction was heated to 80° for 3 hours, and then cooled to room temperature. Aqueous NH_4Cl was added, and the mixture was extracted with dichloromethane, dried with Na_2SO_4 and concentrated to give solid product.

Synthesis of primary amides (5a-g) from aldoximes (4a-g)

Here, we use HgNPs as an efficient catalyst for conversion of oxime into amide using toluene as a solvent. The reaction of aldoximes in toluene (10 ml) in the presence of 50 -100µl of the HgNPs catalyst (0.5-1 mol%) at r.t- 85°C for 5-12 h was studied (Table 1). The resulting mixture was stirred until the reaction was completed as indicated by TLC. The resulting precipitate was collected .The crude solid was purified via recrystallization from ethanol to get pure products **5a-g**.

Synthesis of secondary amides (7a-h) from ketoximes (6a-h):

Here, we use HgNPs as an efficient catalyst for conversion of oxime into amide using acetonitrile as a solvent. The reaction of aldoximes in acetonitrile (10 ml) in the presence of 50 µl of the HgNPs catalyst (0.5 mol%) at r.t for 20-90 min was studied (Table 1). The resulting mixture was stirred until the reaction was completed as indicated by TLC. The

resulting precipitate was collected .The crude solid was purified via recrystallization from ethanol to get pure products **7a-h**.

Synthesis of Compound 4g:

The structure of compound **4g** was confirmed from its spectroscopic and analytical data (Supporting Information S44). ^{1}H NMR (500 MHz, $CDCl_3$, ppm) δ = 6.99 (d, *J* = 15 Hz, 2H, ArH), 7.09 (d, *J* = 10 Hz, 2H, ArH), 7.19 (d, *J* = 15 Hz, 2H, ArH), 9.00 (s, 2H, HC=N), 11.49 (br s, 2H, OH). ^{13}C NMR (125 MHz, $CDCl_3$, ppm) δ = 120.35, 127.44, 129.19, 137.94, 144.91, 149.75, 152.71.

Synthesis of Compound 5g:

The structure of compound **5g** was confirmed from its spectroscopic and analytical data (Supporting Information S45). ^{1}H NMR (500 MHz, $CDCl_3$, ppm) δ = 6.99 (d, *J* = 15 Hz, 2H, ArH), 7.09 (d, *J* = 10 Hz, 2H, ArH), 7.19 (d, *J* = 15 Hz, 2H, ArH), 8.84 (br s, 4H, NH). ^{13}C NMR (125 MHz, $CDCl_3$, ppm) δ = 123.42, 125.76, 128.66, 129.34, 130.68, 137.78, 138.26, 147.49, 158.51, 170.49.

Synthesis of Compound 6h:

The structure of compound **6h** was confirmed from its spectroscopic and analytical data (Supporting Information S60). ^{1}H NMR (500 MHz, $CDCl_3$, ppm) δ = 6.95 (d, *J* = 10 Hz, 4H, ArH), 7.19 (t, *J* = 7.5 Hz, 4H, ArH), 7.25-7.31 (m, 12H, ArH), 11.05 (br s, 1H, OH). ^{13}C NMR (125 MHz, $CDCl_3$, ppm) δ = 125.31, 127.44, 127.97, 128.01, 128.49, 129.32, 130.13, 130.75, 133.07, 154.49, 165.86.

Synthesis of Compound 7h:

The structure of compound **7g** was confirmed from its spectroscopic and analytical data (Supporting Information S61). ^{1}H NMR (500 MHz, $CDCl_3$, ppm) δ = 6.88-6.91 (dd, *J* =7.5 Hz, 2H, ArH), 6.91-6.92 (dd, *J* = 7.5 Hz, 2H, ArH), 6.99-7.01 (d, *J* = 10 Hz, 3H, ArH), 7.02-7.06 (m, 4H, ArH), 7.08-7.11 (m, 3H, ArH), 7.11-7.18 (m, 2H, ArH), 7.21-7.29 (m, 4H, ArH), 10.13 (brs, 1H, NH). ^{13}C NMR (125 MHz, $CDCl_3$, ppm) δ = 126.21, 126.84, 127.23, 128.02, 128.06, 128.13, 128.32, 129.12, 130.00, 130.60, 133.59, 135.46, 138.38, 138.77, 142.26, 178.40.

Synthesis of mercury Nanoparticles (HgNPs):

Aqueous solution of 0.1 M $HgCl_2$ (110 μL) was added to a 3 ml solution of compound **3** (0.2 mM) in H_2O/THF (1:1, v/v). The reaction was stirred at room temperature for 12 min and formations of nanoparticles take place. These nanoparticles solution was used as such in the catalytic experiment.

Table S1: Comparison of present method over other reported procedure in literature for the preparation of HgNPs

S. No.	Publication	Reagents Used	Method of formation of HgNPs	Reaction time to prepare HgNPs	Reaction temp. (in °C)	Reducing agent or surfactants	Size of HgNPs
1	**Present manuscript**	**Compound 3 in Water/THF and $HgCl_2$**	**Wet chemical method**	**12 min**	**Room Temperature**	**No**	**5-20 nm**
2	*Sensors and Actuators B,* 2012, **173**, 745-751	0.02 M ($HgCl_2$), 1 M HCl solution, 0.4 M NaOH, 0.1 M hydrazine and 0.5% ibuprofen	Wet Chemical	1.5 min	Room temperature	Hydrazine ibuprofen	2-9 nm
3	*Chem. Mater.* 2011, **23**, 5231-5236	Mercury(I) nitrate dehydrate, HNO_3, Polyvinyl alcohol	Chemical method	10 min	25^0C	poly(vinyl alcohol)	≥15 nm
4	*Bioresource Technology* 2011, **102** ,4281-4284	Enterobacter sp. Strain maintained at 4°C in agar slants	Microbial synthesis	10 min	4^0C	Bacterial strain	2-5 nm (at pH 8.0)
5	*Applied Surface Science*, 2009, **256**, 438-442	Bacterial cell (DH5α),10 mM mercuric acetate	Microbial synthesis	-	-	Bacterial strain	5-10 nm
6	*Appl. Phys. Lett.* 2009, **94**.	DNA, EDTA, Nucleic bases	templated on plasmid DNA	-	-	EDTA	50 nm to 10 μm
7	*Adv. Mater.* 2008, **20**, 1000-1002	$Hg(CH_3)_2$ in N_2 atm. Followed by heating	RAPET. Method	3 h	800˚C	No	0.5 μm
8	*Acoustical Physics* 2006, **52**, 2	Bulk mercury	Ultrasonic Method (melting and freezing processes)	-	Room temp.	-	6-8 nm

Table S2: Comparison of catalytic activity of HgNPs for formation of primary amides from aldehydes via aldoximes over other reported methods:

Sr. No.	Publication	Catalyst used	Catalyst Amount	Nano catalysis	Reusability	Reaction Time	Temp (in ˚C)
1.	**Present manuscript**	**HgNPs**	**0.5[a] -1[b]**	**Yes**	**Yes**	**5[a]- 12[b] h**	**RT[a]-85˚C [b]**
2.	*Catal. Sci. Technol*., 2015, **5**,199–205	NH_2/SBA-15/Cu and SBA-15/En–Cu	5 mol%	No	Yes	2h	80°C
3.	*Catal. Sci. Technol*., 2014, **4**, 988–996	$[Cp^*Ir(H2O)_3][OTf]_2$	1.5 mol%	No	No	12h	110°C
4.	*Green Chem*., 2013, **15**, 2447–2456	arene–ruthenium(II) complexes	3 mol%	No	Yes	7h	100˚C
5.	*Org. Biomol.chem,* 2013*,* **11**, 2466–2472	$Pd(en)(NO_3)_2$	10 mol%	No	No	3.5-16h	60˚C
6.	*Adv. Synth. Catal*. 2011, **353**, 3262 – 3268	$RhCl(PPh_3)_3$	0.1-10 mol%	No	No	24h	110°C
7.	*J. Org. Chem*., 2010, 1197–1202	$[(IPr)Au(NTf_2)]$, $AgBF_4$	5 mol%	No	No	20h	100°C
8.	*Adv. Synth. Catal.* 2010, **352**, 288 – 292	$Pd(OAc)_2$	5 mol%	No	No	12h	125°C
9.	*Adv. Synth. Catal.* 2009, **351**, 1807 – 1812	Rh catalyst	1mol %	No	No	6h	80°C
10.	*Chem. Asian J.* 2008, **3,** 1715 – 1721	$Rh(OH)_x/Al_2O_3$	4 mol%	No	Yes	7h	160°C
11.	*Angew. Chem. Int. Ed.* 2007, **46**, 5202 –5205	$Rh(OH)_x/Al_2O_3$	4 mol %	No	Yes	7h	160°C

[a] electron donating groups; [b] electron withdrawing groups

Table S3: Comparison of catalytic activity HgNPs for the formation of secondary amides from ketoximes over other reported methods:

S. No	Publication	Catalyst used	Catalyst Amount	Nano catalysis	Reusability	Reaction time	Temp. required (in °C)
1	**Present manuscript**	**HgNPs**	**0.5 mol%**	**Yes**	**Yes**	**30-90 min**	**80°C**
2	*Tetrahedron Letters* 2014, **55**, 1136-1140	H3PW12O40 (DTPA)	0.05 mmol	No	Yes	2-6.5 h	Refluxing
3	*J.Org. Chem*., 2013, **78**, 4297-4302	Tosyl chloride (TsCl)	5-30 mol%	No	No	2 h	90°C
4	*Tetrahedron Letters,*2010, **51**, 739-743	Bromodimethylsulfonium bromide(BDMS), imidazolium-based ionic liquid [bmim]PF_6	(20 mol%)	No	Yes	2h	80°C
5	*Tetrahedron Letters* 2007, **48**, 2639-2643	Diethyl chlorophosphate	5 mmol	No	No	20 min	Reflux
6	*J. Org. Chem.* 2007, **72**, 4536-4538	$HgCl_2$	12 mol%	No	No	8 h	80
7	*Journal of Molecular Catalysis A*: *Chemical* 2006, **250**, 100–103	Silica sulphate	100 mg	No	Yes	3 h	microwave irradiation
8	*Tetrahedron Letters* 2005, **46,** 671-674	chlorosulfonic acid	0.4 ml, 6 mmol	No	No	0.5 h	90
9	*Tetrahedron Letters,*2003, **44**, 755-756	Chloral hydrate	0.5mmol	No	No	6.5 h	140
10	Tetrahedron Letters 2002,**43**, 2455-2457	Metaboric acid	3 mmol	No	No	17 h	140-145
11	*Org. Lett.,*2001, **3**, 2	$[RhCl(cod)]_2$ $(p\text{-}tol)_3P$ CF_3SO_3H	1-5mol%	No	No	3 h	Reflux

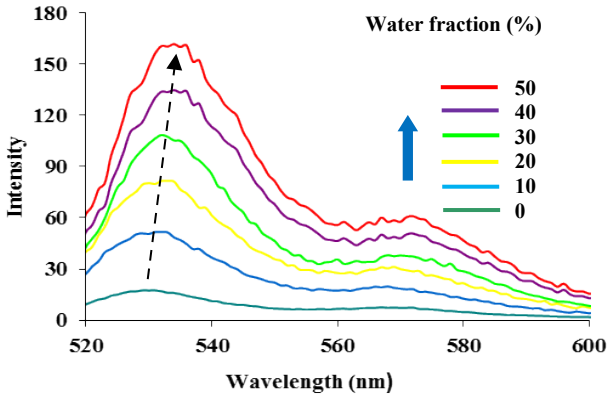

Fig. S1 Fluorescence spectrum of derivative **3** (5 μM) showing the variation of fluorescence intensity in various H_2O/THF mixtures; λ_{ex} = 485 nm.

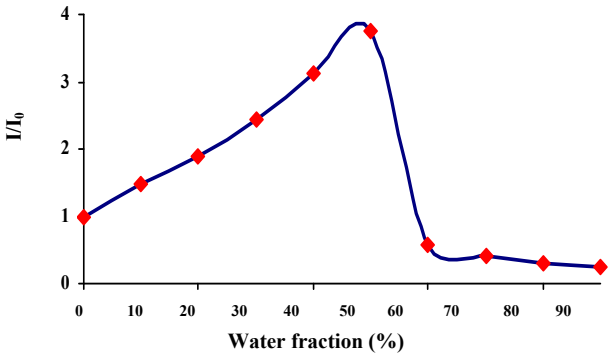

Fig. S2 Spectra showing the variation of fluorescence intensity of derivative **3** (5 μM) in H_2O/THF mixture (0 to 90% volume fraction of water in THF); λ_{ex} = 485 nm.

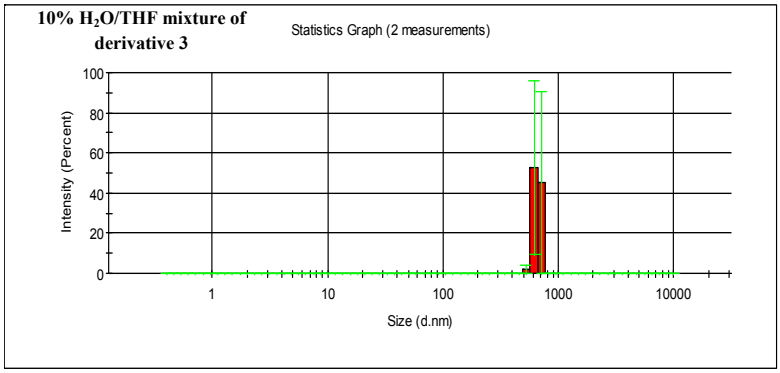

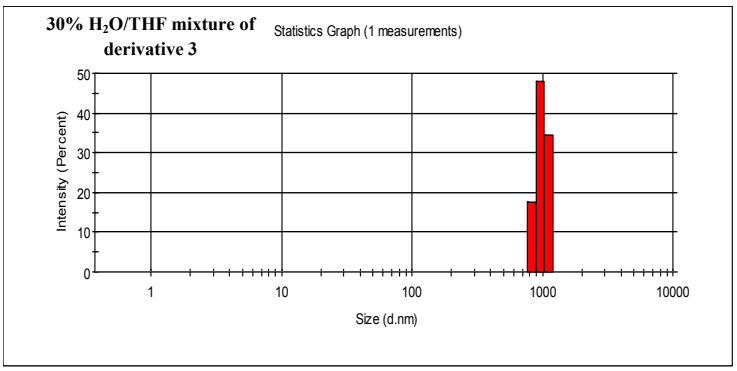

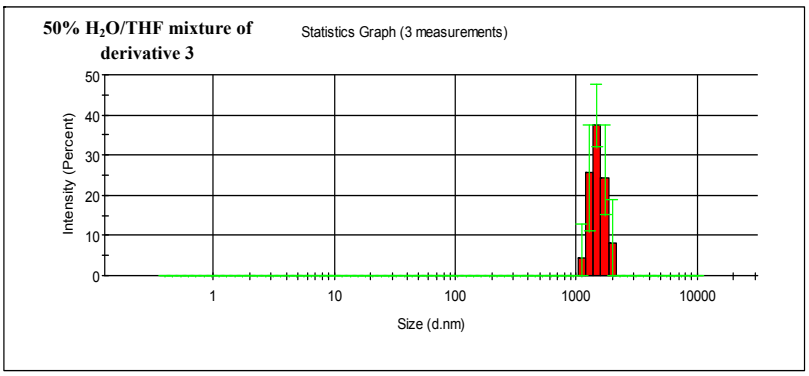

Fig. S3 Dynamic light scattering (DLS) results showing the variation in particle size diameter with increasing water content in THF solution of **3**. (A) **10%** (B) **30%** and (C) **50%** water content in THF solution of **3**.

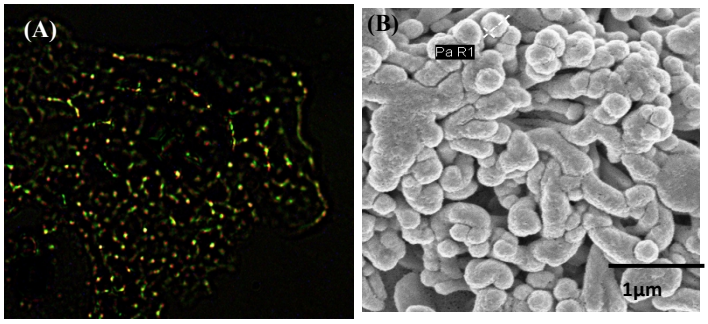

Fig. S4 (A) Polarized optical micrographs of derivative **3** at room temperature through crossed polarizing filters (B) SEM images of **3** showing the formation of aggregates in water/THF solution (1:1 v/v). Scale bar1µm

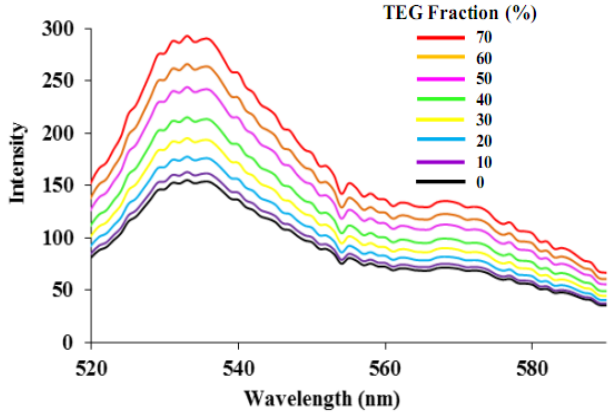

Fig. S5 Fluorescence spectra of compound **3** (5 µM) showing the variation of fluorescence intensity in TEG/THF mixture (0 to 70% volume fraction of TEG in THF); λ_{ex} = 485 nm.

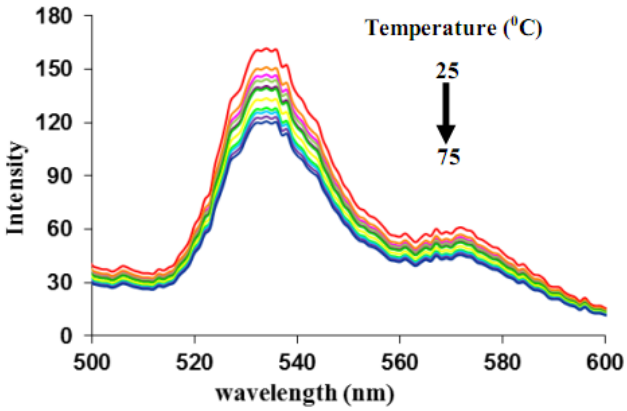

Fig. S6 Fluorescence spectra of derivative **3** (5 µM) showing the variation of fluorescence intensity with increase in temperature in H_2O/THF mixture (1:1, v/v); λ_{ex} = 485 nm.

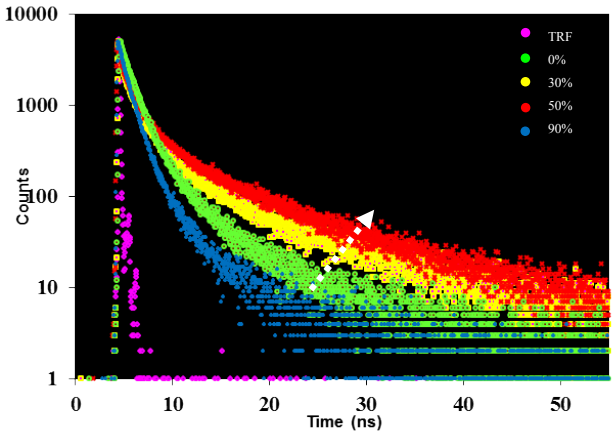

Fig. S7 Exponential fluorescence decays of **3** on addition of water fraction measured at 530 nm. Spectra were acquired in Water/THF mixture (0 to 50% volume fraction of water in THF), λ_{ex}= 486 nm.

Water fraction %	**Quantum Yield (Φ_f)**	**A_1/A_2**	**τ_1 (ns)**	**τ_2 (ns)**	**k_f (10^9 S^{-1})**	**k_{nr} (10^9 S^{-1})**
0	0.0004	56/44	**1.09**	6.43	0.00036	0.917
50	0.006	30/70	1.28	**8.85**	0.00067	0.112

Table S4 Fluorescence lifetime of derivative **3** in absence and presence of water (50%) in THF for the emission at 530 nm. **A_1, A_2:** fractional amount of molecules in each environment. **τ_1, τ_2** and **τ_{avg}:** bi-exponential and average life time of aggregates in 50 vol% of water in THF; **k_f:** radiative rate constant ($k_f = \Phi_f/\tau_{avg}$); **k_{nr}:** non-radiative rate constant ($k_{nr} = (1- \Phi_f)/\tau_{avg}$); λ_{ex}= 486 nm.

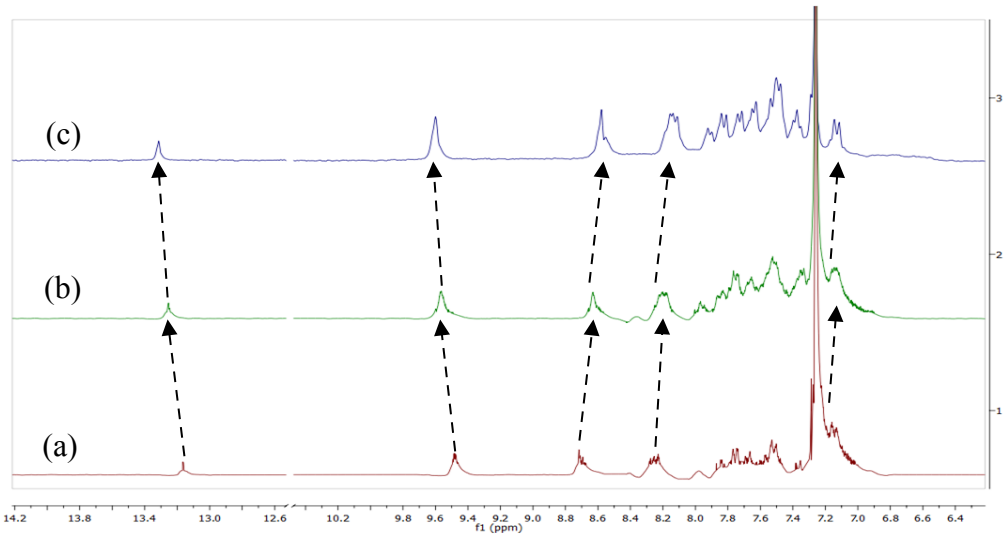

Fig. S8 Concentration dependent ^{1}H NMR spectrum of compound **3**, (a) 2 mg (b) 5 mg and (c) 10 mg each in 0.6 ml $CDCl_3$. NMR frequency is 300 MHz.

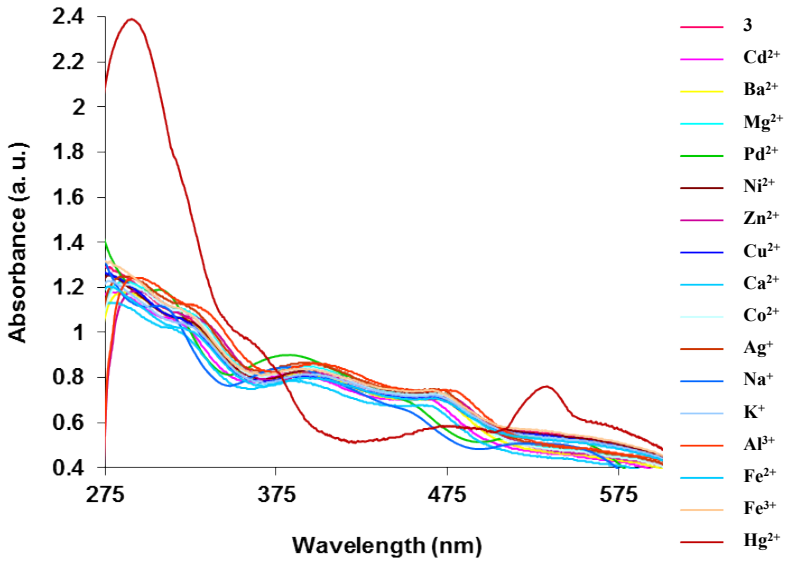

Fig. S9A UV-vis spectra of derivative **3** (5 μM) upon additions of 18 equiv. of various metal ions as their chloride salt in H_2O/THF (1:1, v/v) mixture.

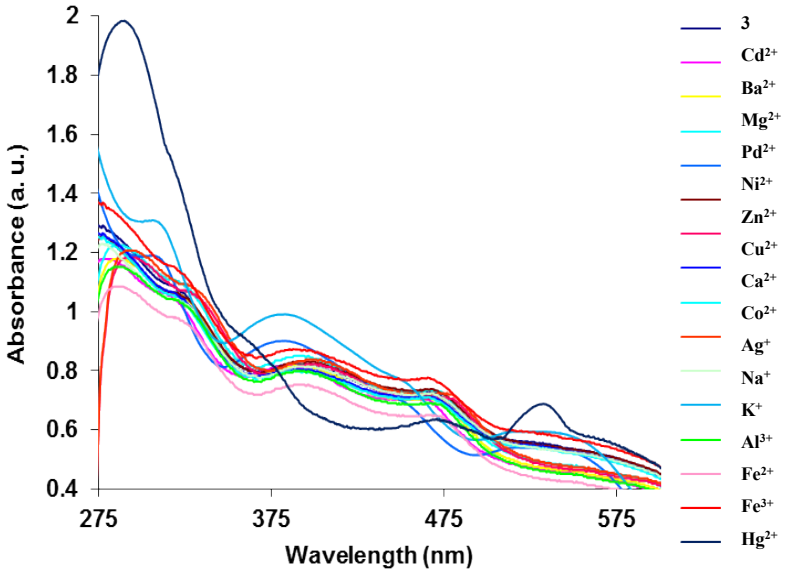

Fig. S9B UV-vis spectra of derivative **3** (5 μM) upon additions of 18 equiv. of various metal ions as their perchlorate salt in H_2O/THF (1:1, v/v) mixture.

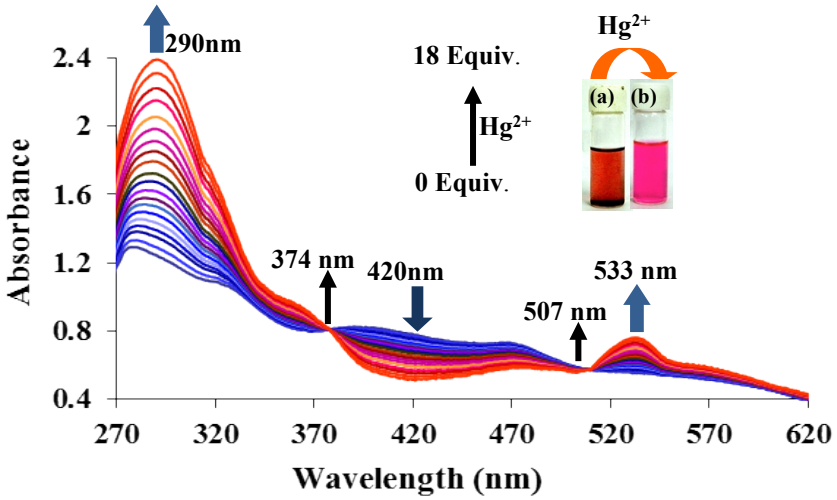

Fig. S10 UV−vis spectra of compound **3** (5 μM) showing the response to the Hg^{2+} ion (0-18 equiv.) in H_2O/THF (1:1, v/v) mixture, Inset photographs (Under 365 nm UV-light) (a) before and (b) after the addition of Hg^{2+} ion.

Regression Statistics	
Multiple R	0.996201
R Square	0.992016
Intercept	1.200389
Slope	0.100172

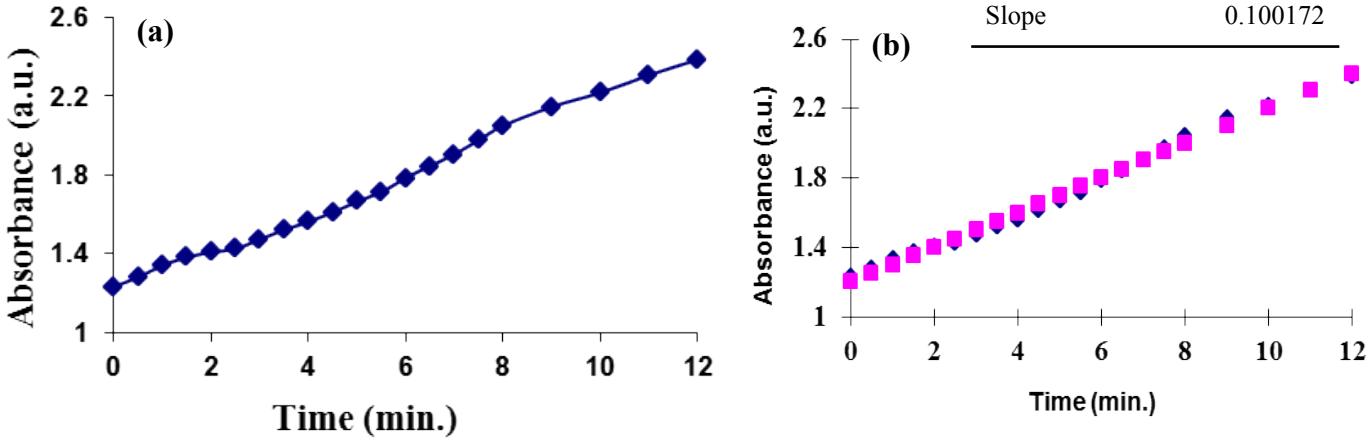

Fig. S11 Graphical representation of the rate of formation of HgNPs of derivative **3**; (a) Time (min) vs. absorbance plot at 290 nm; (b) regression plot of a.

The first order rate constant for the formation of nanoparticles was calculated from the changes of intensity of absorbance of aggregates of derivative **3** in the presence of Hg^{2+} ions at different time interval.

From the time vs. absorbance plot at fixed wavelength 290 nm by using first order rate equation we get the rate constant = k = slope×2.303 = 0.100172×2.303 = 0.230 min^{-1}= **3.84×10^{-3} S^{-1}**.

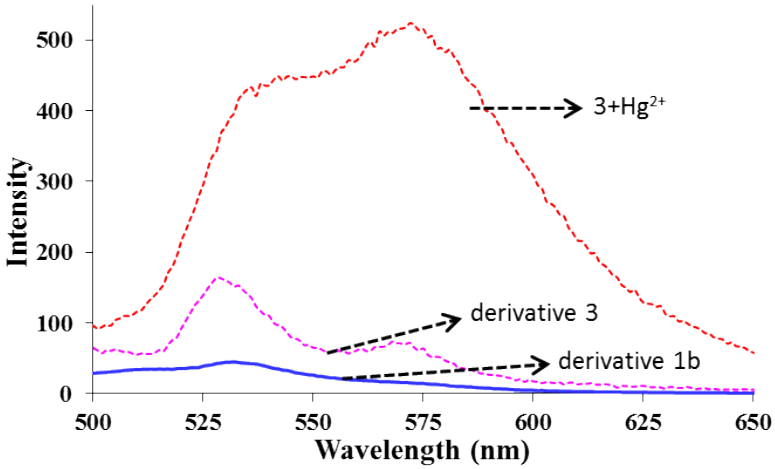

Fig. S12 Fluorescence spectrum of derivative **1b** (5 μM) (blue line), derivative **3** (pink dotted line), derivative **3-Hg^{2+}** (red dotted line) showing the variation of fluorescence in H_2O/THF mixtures (1:1v/v). λex = 485 nm.

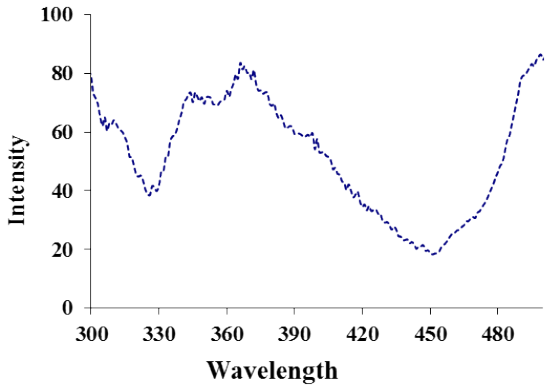

Fig. S13 Fluorescence excitation spectrum of **3** in H_2O/THF (1:1, v/v) mixture addition of Hg^{2+} ions for the emission at 570 nm (λ_{em} = 570 nm).

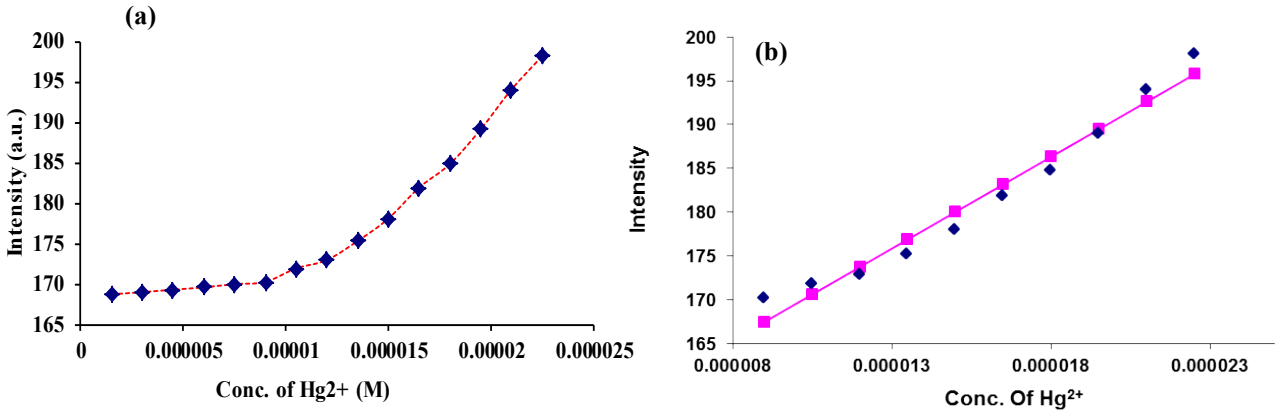

Fig. S14 (a) Showing the fluorescence intensity of compound **3** and (b) Calibrated curve showing the fluorescence intensity of compound **3** at 570 nm as a function of Hg^{2+} ions concentration (equiv.) in H_2O/THF (1:1, v/v) buffered with HEPES, pH =7.05, λ_{ex}= 485nm.

Multiple R = 0.983094,

R^2 = 0.966474,

Standard deviation = 0.005,

Observation = 10,

Intercept = 148.60,

Slope = 2095636

The detection limit was calculated based on the fluorescence titration. To determine the S/N ratio, the emission intensity of receptor **3** without Hg^{2+} was measured by 10 times and the standard deviation of blank measurements was determined. The detection limit is then calculated with the following equation:

DL = 3 × SD/S

Where SD is the standard deviation of the blank solution measured by 10 times; S is the slope of the calibration curve.

From the graph we get slope

S =**2095636**, and SD value is 0.005

Thus using the formula we get the Detection Limit **(DL) = 3 × 0.005/2095636 = 7.15 × 10^{-9} M = 7.15 nM**

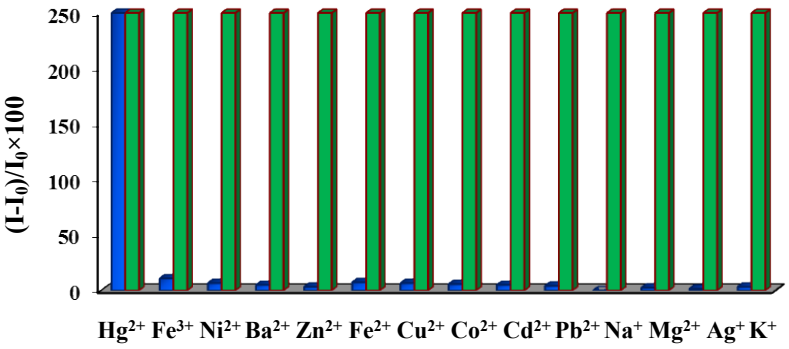

Fig. S15A Fluorescence response of **3** (5.0 μM) to various metal ions of **chloride salts** (36 equiv.) in H_2O/THF (1:1, v/v) mixture buffered with HEPES; pH = 7.05; λ_{ex} = 485 nm. Bars represent the emission intensity ratio $(I-I_0)/I_0\times100$ (I_0 and I are the initial and final fluorescence intensity at 570 nm before and after the addition of metal ions). (a) Blue bars represent selectivity of **3** upon addition of different metal ions. (b) Green bars represent competitive selectivity of receptor **3** toward Hg^{2+} ions (18 equiv.) in the presence of other metal ions (36 equiv.).

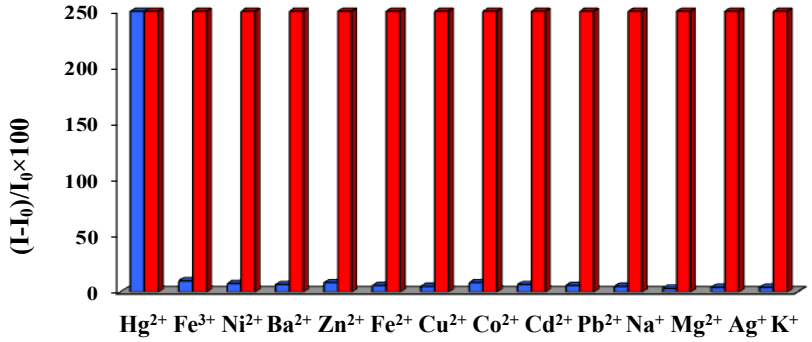

Fig. S15B Fluorescence response of **3** (5.0 μM) to various metal ions of **perchlorate salts** (36 equiv.) in H_2O/THF (1:1, v/v) mixture buffered with HEPES; pH = 7.05; λ_{ex} = 485 nm. Bars represent the emission intensity ratio $(I-I_0)/I_0\times100$ (I_0 and I are the initial and final fluorescence intensity at 570 nm before and after the addition of metal ions). (a) Blue bars represent selectivity of **3** upon addition of different metal ions. (b) Green bars represent competitive selectivity of receptor **3** toward Hg^{2+} ions (18 equiv.) in the presence of other metal ions (36 equiv.).

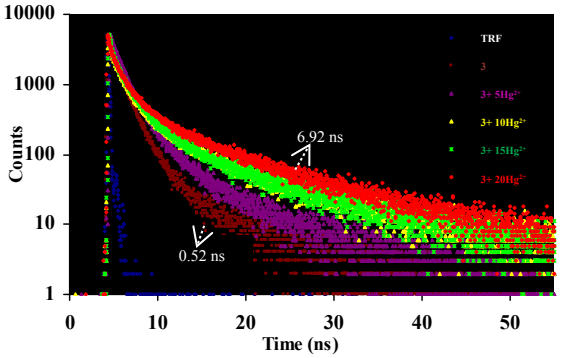

Fig. S16 Exponential fluorescence decays of **3** on addition of Hg^{2+} ions measured at 570 nm. Spectra were acquired in H_2O/THF (1:1, v/v) mixture buffered with HEPES; pH = 7.05; λex = 486 nm

Hg^{2+} (equiv.)	Quantum Yield	A_1/A_2	τ_1 (ns)	τ_2 (ns)	k_f (10^9 S^{-1})	k_{nr} (10^9 S^{-1})
0	0.006	79/21	**0.523**	5.58	0.0114	1.9
18	0.12	35/65	2.96	**6.92**	0.017	0.12

Table S5 Fluorescence lifetime of derivative **3** in absence and presence of Hg^{2+} ions (18 equiv.) in H_2O/THF (1:1, v/v) mixture buffered with HEPES; pH = 7.05; at 570 nm. **A_1**, **A_2:** fractional amount of molecules in each environment. ***τ_1*** and ***τ_2*:** biexponential life time of aggregates in 50 vol% of water in THF; ***k_f*:** radiative rate constant ($K_f = \Phi_f/\tau_{avg}$); ***K_{nr}*:** non-radiative rate constant ($K_{nr} = (1- \Phi_f)/\tau_{avg}$); λ_{ex}= 486 nm.

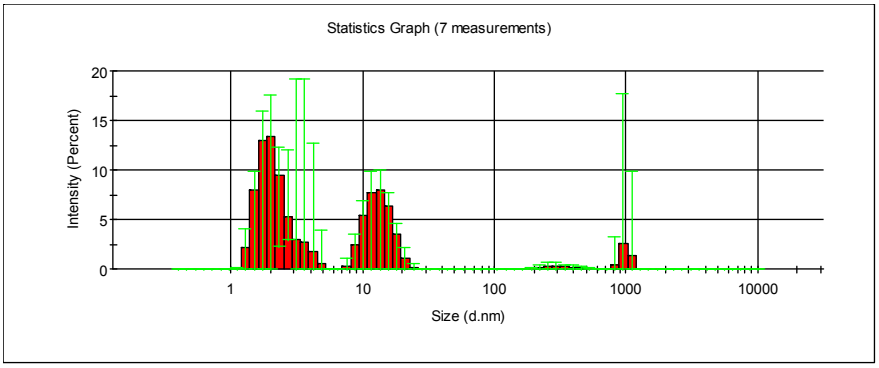

Fig. S17 Dynamic light scattering (DLS) results showing the variation in particle size of derivative **3**+Hg^{2+} ion in presence of Water/THF (1:1, v/v) mixture.

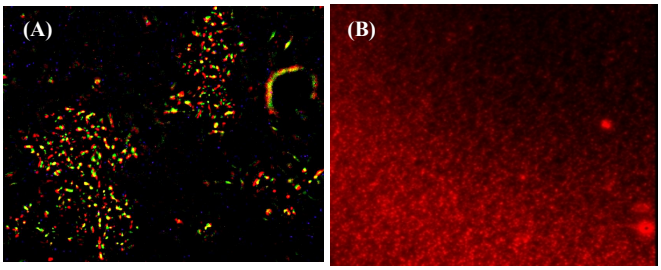

Fig. S18 (A) Polarized optical micrographs and (B) Confocal image of compound **3** in the H_2O-THF (1:1, v/v) solvent mixture in presence of Hg^{2+} ions; λ_{ex} = 485 nm.

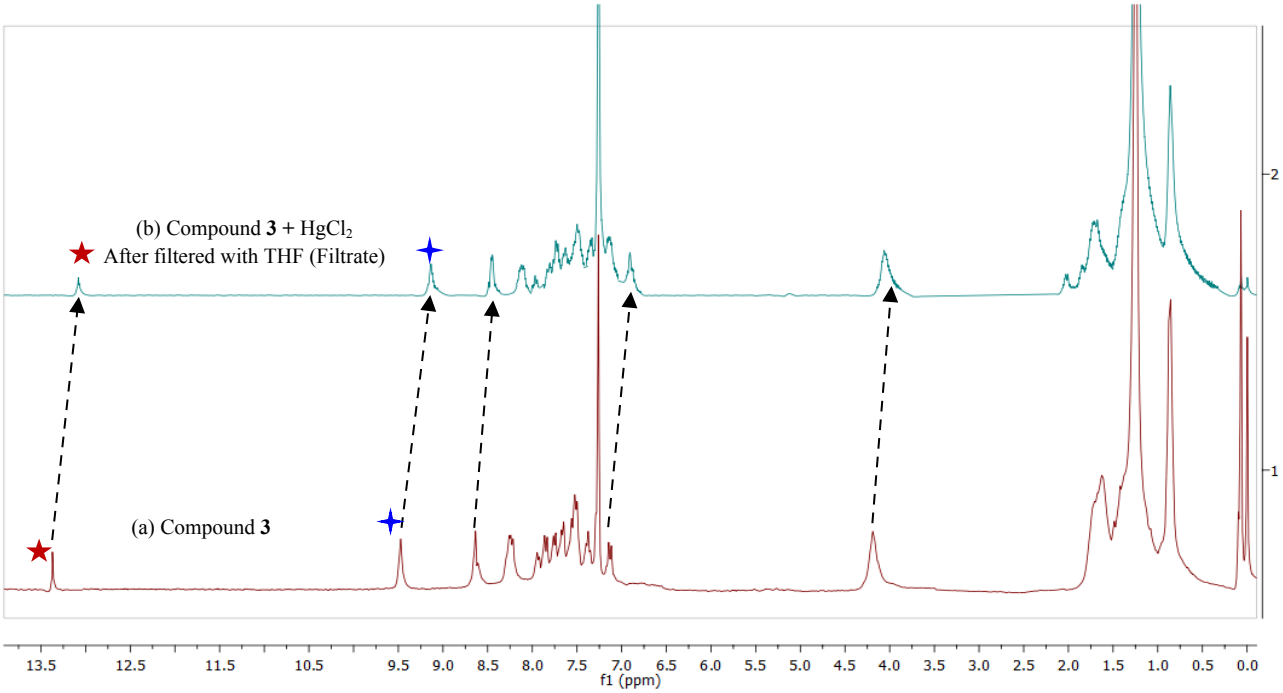

Fig. S19 Overlay ^{1}H NMR spectra of (a) compound **3** and (b) compound **3** + **$HgCl_2$** after filtration with THF in $CDCl_3$.

(a) Compound 3 (δ_3, ppm)	**(b) Compound 3 + Hg^{2+}**, after filtration by THF (δ_F, ppm)	$\Delta\delta_1 = \delta_3 - \delta_F$
★ 13.31 (s, -OH)	13.16	0.15
✦ 9.47 (s, -N=CH)	9.32	0.15
8.63 (s, aromatic)	8.48	0.15
8.19 (d, aromatic)	8.16	0.03
7.93 (d, aromatic)	7.90	0.03
7.85 (m, aromatic)	7.78	0.07
7.75 (d, aromatic)	7.68	0.07
7.66 (d, aromatic)	7.58	0.08
7.52 (t, aromatic)	7.46	0.06
7.37 (t, aromatic)	7.28	0.09
7.12 (d, aromatic)	7.06	0.06
4.19 (t, -NCH_2)	4.12	0.07

Table S6 Change in chemical shift (δ) value of ^{1}H NMR spectra (a) compound **3** and (b) compound **3** + **$HgCl_2$** after filtration with THF in $CDCl_3$.

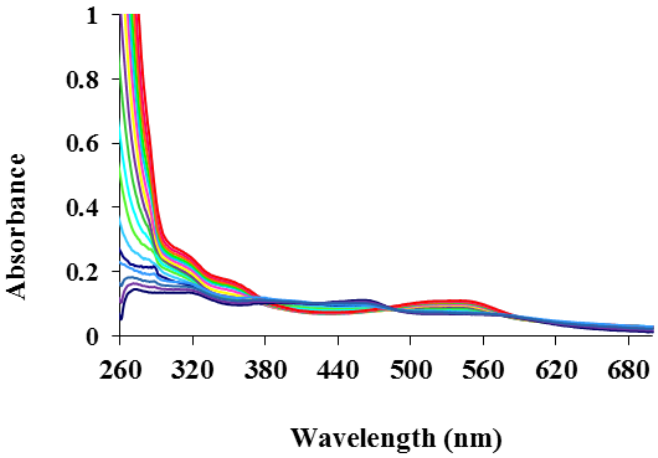

Fig S20 UV-vis spectra of derivative **3** (5 μM) showing the response to the Hg^{2+} ion (0-18 equiv.) in THF

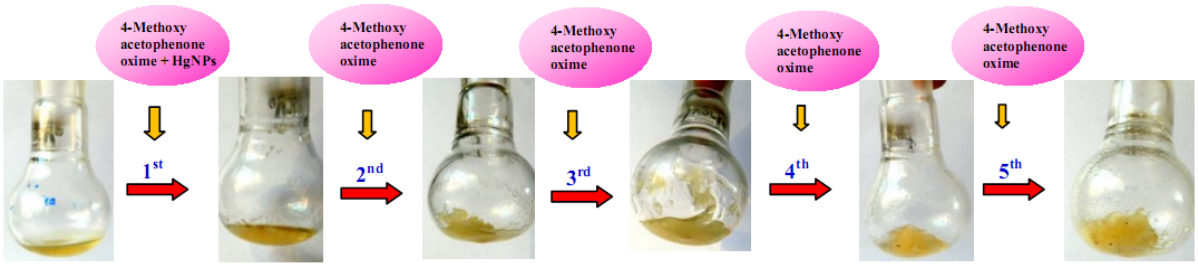

Fig S21 Catalyst-reusability in rearrangement reaction of 4-methoxy acetophenone oxime **(6b)** entry 2 in Table S7.

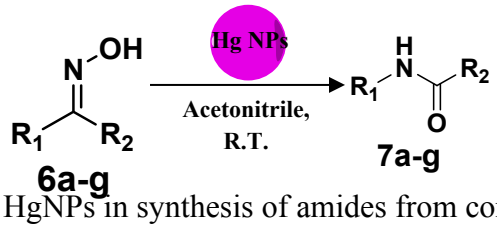

Scheme 2: Catalytic activity of HgNPs in synthesis of amides from corresponding ketoximes.

Table S7 HgNPs catalysed Beckmann rearrangement of various ketoximes to corresponding amides/lactams.

Entry	Reactant (Ketoxime)	Product (Amide/lactam)	Time	(%) Yield	Mp (Lit.)
1	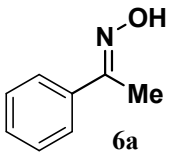 6a	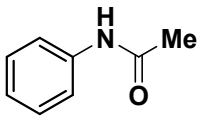 7a	30min	97	114(114-115)[3a]
2	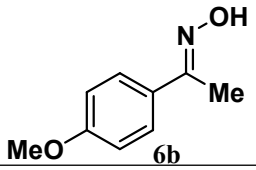 6b	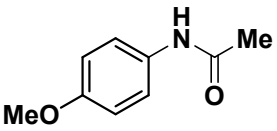 7b	20min	98	129(130)[3b]
3	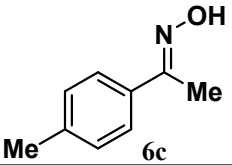 6c	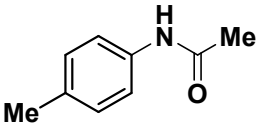 7c	25min	94	145(151)[3b]
4	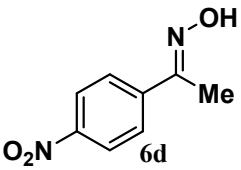 6d	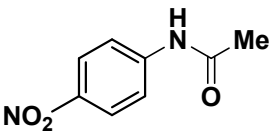 7d	40min	91	214(216)[3b]
5	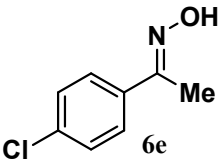 6e	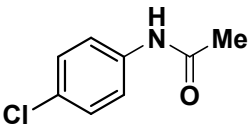 7e	1h	92	178(179)[3b]
6	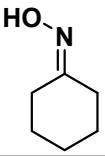 6f	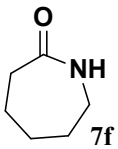 7f	1.5h	86	69(69)[3c]
7	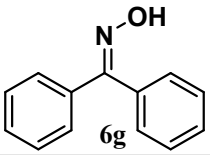 6g	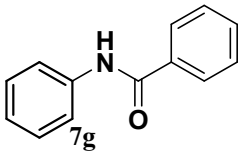 7g	1.2h	94	163(162-165)[3a]

[3a] A. R. Sardarian, Z. S. -Fard, H. R. Shahsavari and Z. Ebrahimi, *Tetrahedron Letters*, 2007, **48**, 2639; [3b]A. R. Katritzky, U. Maran, M. Karelson and V. S. Lobanov, *J. Chem. Inf. Comput. Sci.*, 1997, **37**, 913; [3c] D. Crespy and K. Landfester, *Macromolecules*, 2005, **38**, 6882.

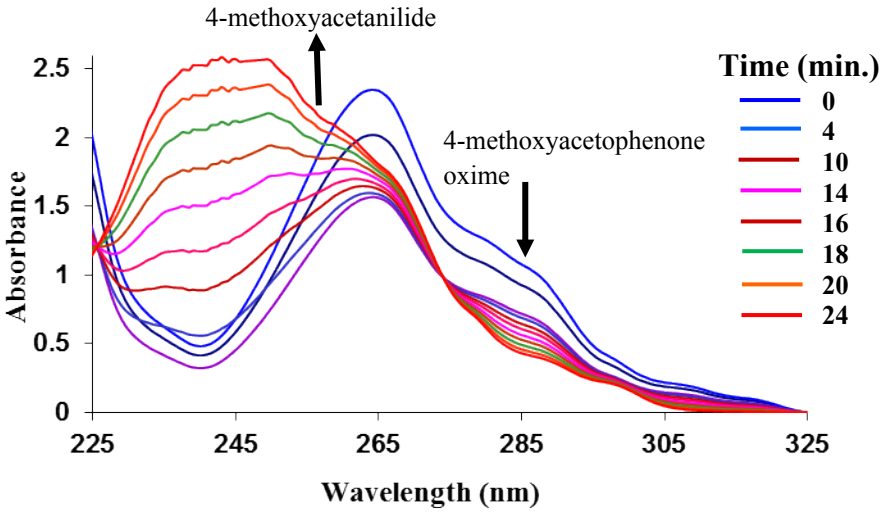

Fig. S22 UV-vis spectra showing conversion of 4-methoxyacetophenone oxime **(6b)** to 4-methoxyacetanilide **(7b)** by *in situ* generated HgNPs in acetonitrile at different time interval (24 min).

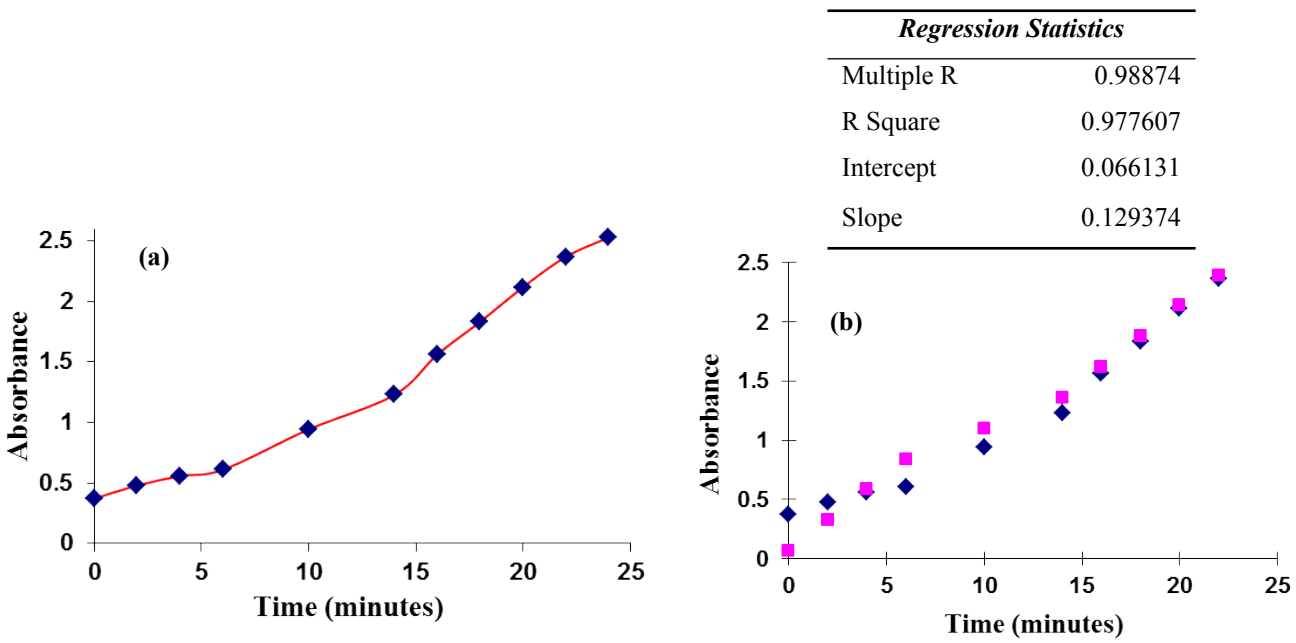

Regression Statistics	
Multiple R	0.98874
R Square	0.977607
Intercept	0.066131
Slope	0.129374

Fig. S23 Graphical representation of the rate of formation of 4-methoxyaacetanilide (a) Time (min) vs. absorbance plot at 241 nm (b) regression plot of a.

The first order rate constant for the formation of 4-methoxyaacetanilide **(7b)** was calculated from the changes of intensity of absorbance of 4-methoxyacetophenone oxime **(6b)** in the presence of HgNPs at different time interval.

From the time vs. absorbance plot at fixed wavelength[2] 241 nm by using first order rate equation we get the rate constant = k = slope×2.303 = 0.129374×2.303 = 0.297 min $^{-1}$ = **4.96×10^{-3} S^{-1}**.

[2] C. J. Giffney and C. J. O Connor, *J. Chem. Soc., Perkin Trans. 2*, 1975, 706.

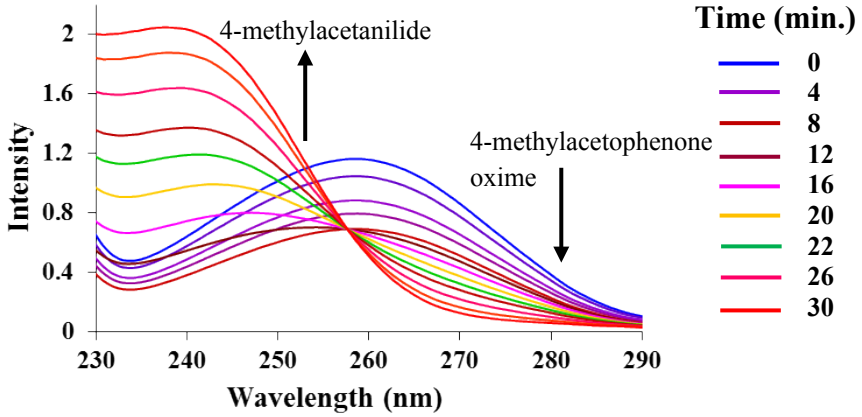

Fig. S24 UV−vis spectra showing conversion of 4-methylacetophenone oxime **(6c)** to 4-methylacetanilide **(7c)** by *in situ* generated HgNPs in acetonitrile at different time interval (30 min.).

Regression Statistics	
Multiple R	0.958614
R Square	0.918946
Intercept	0.056638
Slope	0.057249

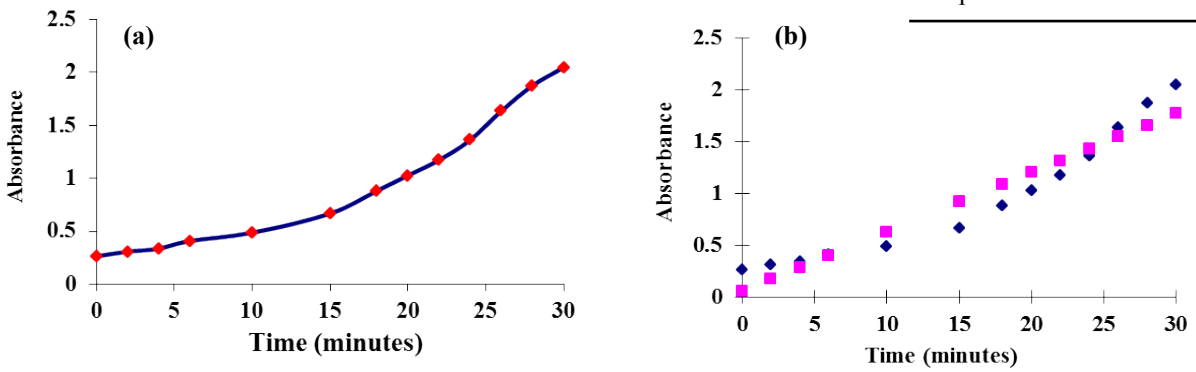

Fig. S25 Graphical representation of the rate of formation of 4-methylacetanilide. (a) Time (min) vs. absorbance plot at 242 nm (b) regression plot of a.

The first order rate constant for the formation of 4-methylacetanilide **(7c)** was calculated from the changes of intensity of absorbance of 4-methylacetophenone oxime **(6c)** in the presence of HgNPs at different time interval.

From the time vs. absorbance plot at fixed wavelength[2] 242 nm by using first order rate equation we get the rate constant = k = slope×2.303 = 0.057249×2.303 = 0.132 min^{-1}= **2.19×10^{-3} S^{-1}**.

[2] C. J. Giffney and C. J. O Connor, *J. Chem. Soc., Perkin Trans. 2*, 1975, 706.

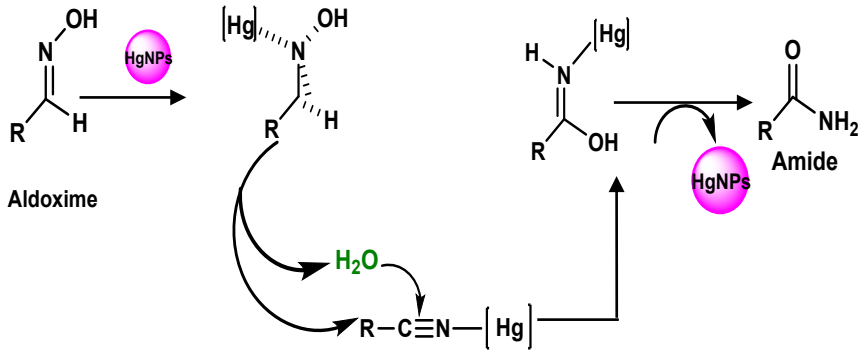

Scheme 3 Proposed Mechanism for rearrangement aldoxime to primary amide.

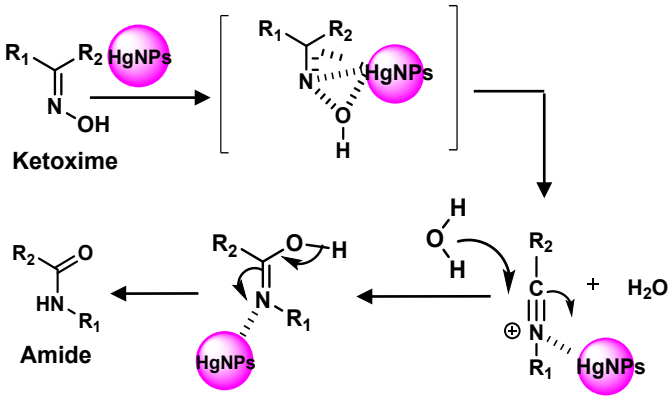

Scheme 4 Proposed Mechanism for rearrangement ketoxime to secondary amide.

Table S8 HgNPs catalysed Beckmann reaction of 4-methoxyacetophenone oxime **(6b)** using various amount of HgNPs

Entry	HgNPs (ppm)	Time	Yield (%)	TON	TOF (h^{-1})
1	5000 (0.5 mol%)	20 min	98	196	588
2	1000 (0.1 mol%)	1.6 h	96	960	600
3	100 (0.01 mol%)	4 h	91	9100	2275
4	10 (0.001 mol%)	12 h	86	86000	7166
5	0 (mol%)	24 h	0	0	0

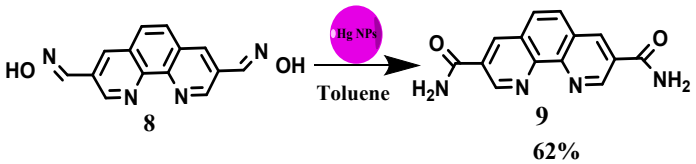

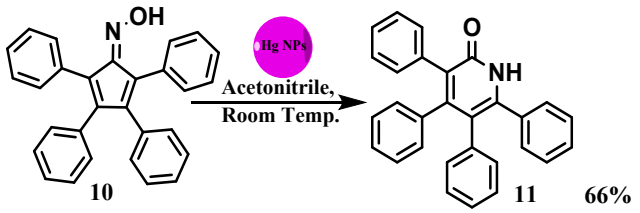

Scheme 5 Synthesis of phenanthroline and cyclopentadieneone based amides using Beckmann rearrangement in the presence of HgNPs (1and 0.5mol% respectively)

^{1}H NMR spectrum of derivative **1b** in $CDCl_3$

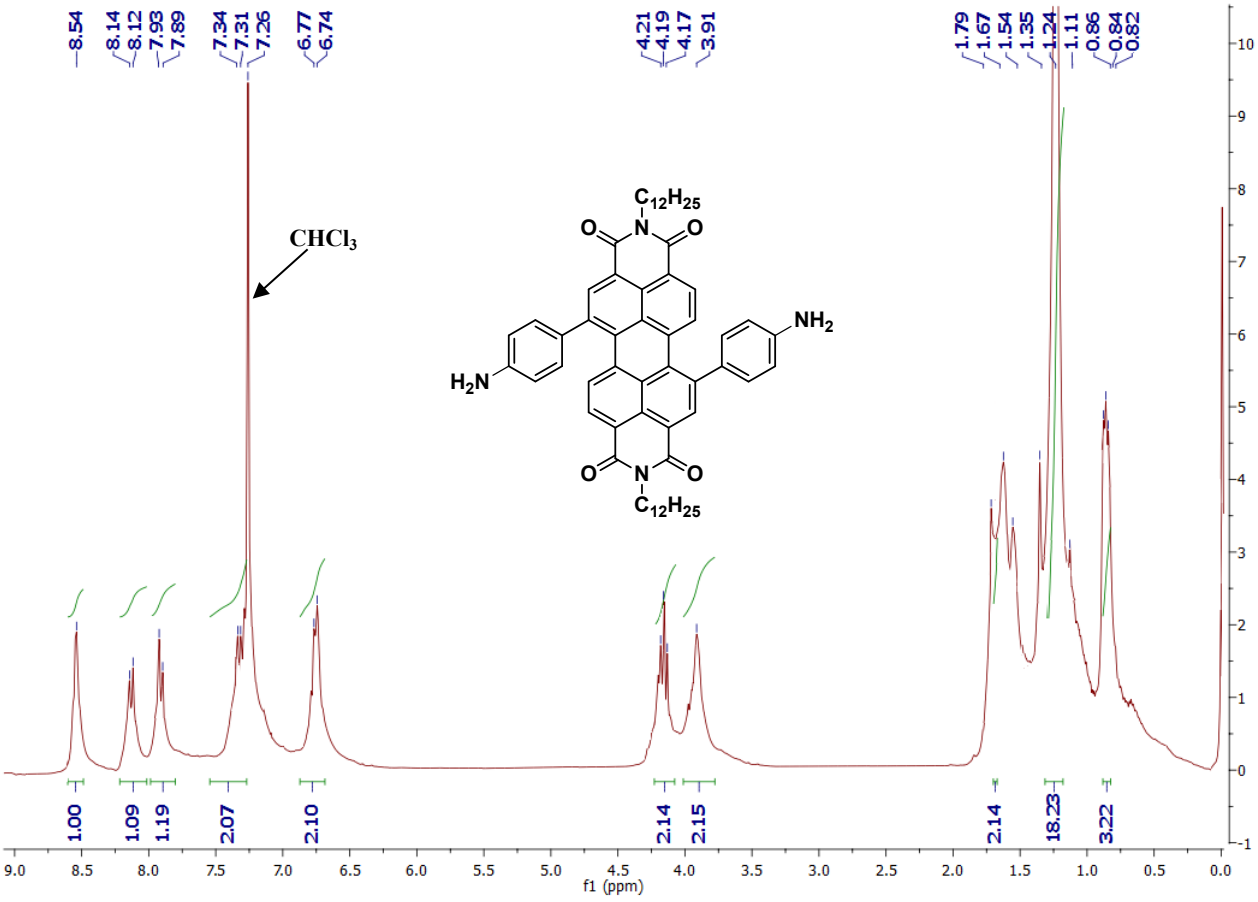

Fig. S26 ^{1}H NMR spectrum of derivative **1b** in $CDCl_3$

^{13}C NMR spectrum of derivative **1b**

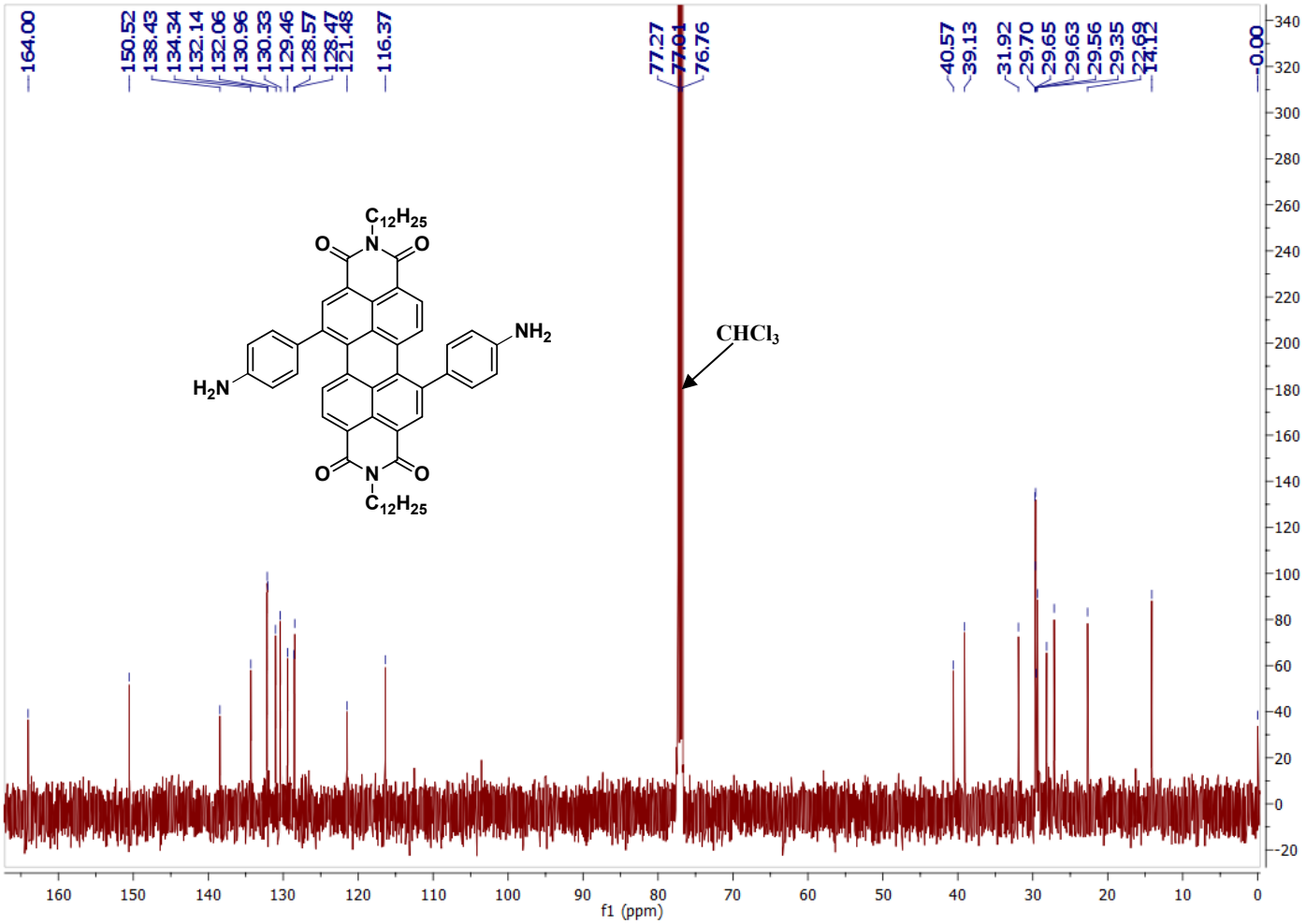

Fig. S27 ^{13}C NMR spectrum of derivative **1b**.

ESI-MS Spectrum of compound 1b:

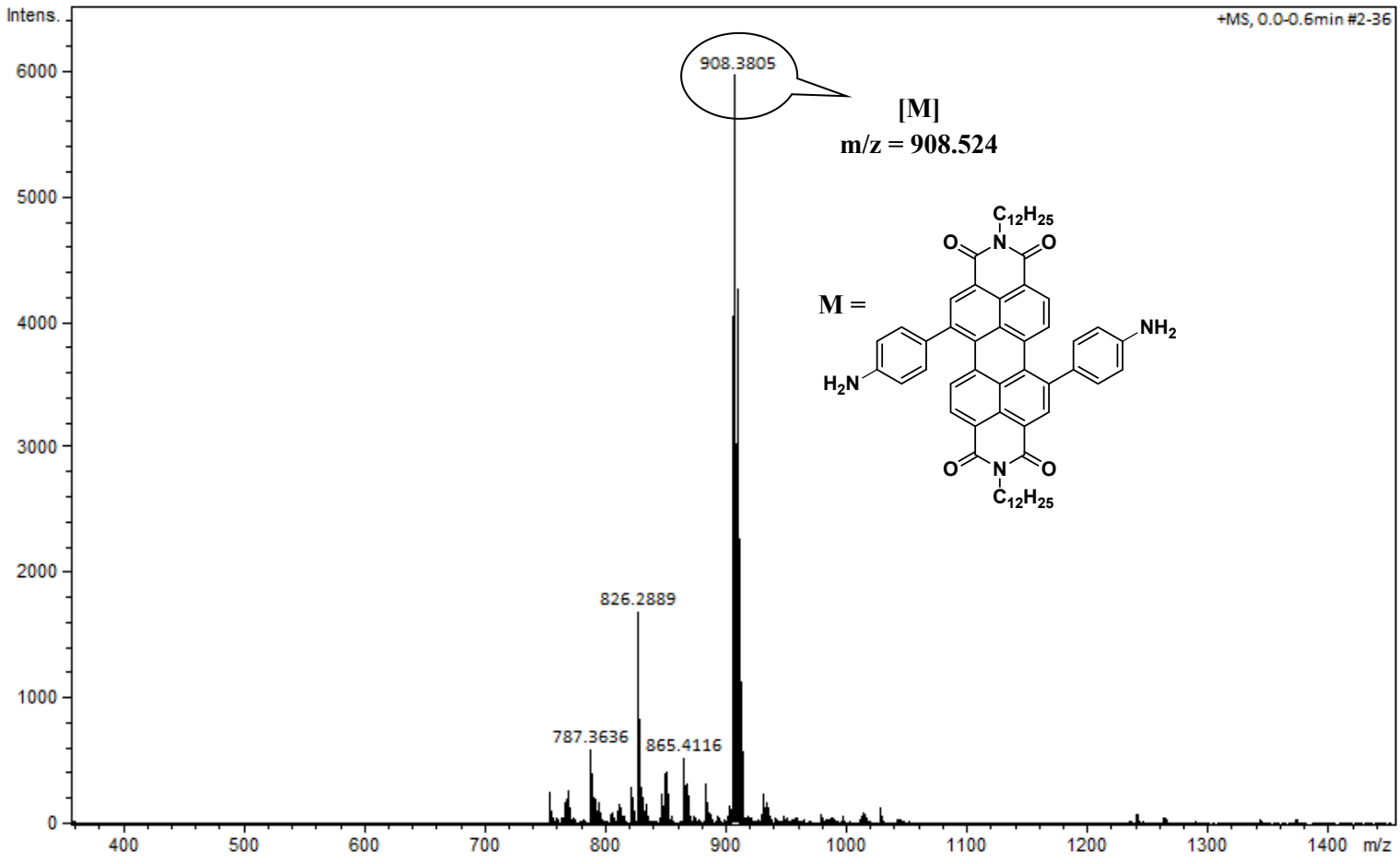

Fig. S28 ESI-MS Mass spectrum of derivative **1b**.

FT-IR Spectrum of compound 1b:

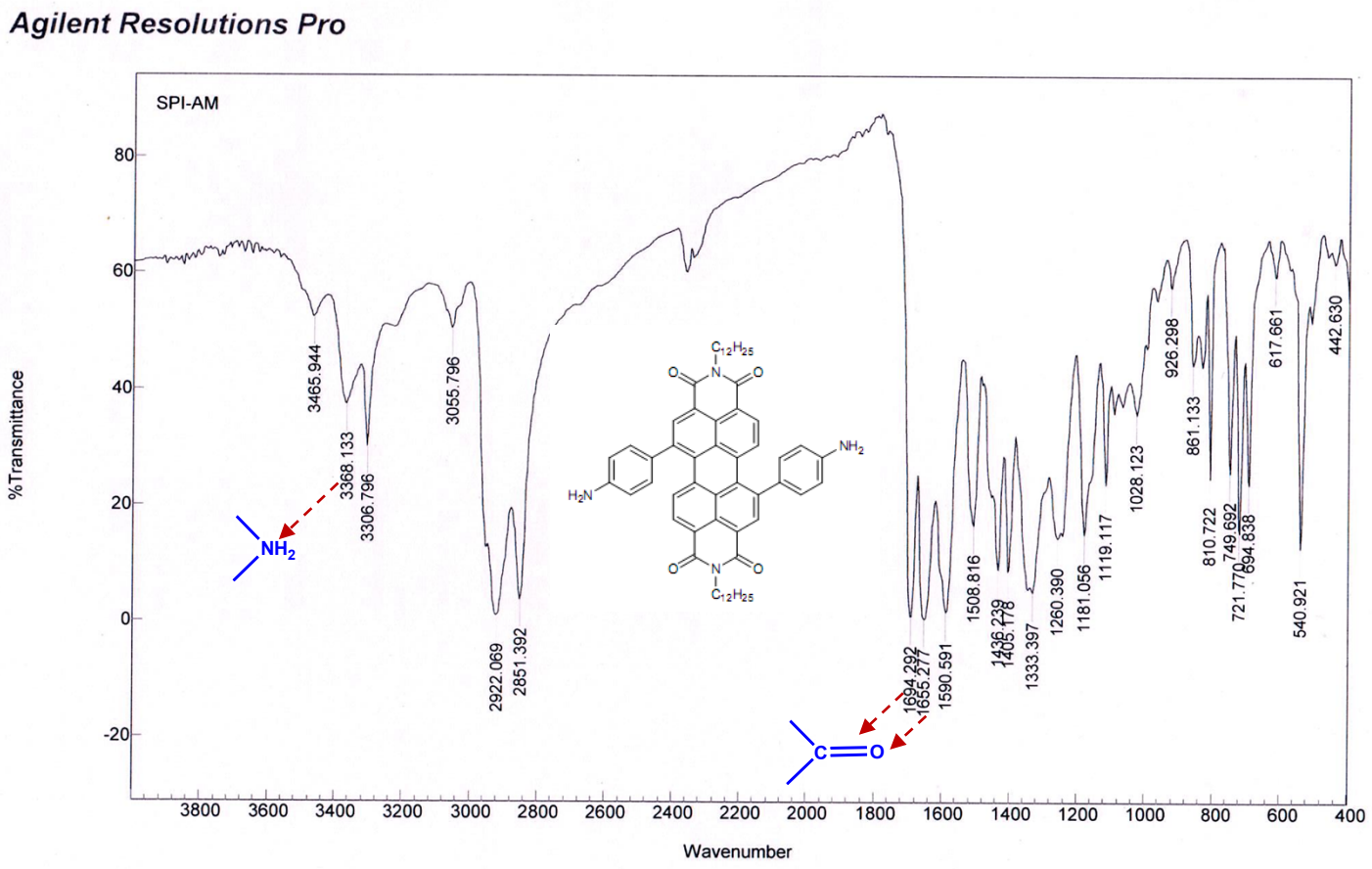

Fig. S29 FT-IR Spectrum of compound 1b:

^{1}H NMR spectrum of derivative **3** in $CDCl_3$

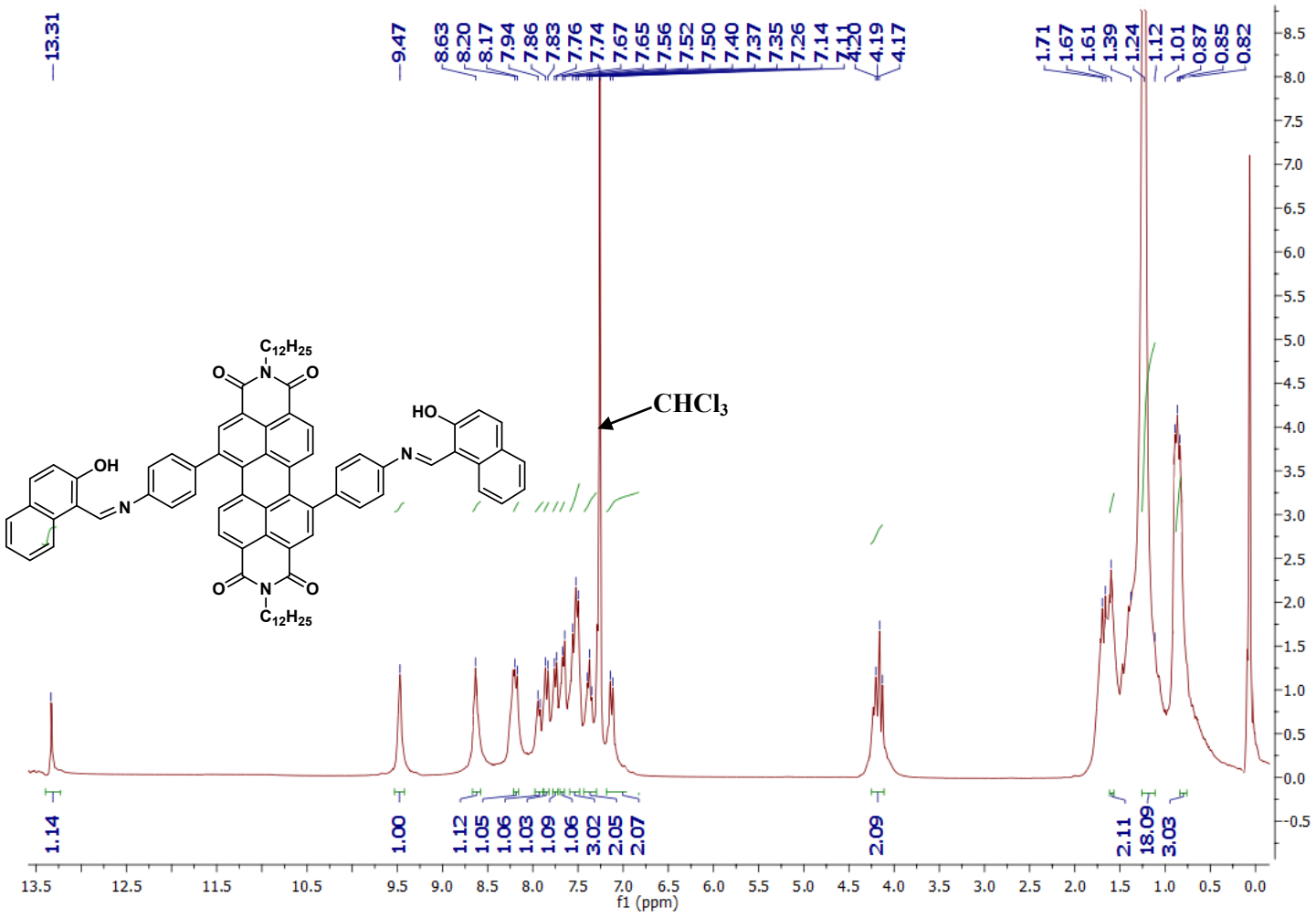

Fig. S30 ^{1}H NMR spectrum of derivative **3** in $CDCl_3$.

^{13}C NMR spectrum of derivative **3**

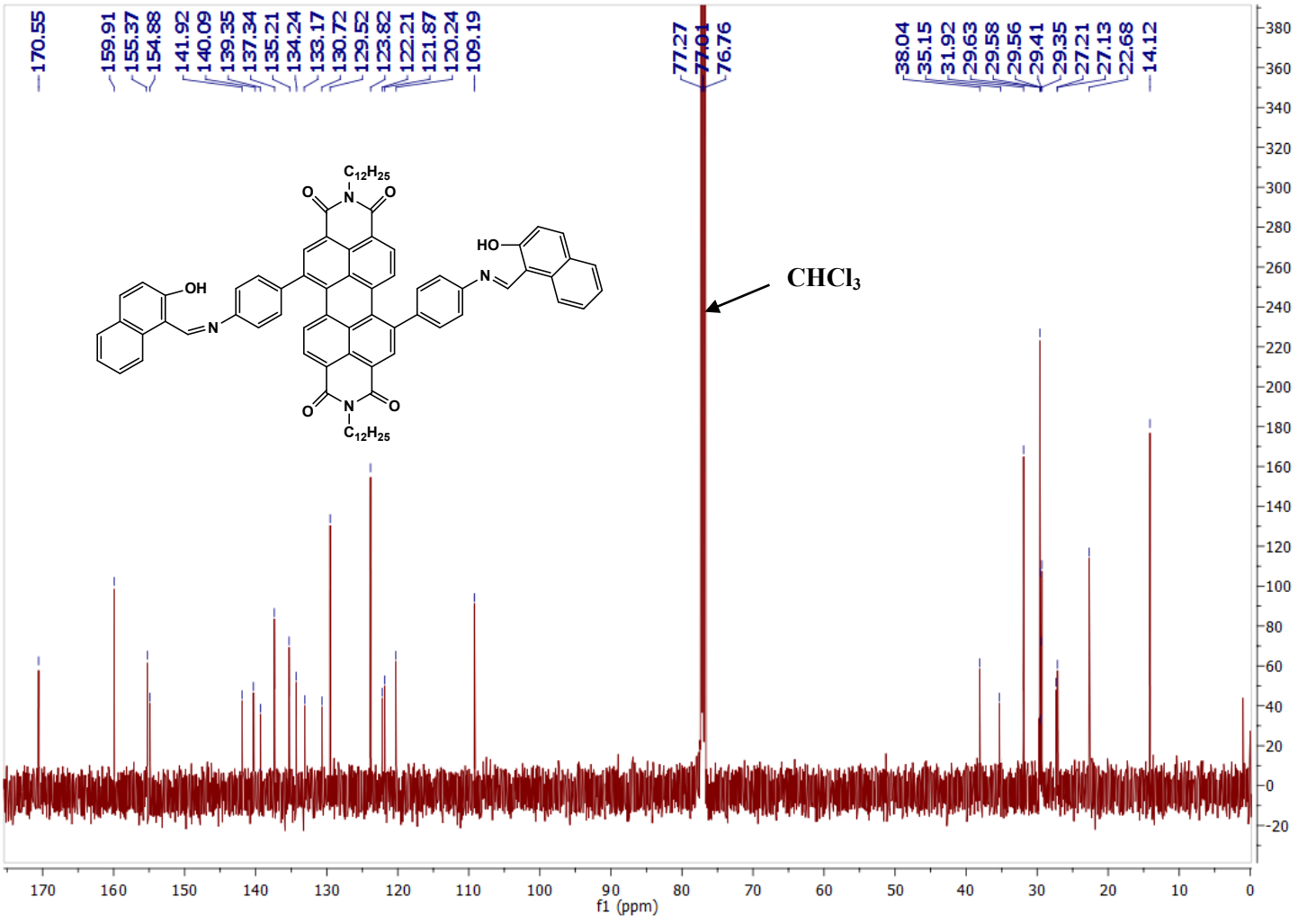

Fig. S31 ^{13}C NMR spectrum of derivative **3** in $CDCl_3$.

Mass spectrum of derivative **3**:

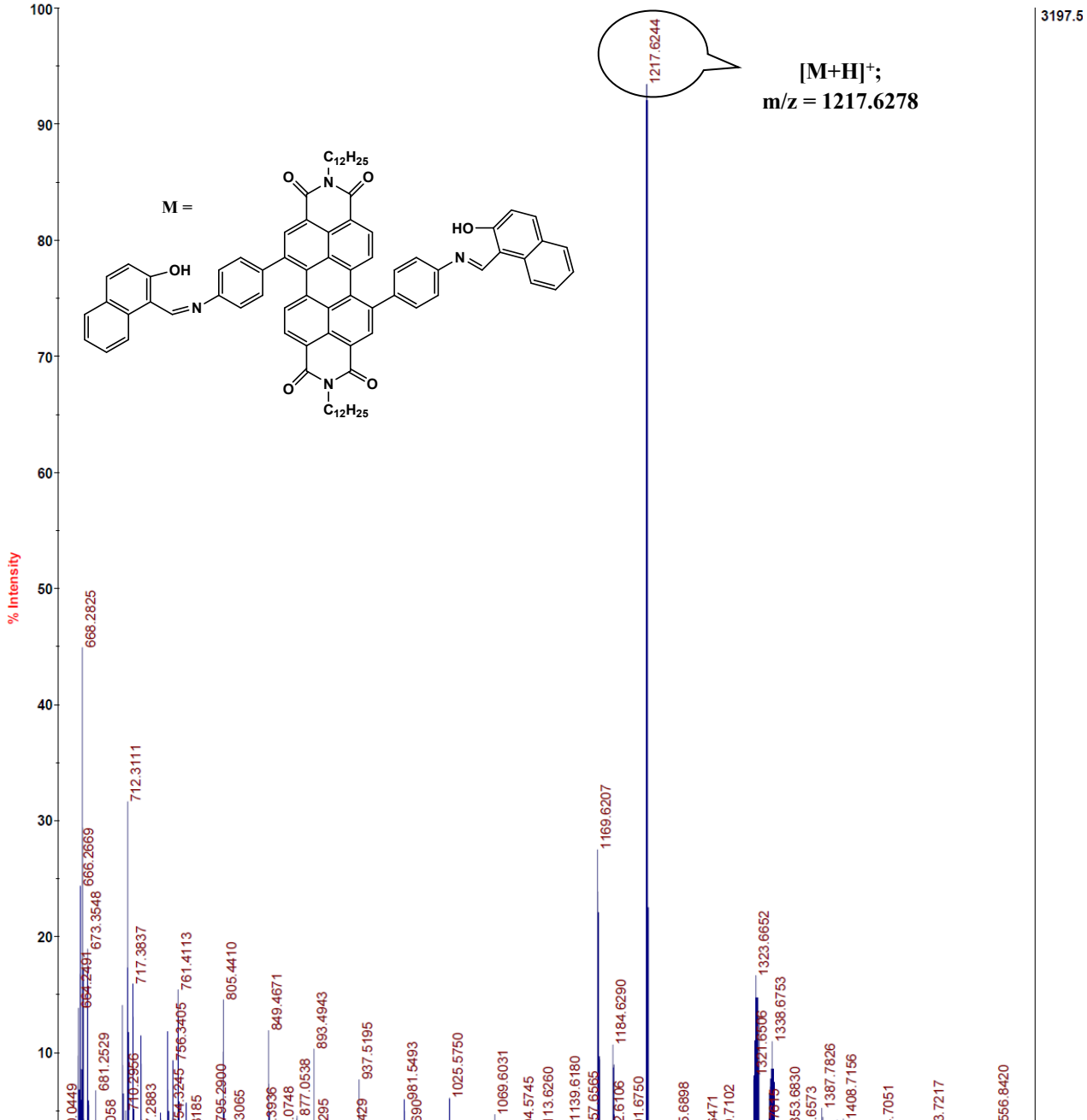

Fig. S32 MALDI-TOF Mass spectrum of derivative **3**

FT-IR Spectrum of compound **3**

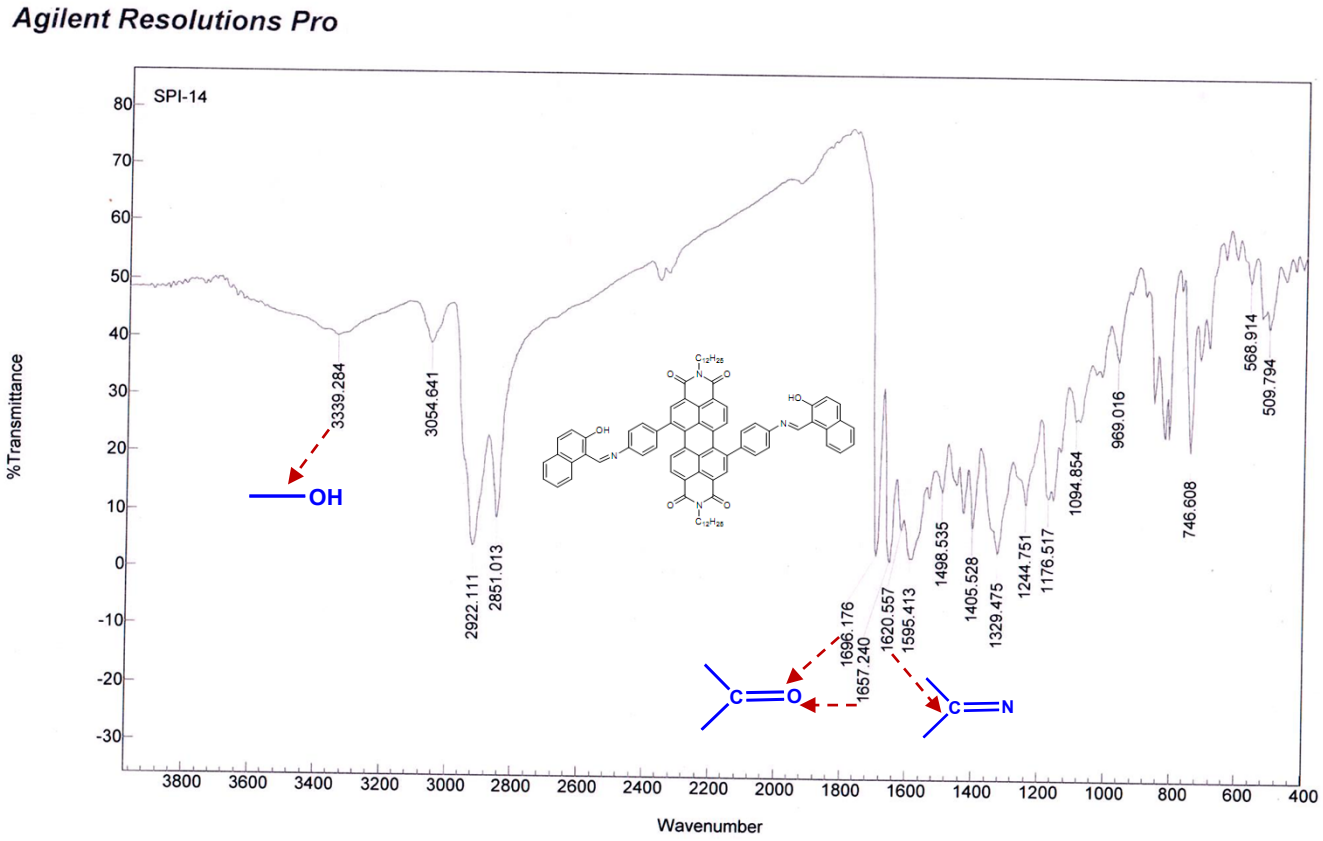

Fig. S33 FT-IR Spectrum of compound **3**.

Fig. S34 ^{1}H NMR spectrum of derivative **4a** in $CDCl_3$

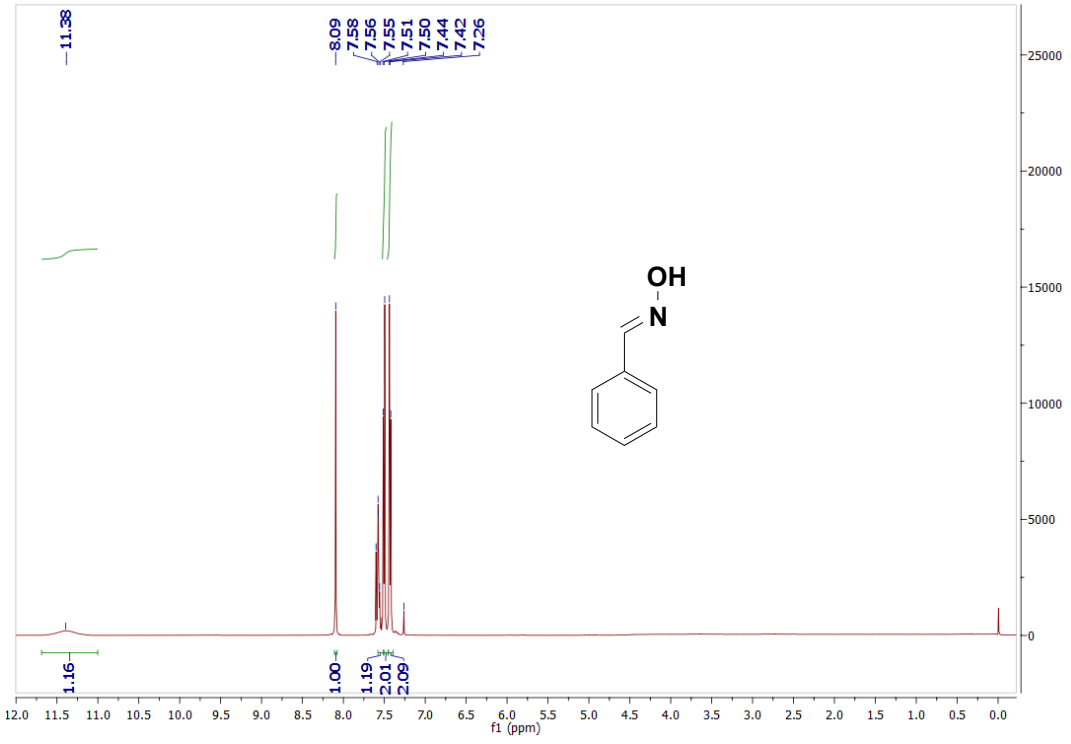

Fig. S35 ^{13}C NMR spectrum of derivative **4a** in $CDCl_3$

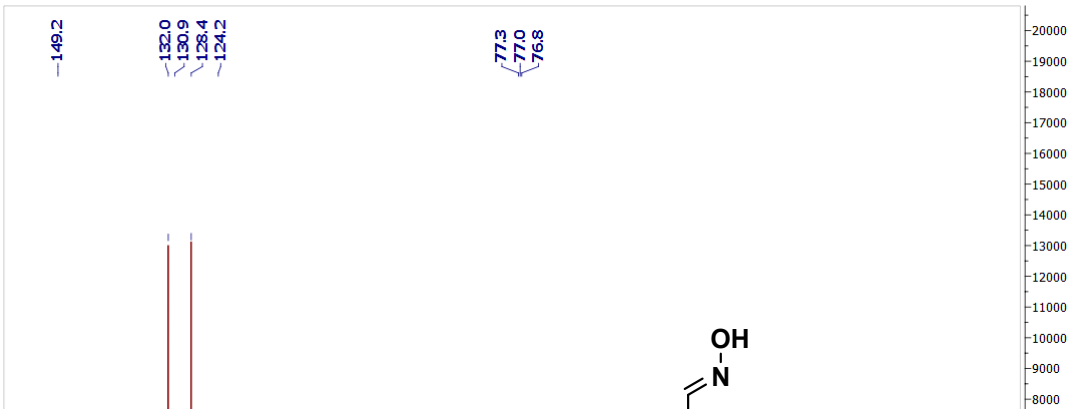

Fig. S36 ^{1}H NMR spectrum of derivative **5a** in $CDCl_3$

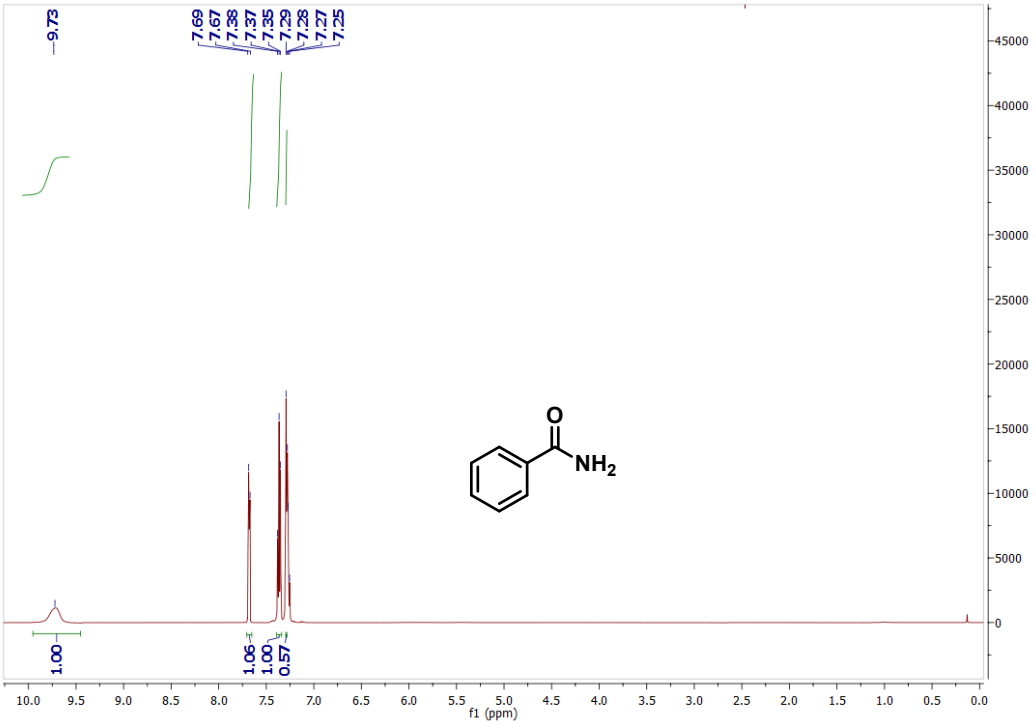

Fig. S37 ^{13}C NMR spectrum of derivative **5a** in $CDCl_3$

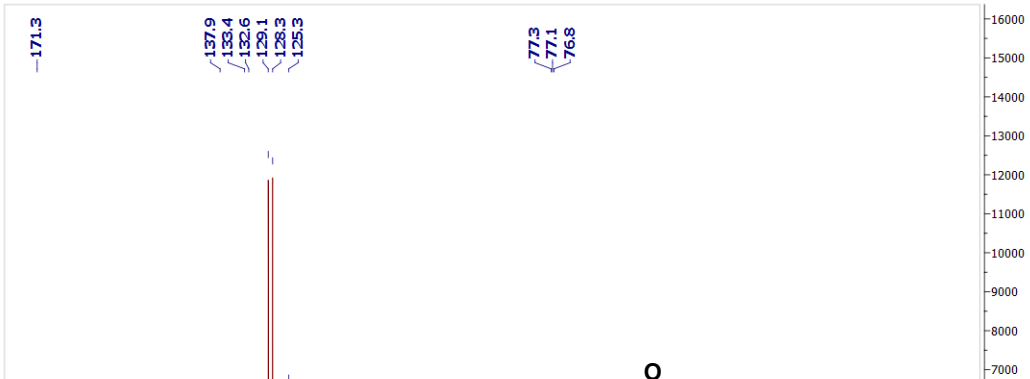

Fig. S38 ^{1}H NMR spectrum of derivative **4b** in $CDCl_3$

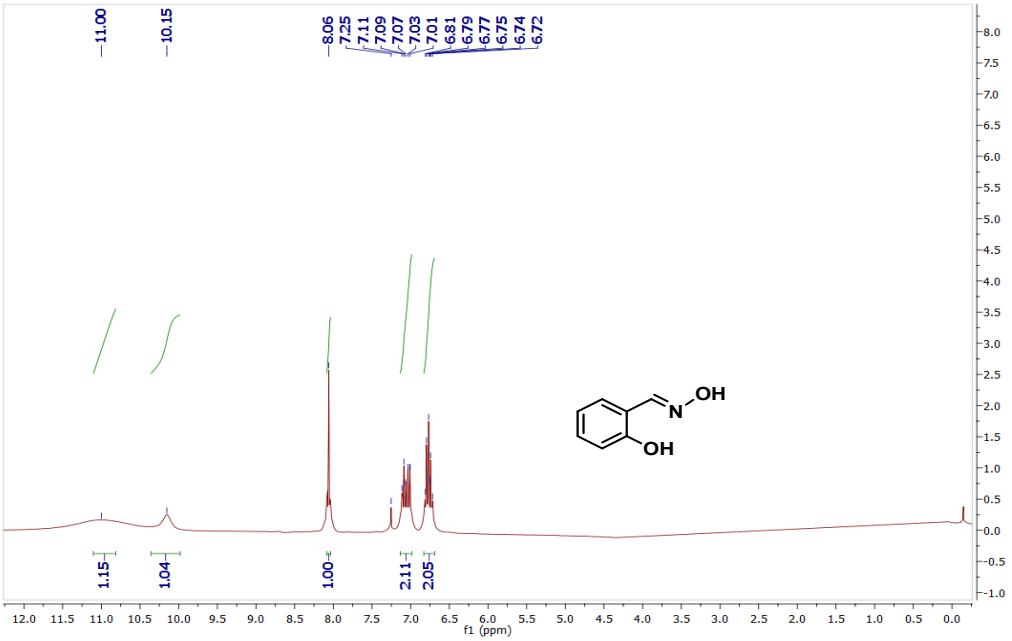

Fig. S39 ^{13}C NMR spectrum of derivative **4b** in $CDCl_3$

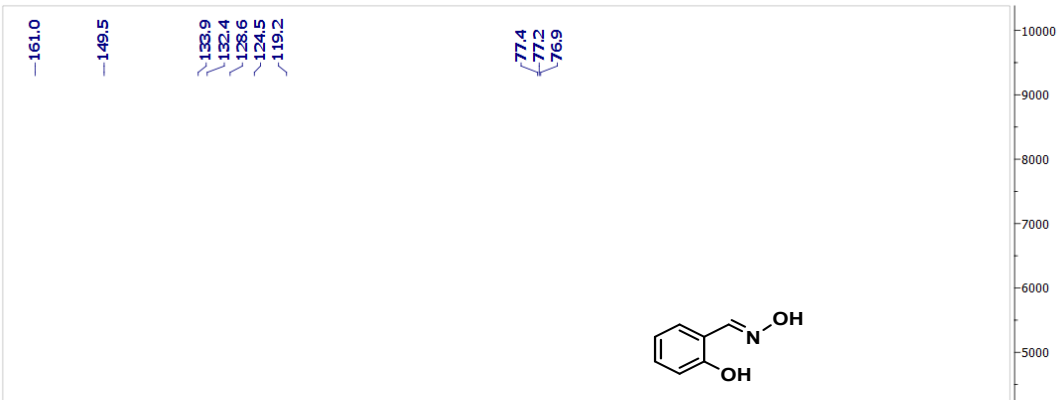

Fig. S40 ^{1}H NMR spectrum of derivative **5b** in $CDCl_3$

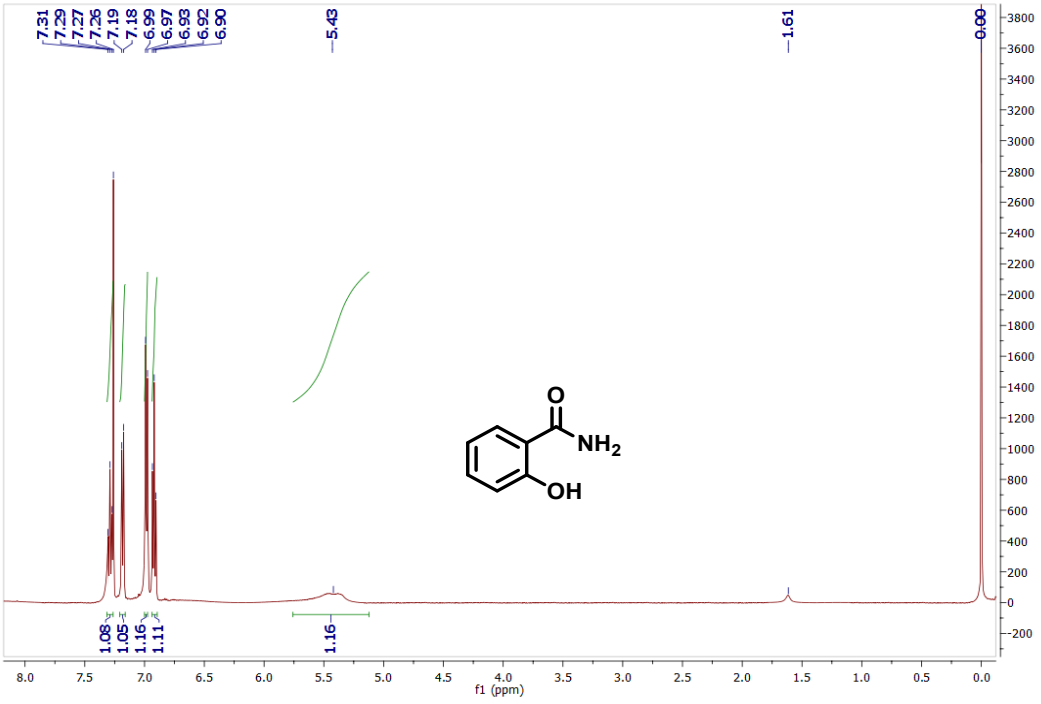

Fig. S41 ^{13}C NMR spectrum of derivative **5b** in $CDCl_3$

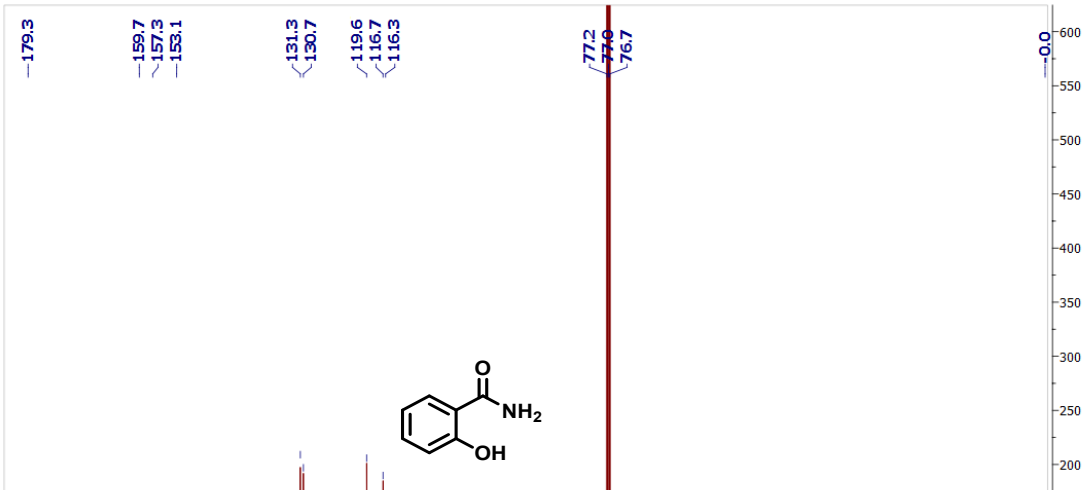

Fig. S42 ^{1}H NMR spectrum of derivative **4c** in $CDCl_3$

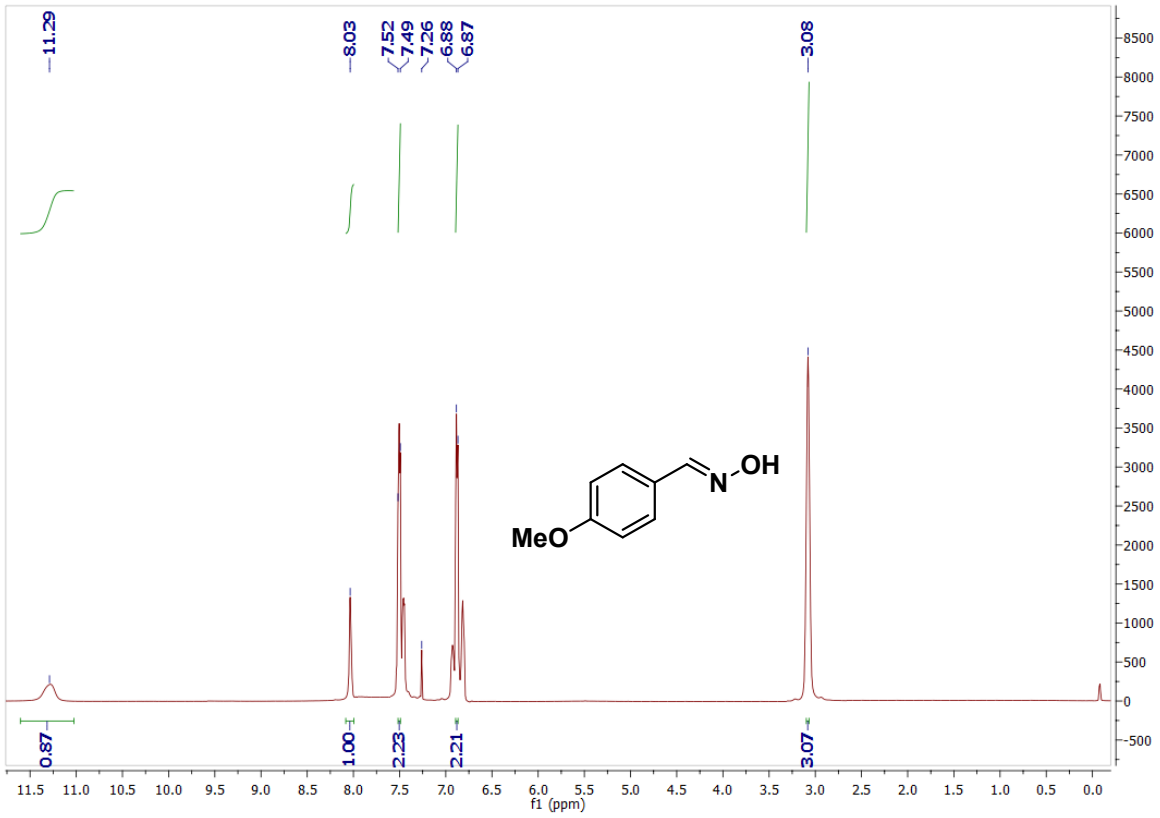

Fig. S43 ^{13}C NMR spectrum of derivative **4c** in $CDCl_3$

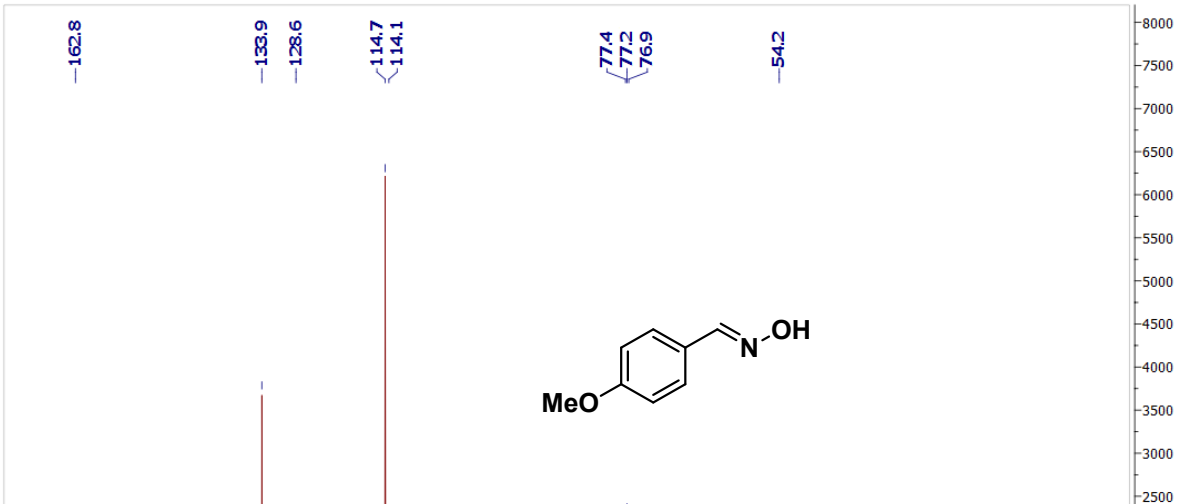

Fig. S44 ^{1}H NMR spectrum of derivative **5c** in $CDCl_3$

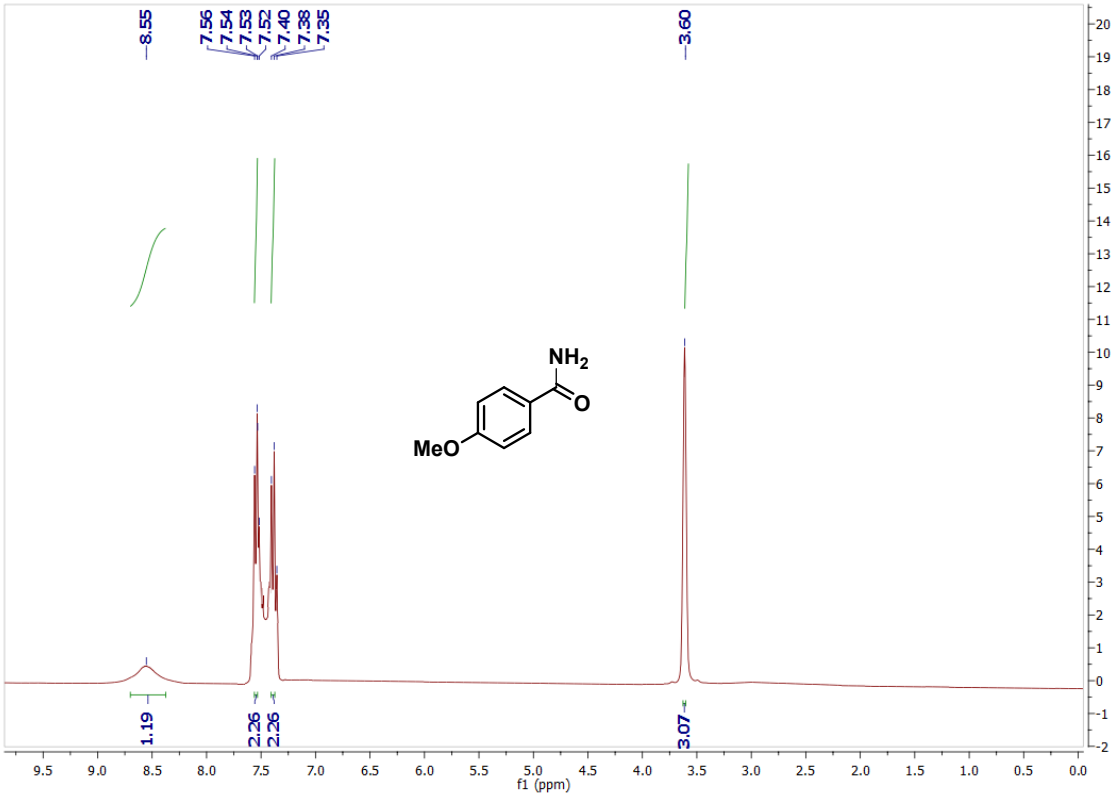

Fig. S45 ^{13}C NMR spectrum of derivative **5c** in $CDCl_3$

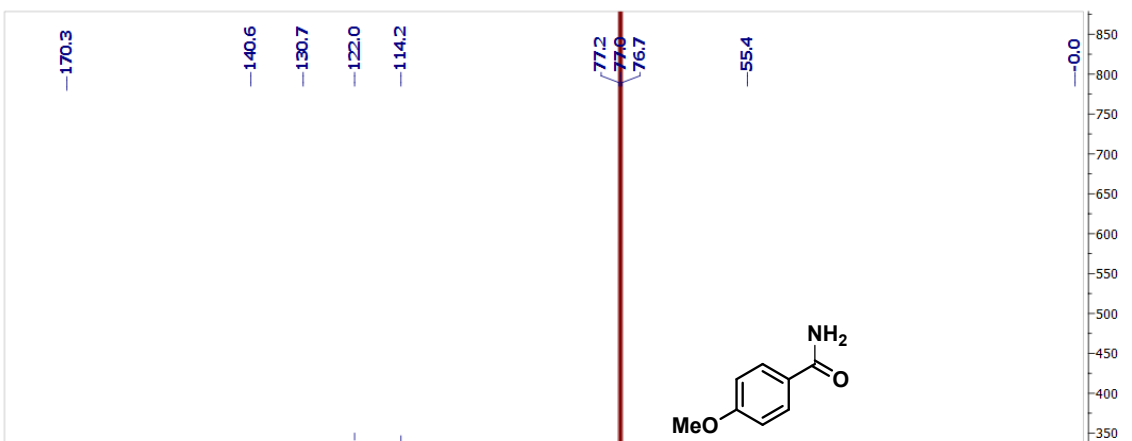

Fig. S46 ^{1}H NMR spectrum of derivative **4d** in $CDCl_3$

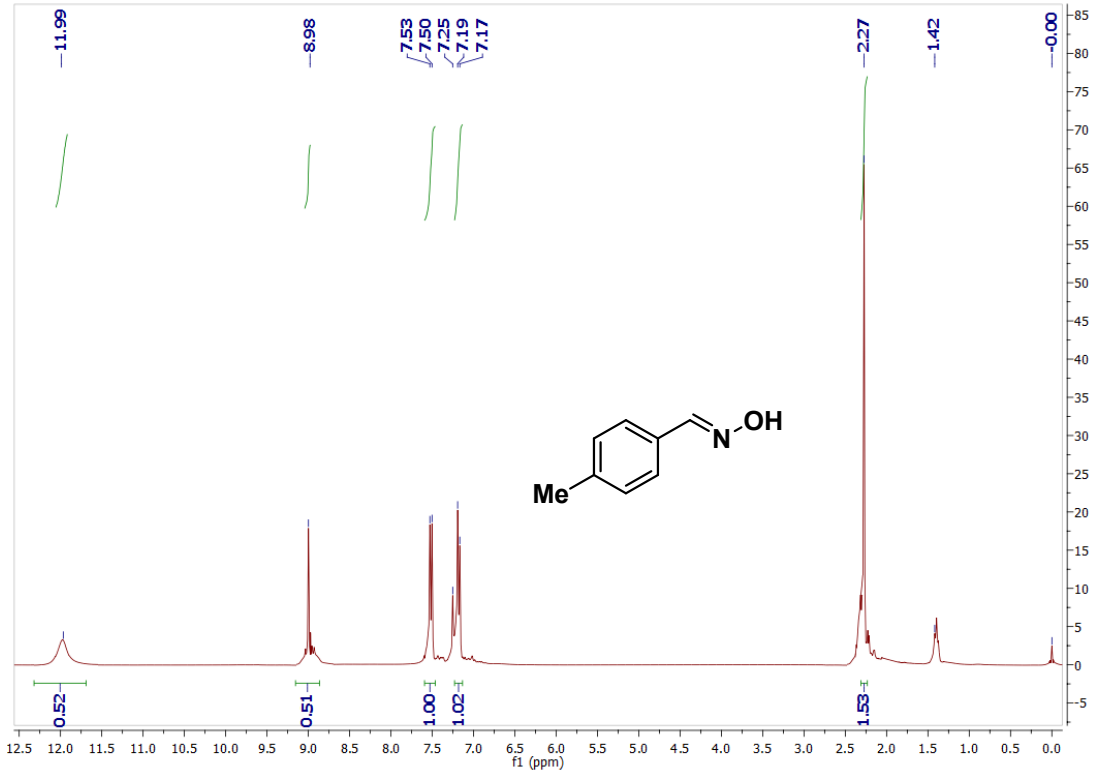

Fig. S47 ^{13}C NMR spectrum of derivative **4d** in $CDCl_3$

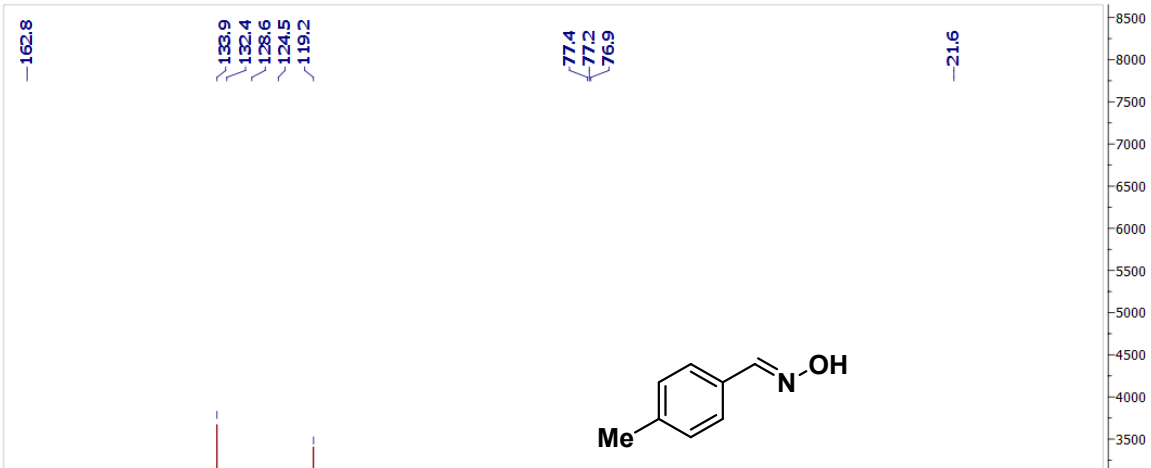

Fig. S48 ^{1}H NMR spectrum of derivative **5d** in $CDCl_3$

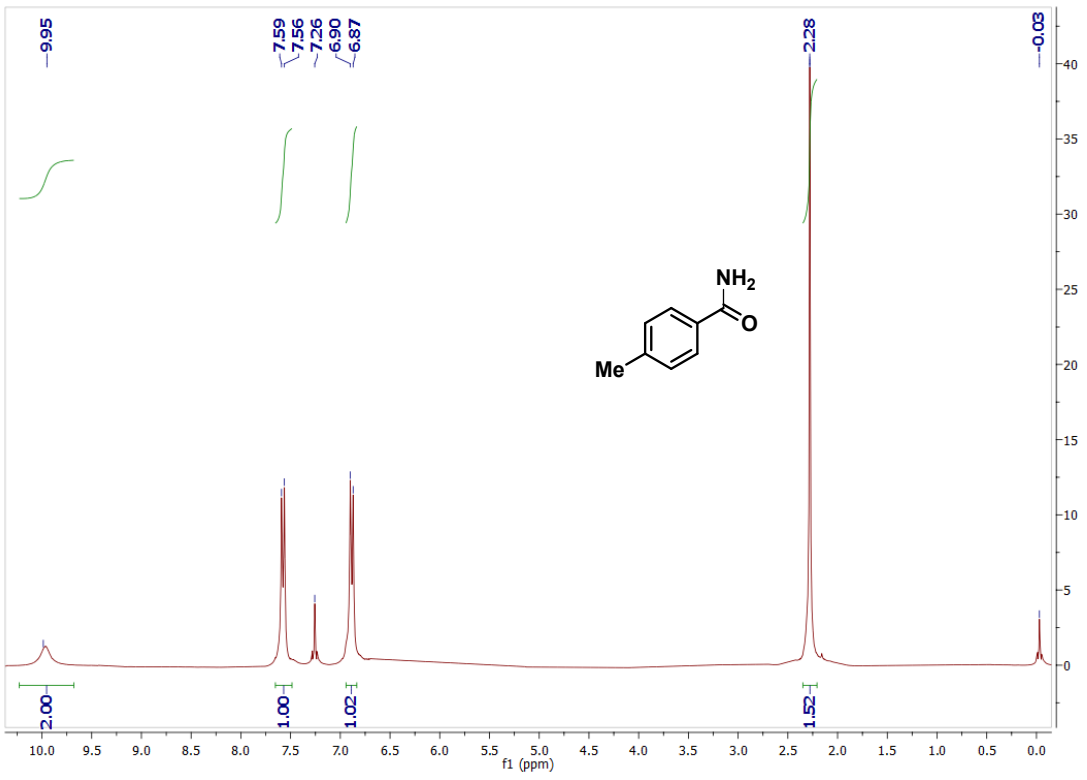

Fig. S49 ^{13}C NMR spectrum of derivative **5d** in $CDCl_3$

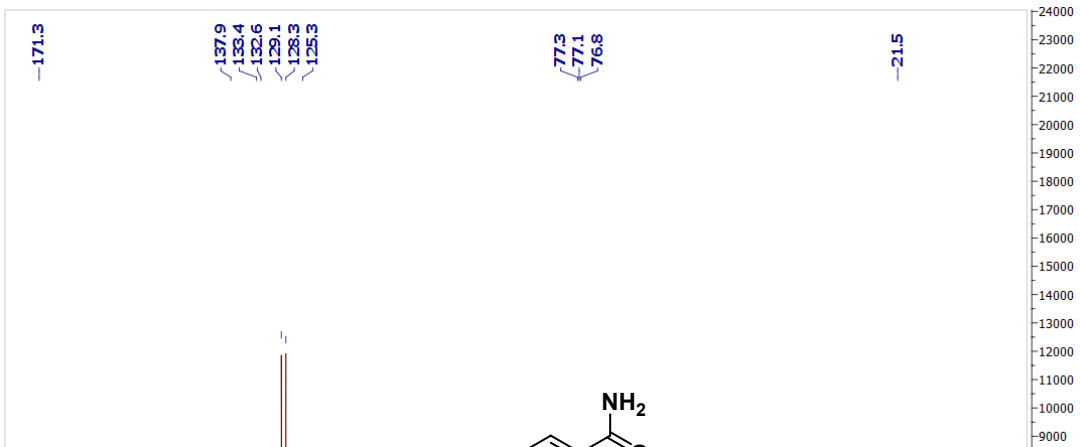

Fig. S50 ^{1}H NMR spectrum of derivative **4e** in $CDCl_3$

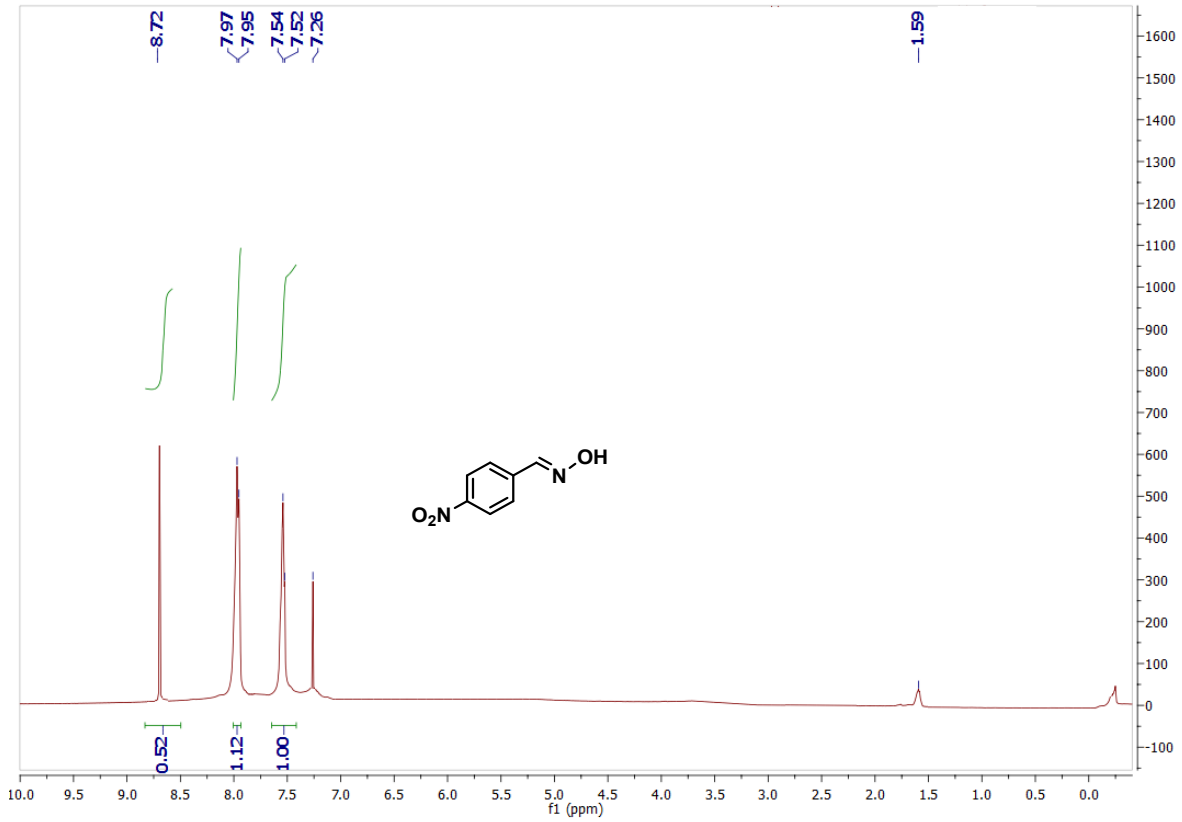

Fig. S51 ^{13}C NMR spectrum of derivative **4e** in $CDCl_3$

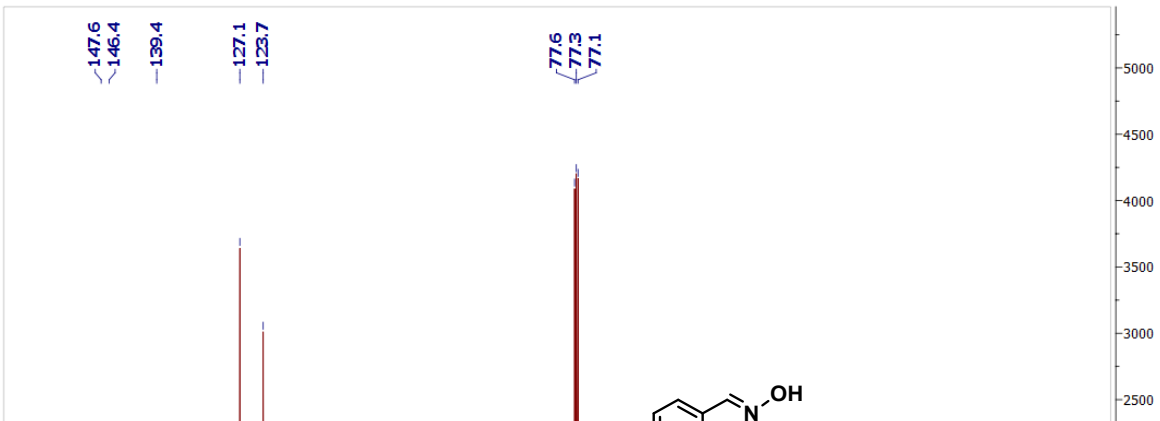

Fig. S52 ^{1}H NMR spectrum of derivative **5e** in $CDCl_3$

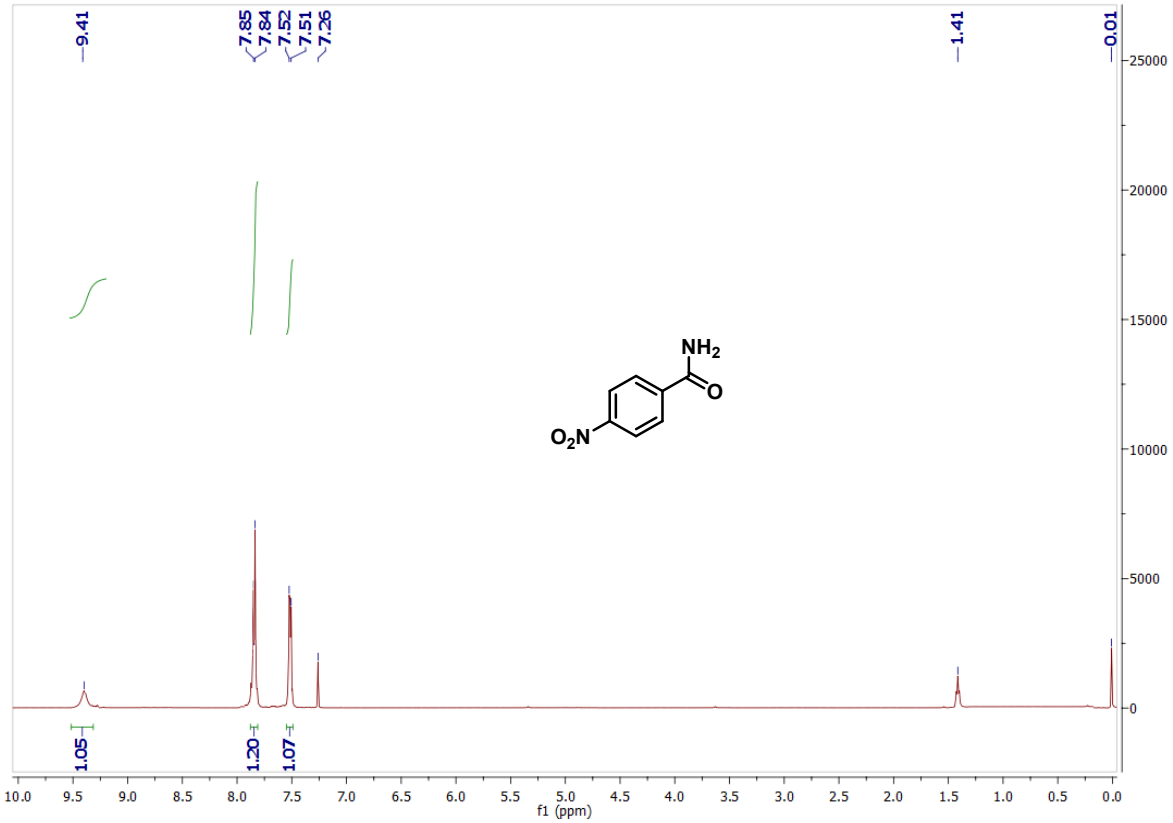

Fig. S53 ^{13}C NMR spectrum of derivative **5e** in $CDCl_3$

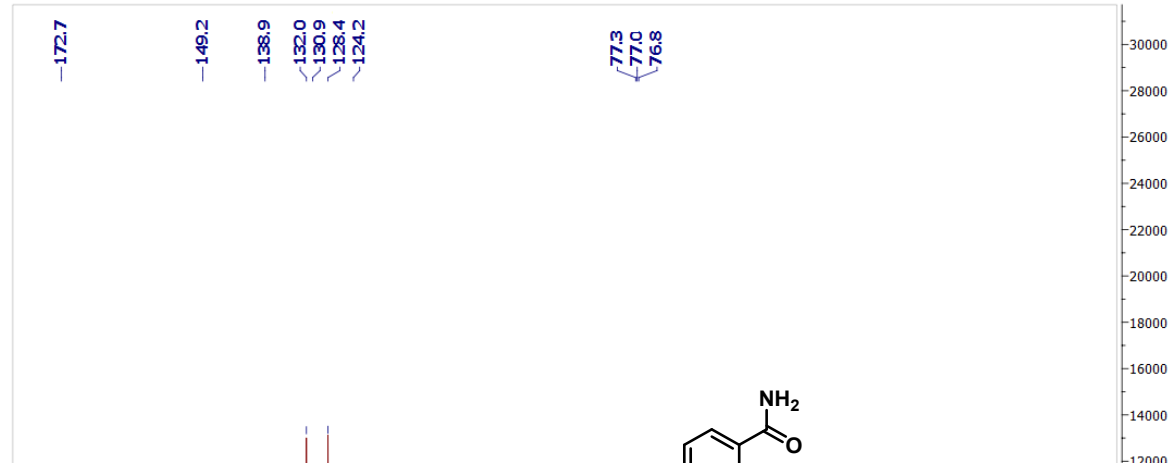

Fig. S54 ^{1}H NMR spectrum of derivative **4f** in $CDCl_3$

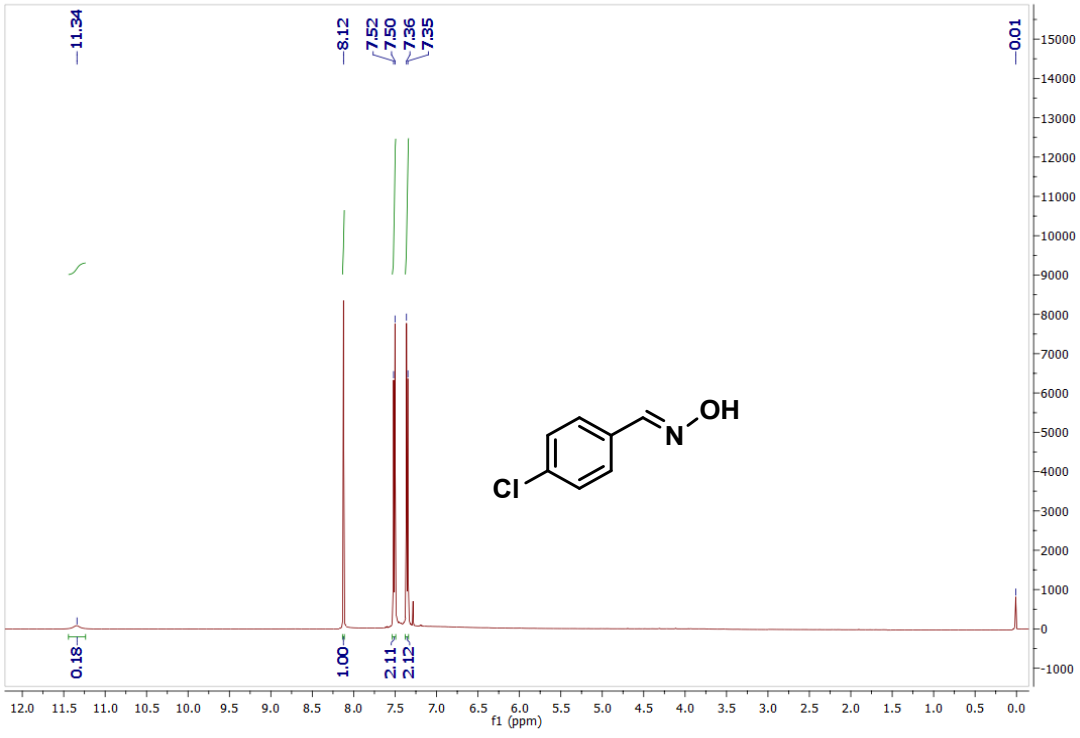

Fig. S55 ^{13}C NMR spectrum of derivative **4f** in $CDCl_3$

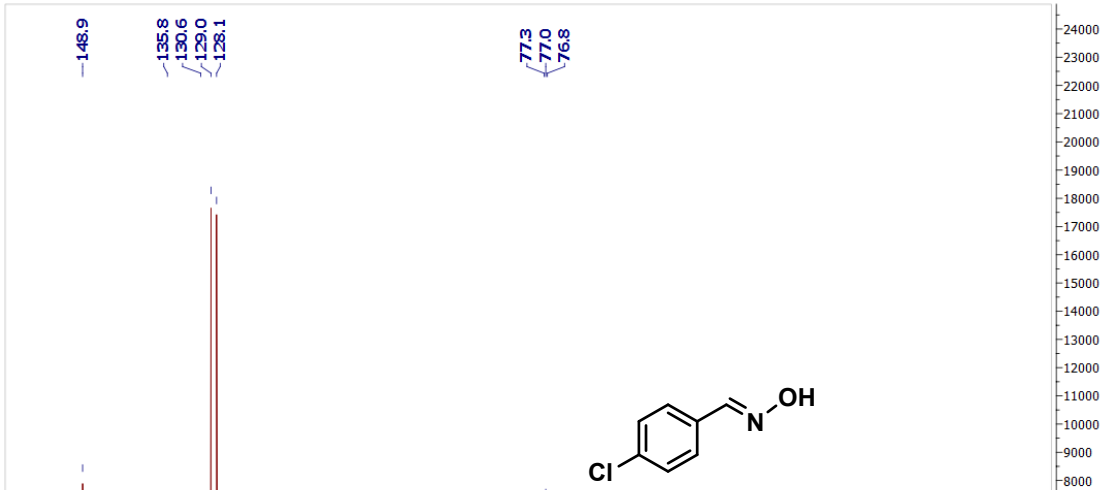

Fig. S56 ^{1}H NMR spectrum of derivative **5f** in $CDCl_3$

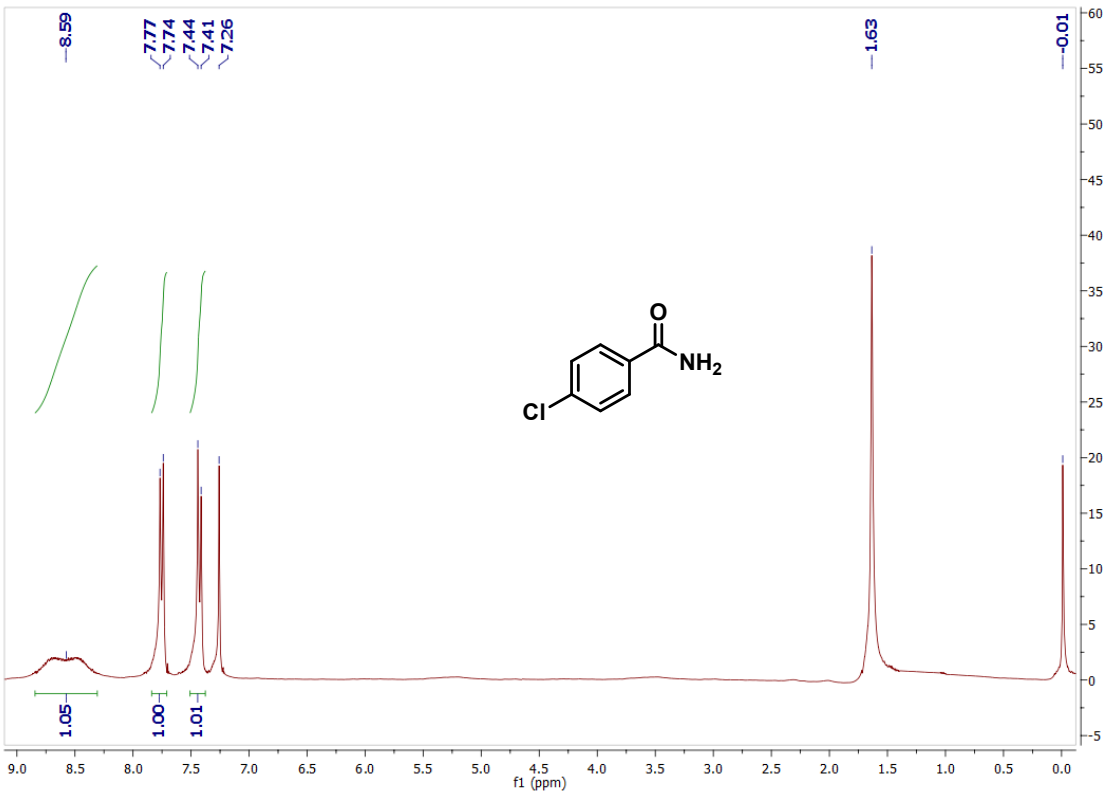

Fig. S57 ^{13}C NMR spectrum of derivative **5f** in $CDCl_3$

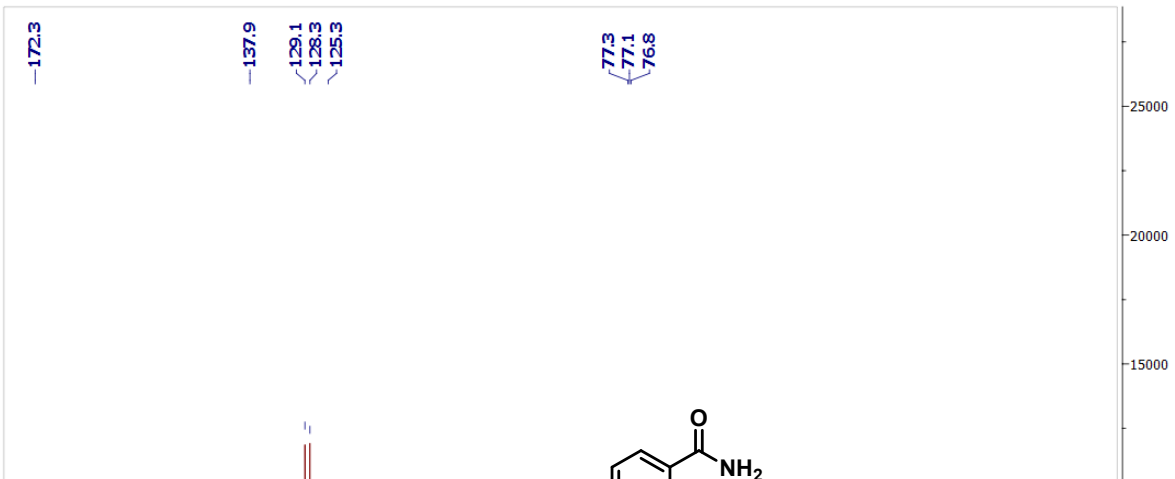

Fig. S58 ^{1}H NMR spectrum of derivative **6a** in $CDCl_3$

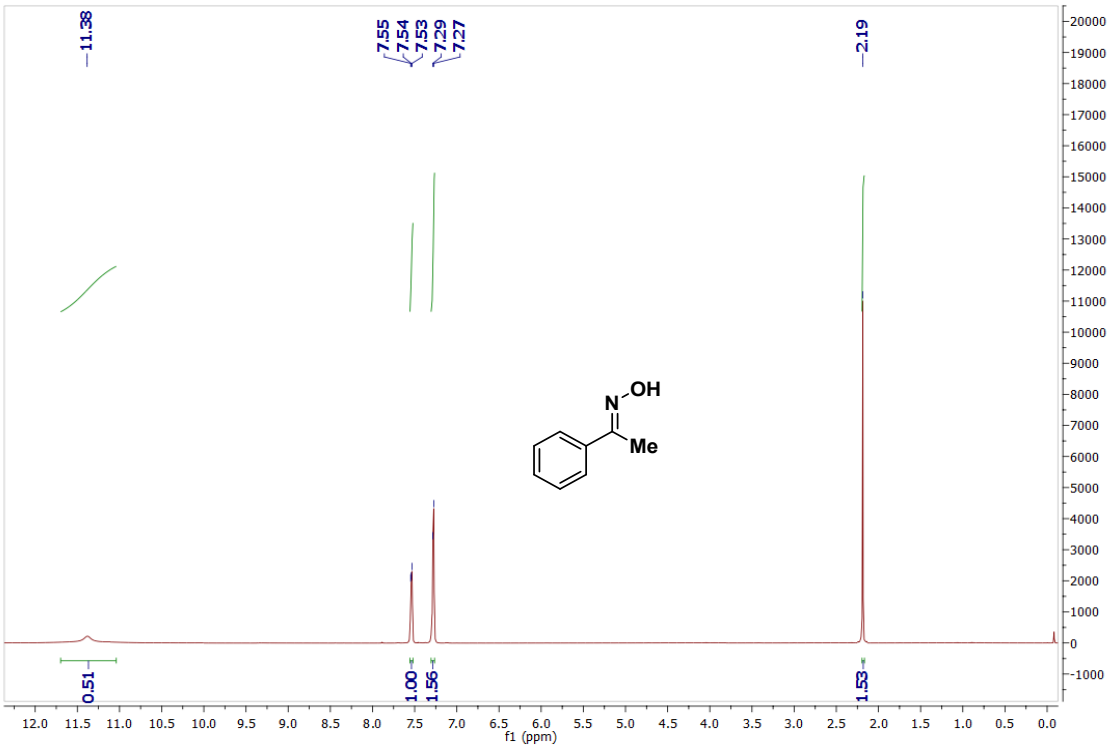

Fig. S59 ^{13}C NMR spectrum of derivative **6a** in $CDCl_3$

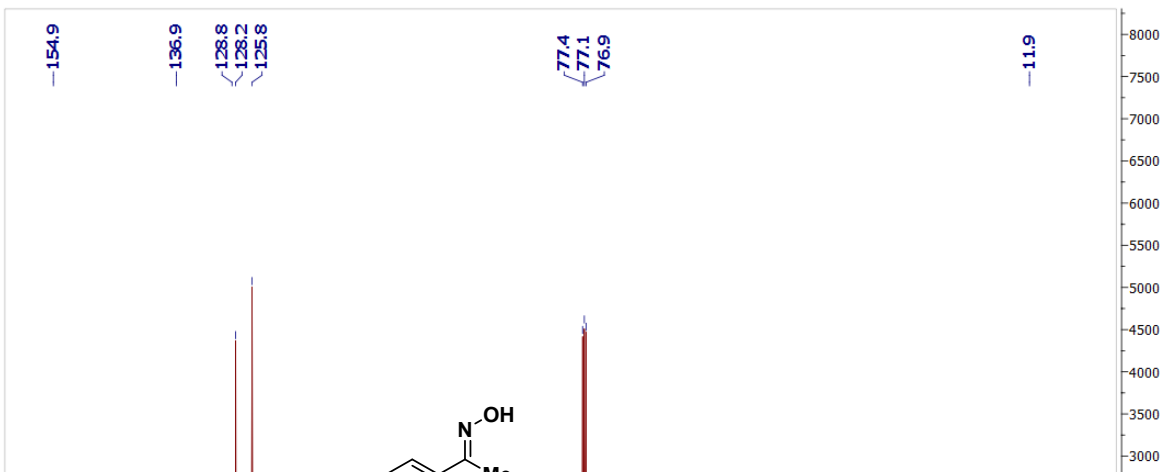

Fig. S60 ^{1}H NMR spectrum of derivative **7a** in $CDCl_3$

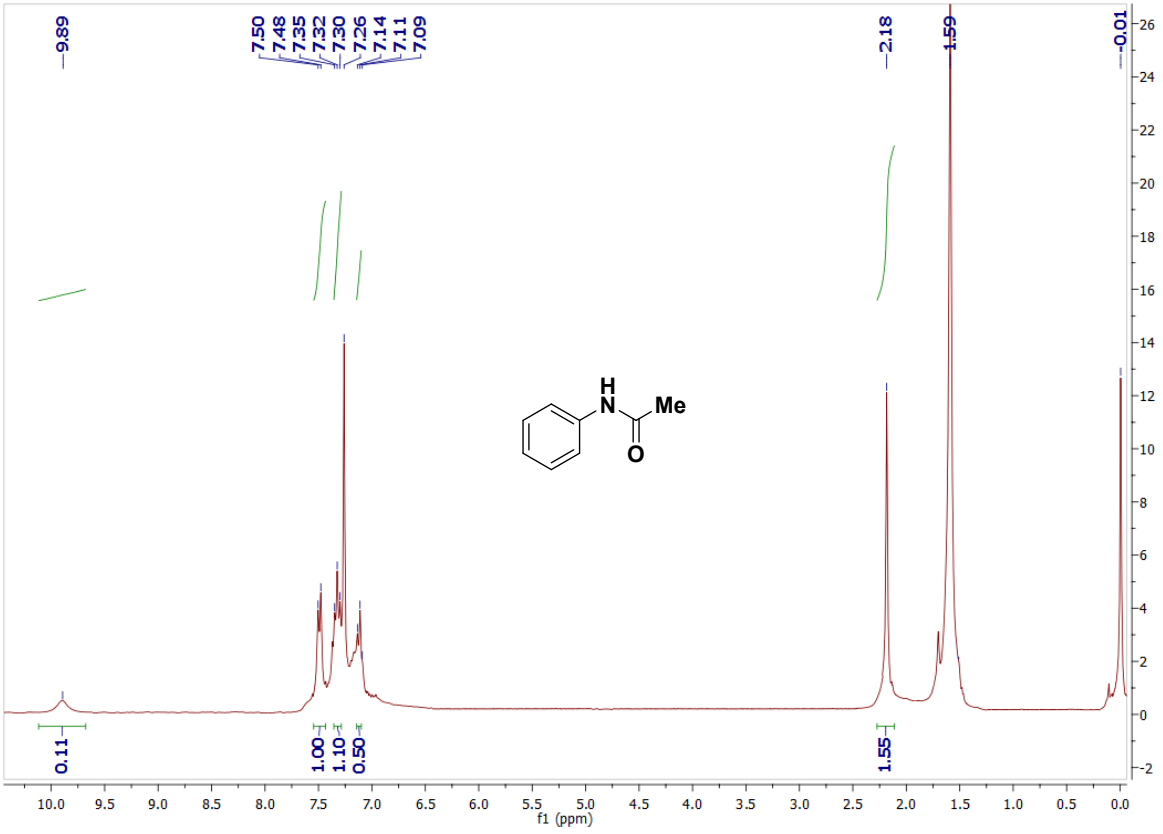

Fig. S61 ^{1}H NMR spectrum of derivative **7a** in $CDCl_3$

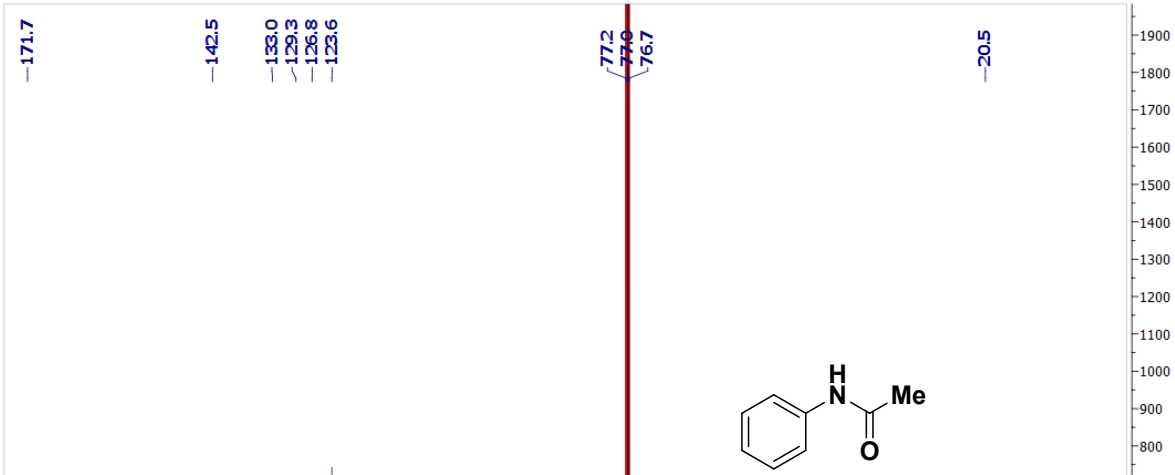

Fig. S62 ^{1}H NMR spectrum of derivative **6b** in $CDCl_3$

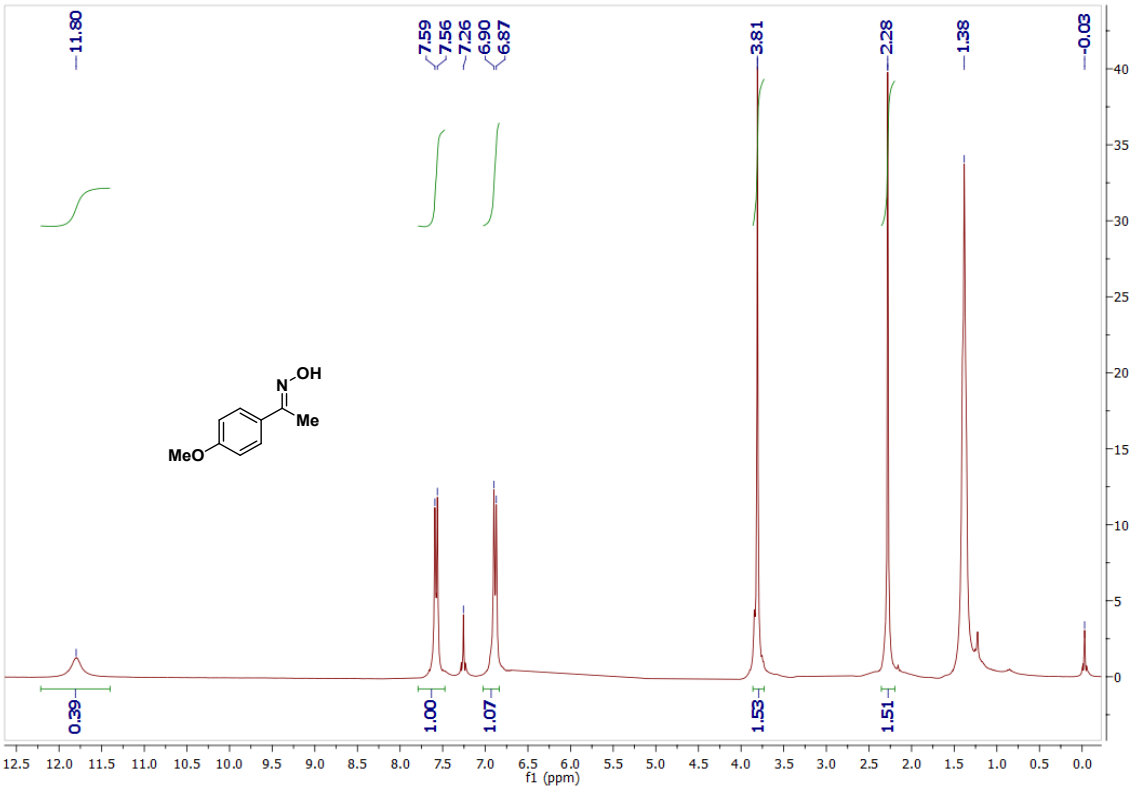

Fig. S63 ^{13}C NMR spectrum of derivative **6b** in $CDCl_3$

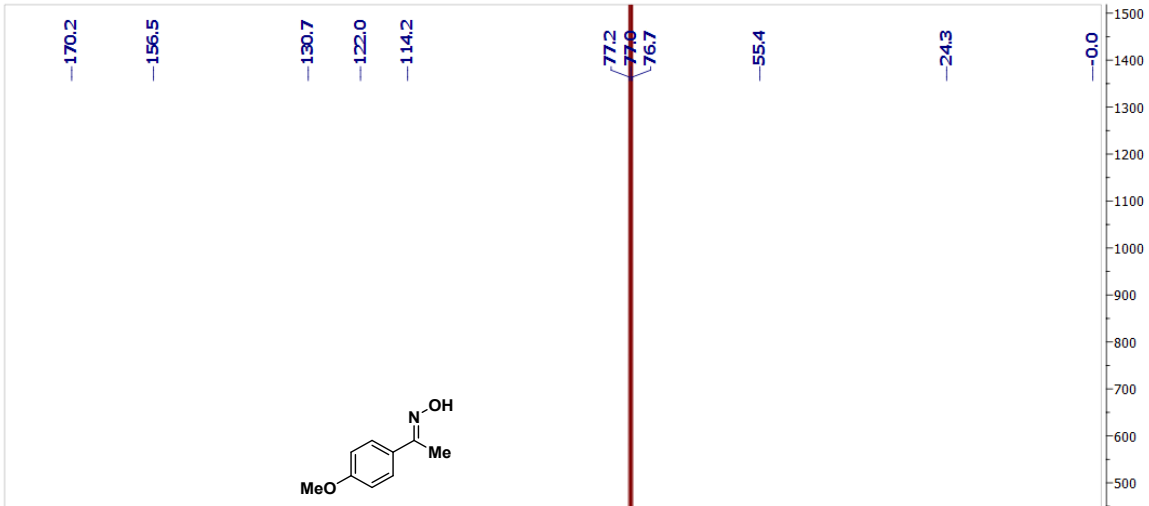

Fig. S64 ^{1}H NMR spectrum of derivative **7b** in $CDCl_3$

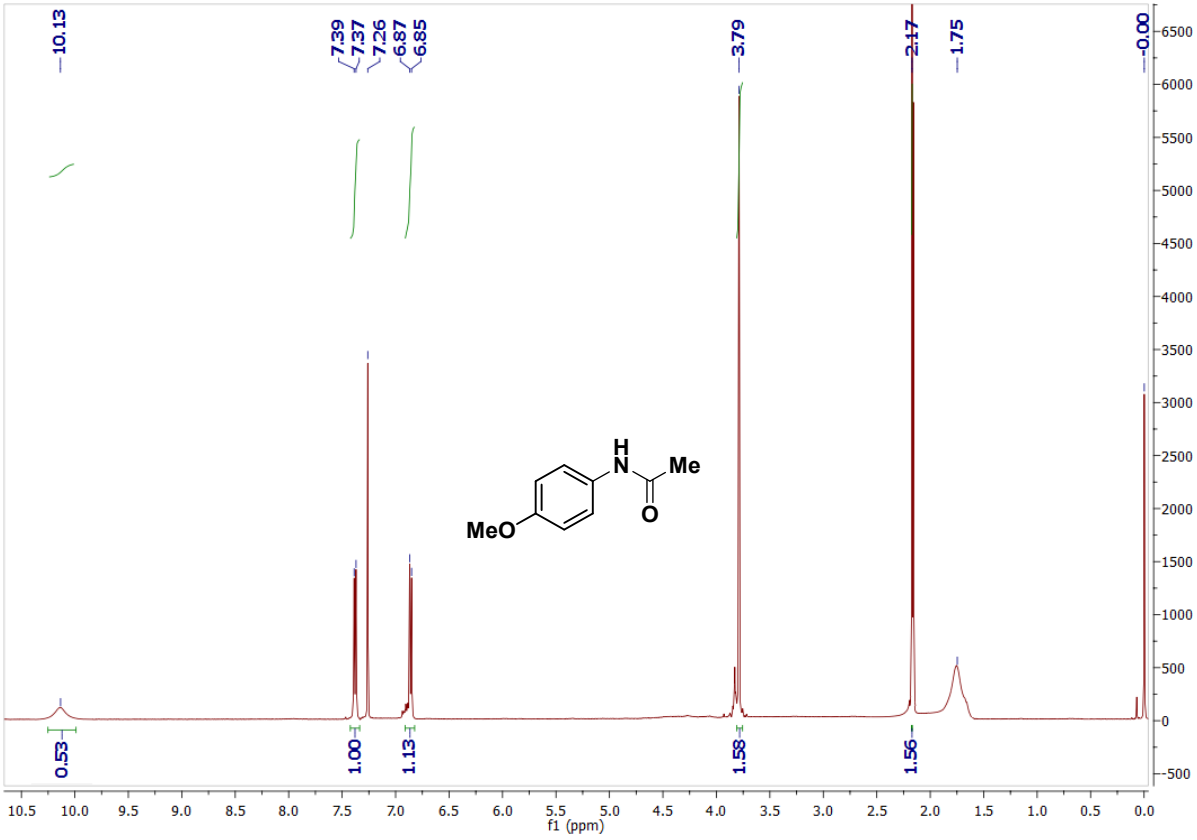

Fig. S65 ^{13}C NMR spectrum of derivative **7b** in $CDCl_3$

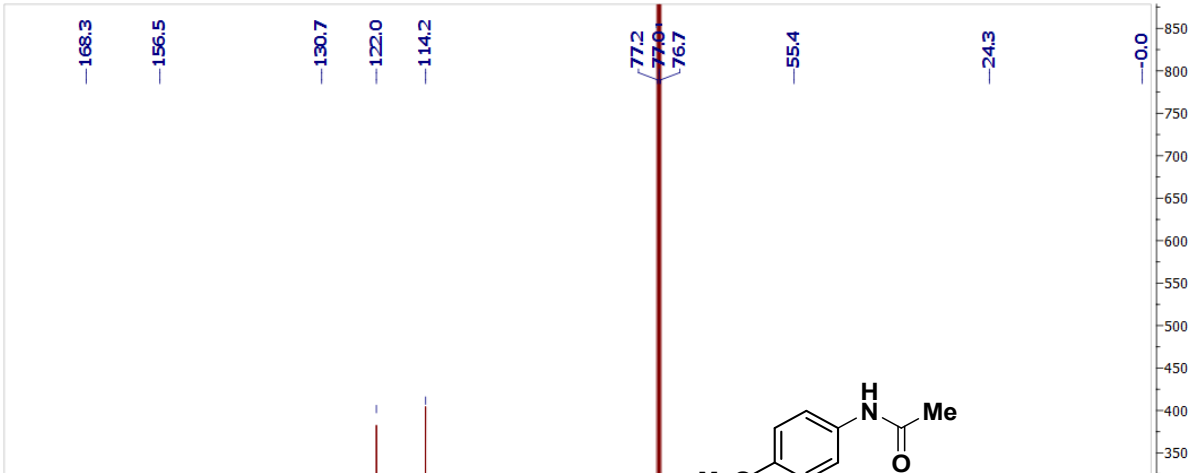

Fig. S66 ^{1}H NMR spectrum of derivative **6c** in $CDCl_3$

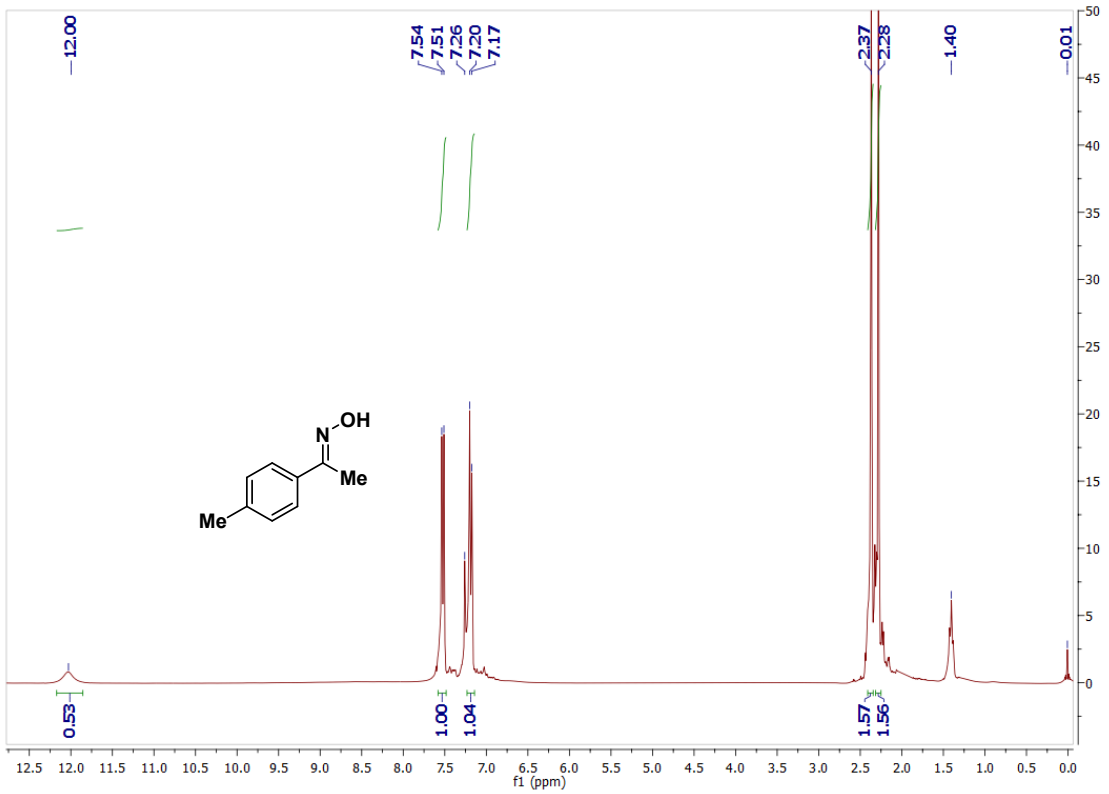

Fig. S67 ^{13}C NMR spectrum of derivative **6c** in $CDCl_3$

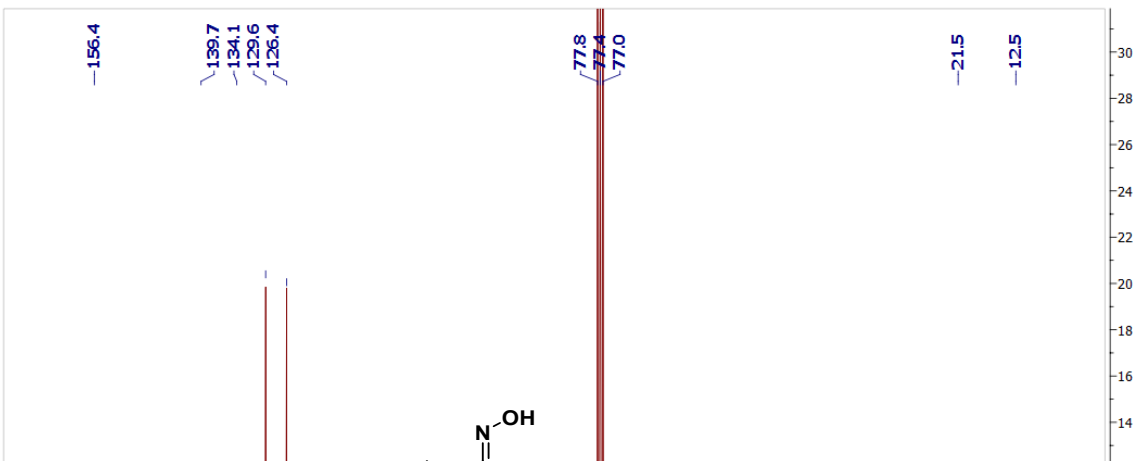

Fig. S68 ^{1}H NMR spectrum of derivative **7c** in $CDCl_3$

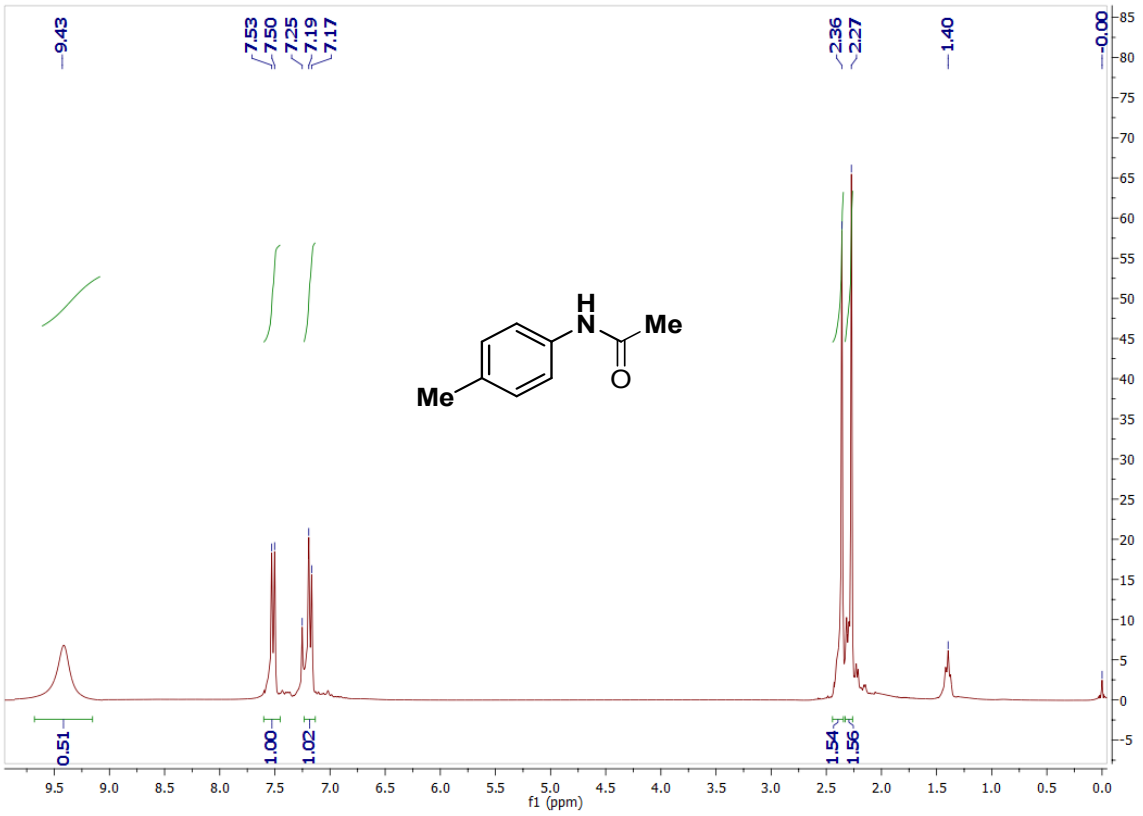

Fig. S69 ^{13}C NMR spectrum of derivative **7c** in $CDCl_3$

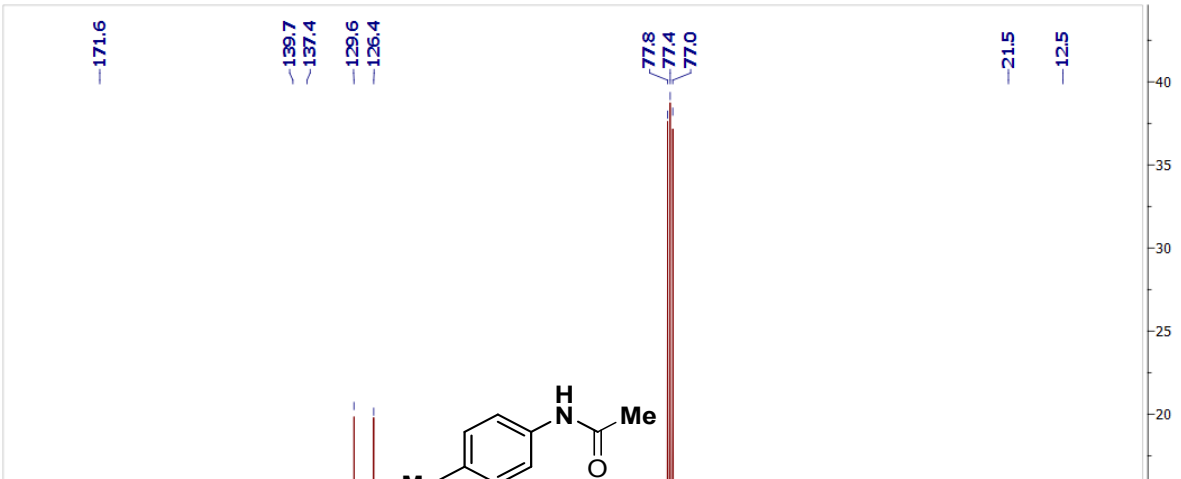

Fig. S70 ^{1}H NMR spectrum of derivative **6d** in $CDCl_3$

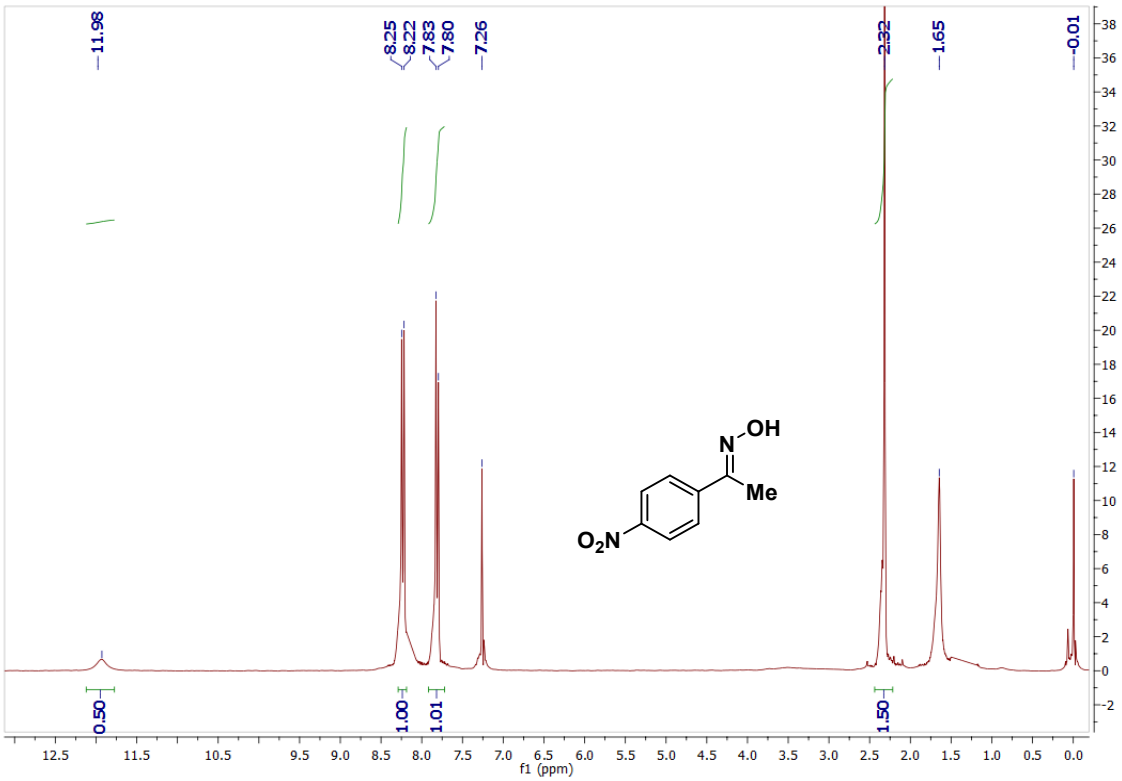

Fig. S71 ^{13}C NMR spectrum of derivative **6d** in $CDCl_3$

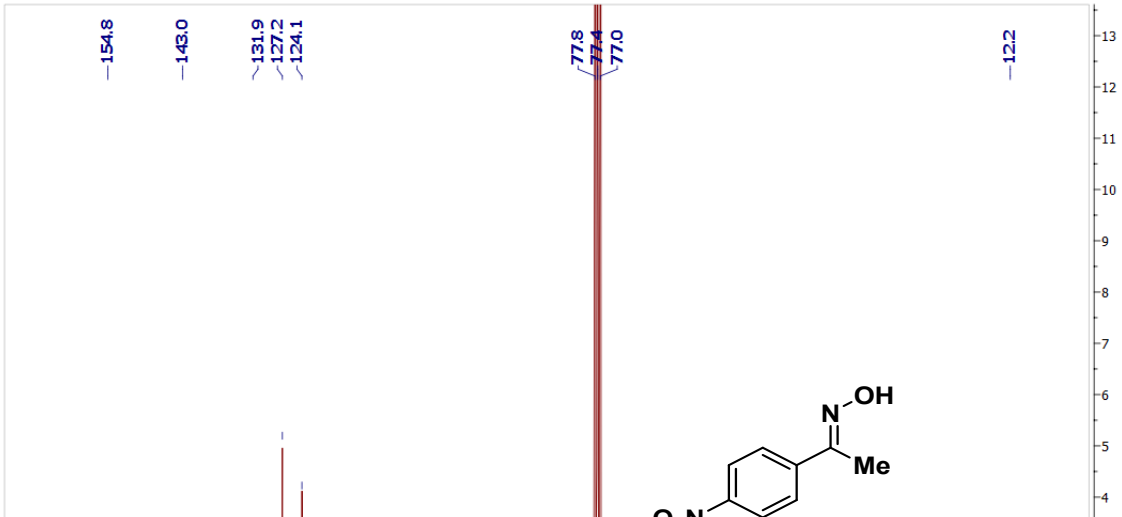

Fig. S72 ^{1}H NMR spectrum of derivative **7d** in $CDCl_3$

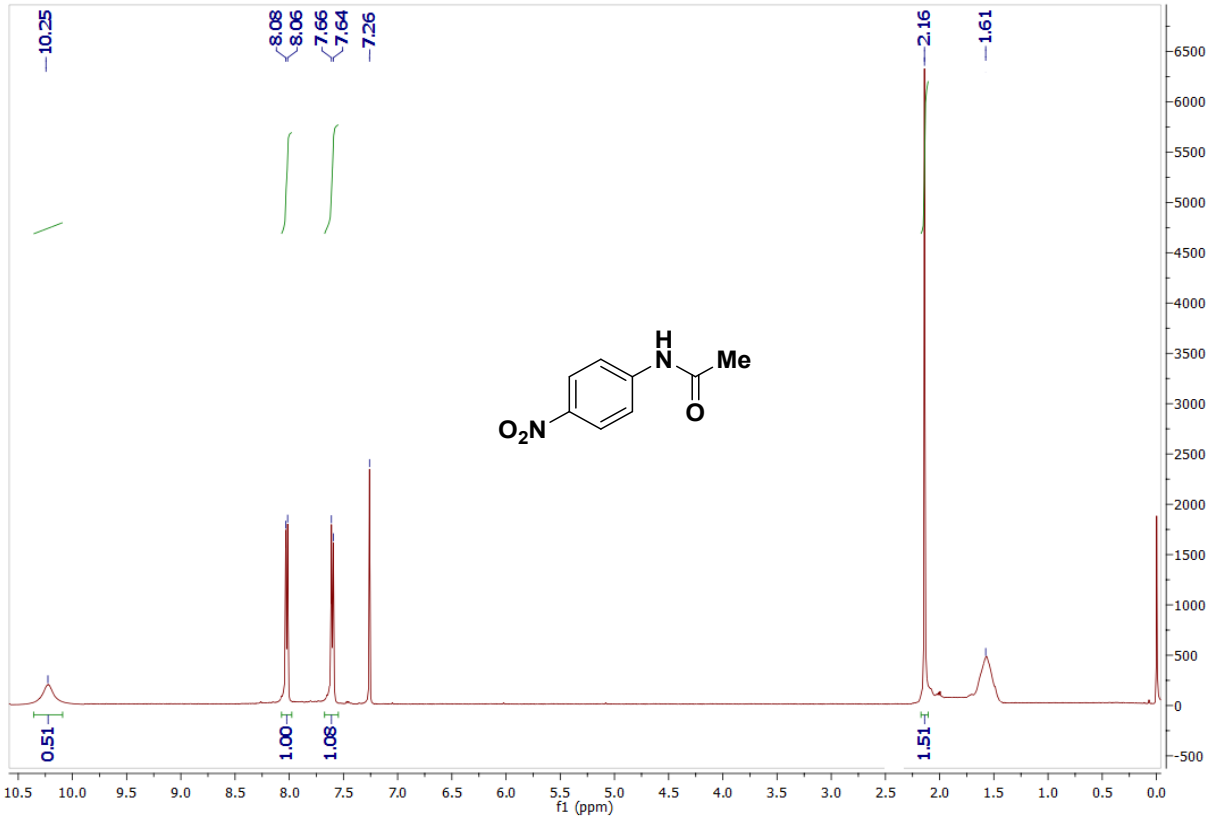

Fig. S73 ^{13}C NMR spectrum of derivative **7d** in $CDCl_3$

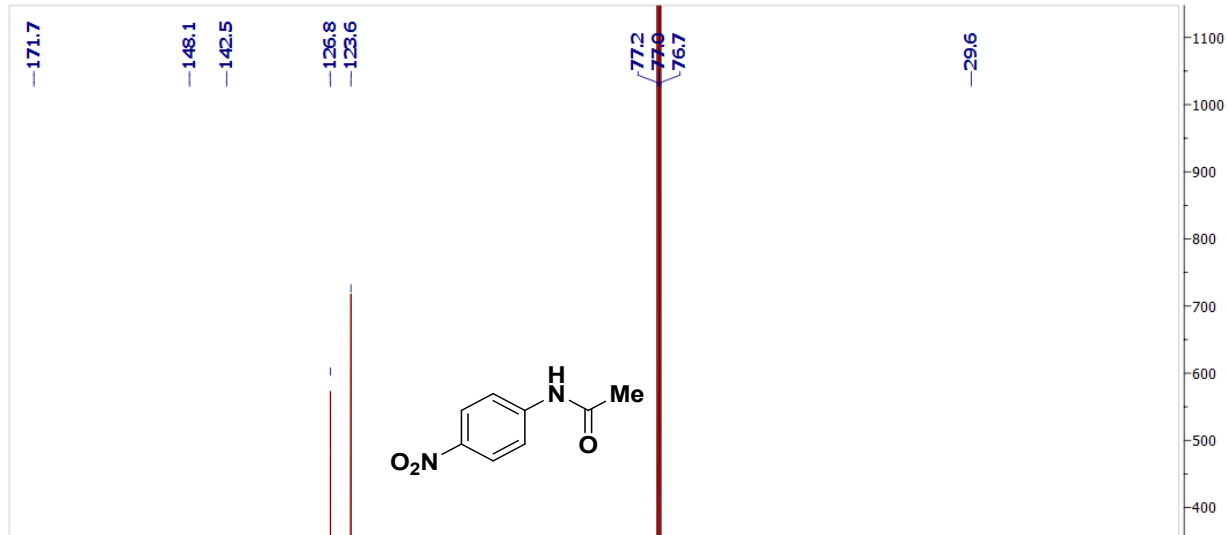

Fig. S74 ^{1}H NMR spectrum of derivative **6e** in $CDCl_3$

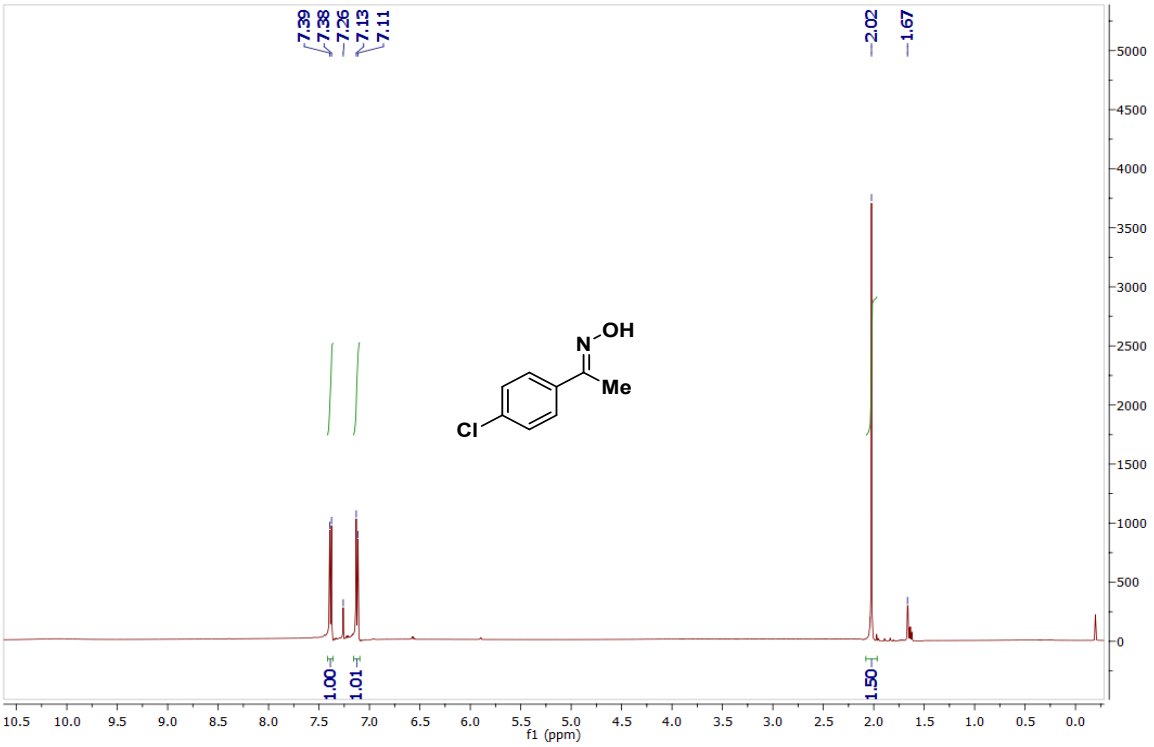

Fig. S75 ^{13}C NMR spectrum of derivative **6e** in $CDCl_3$

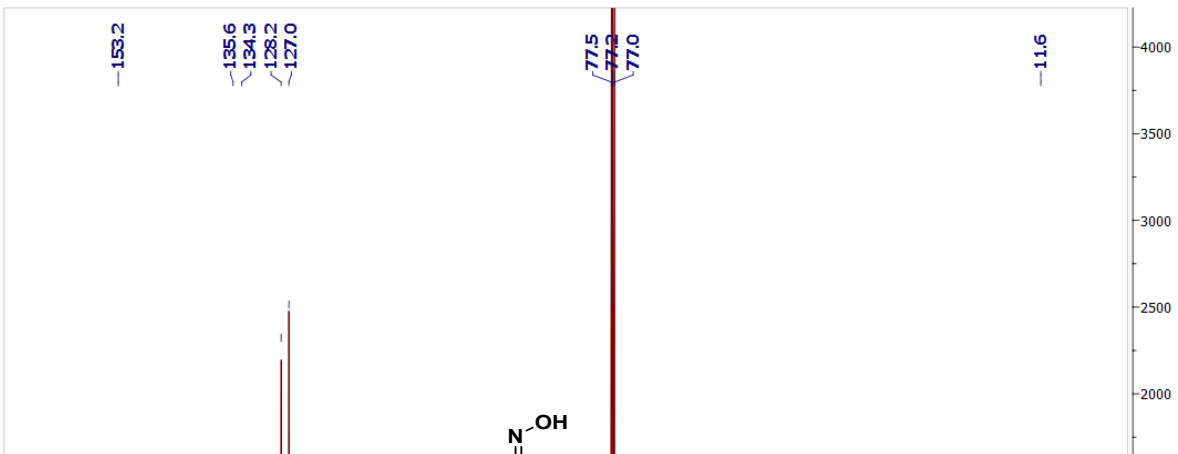

Fig. S76 ^{1}H NMR spectrum of derivative **7e** in $CDCl_3$

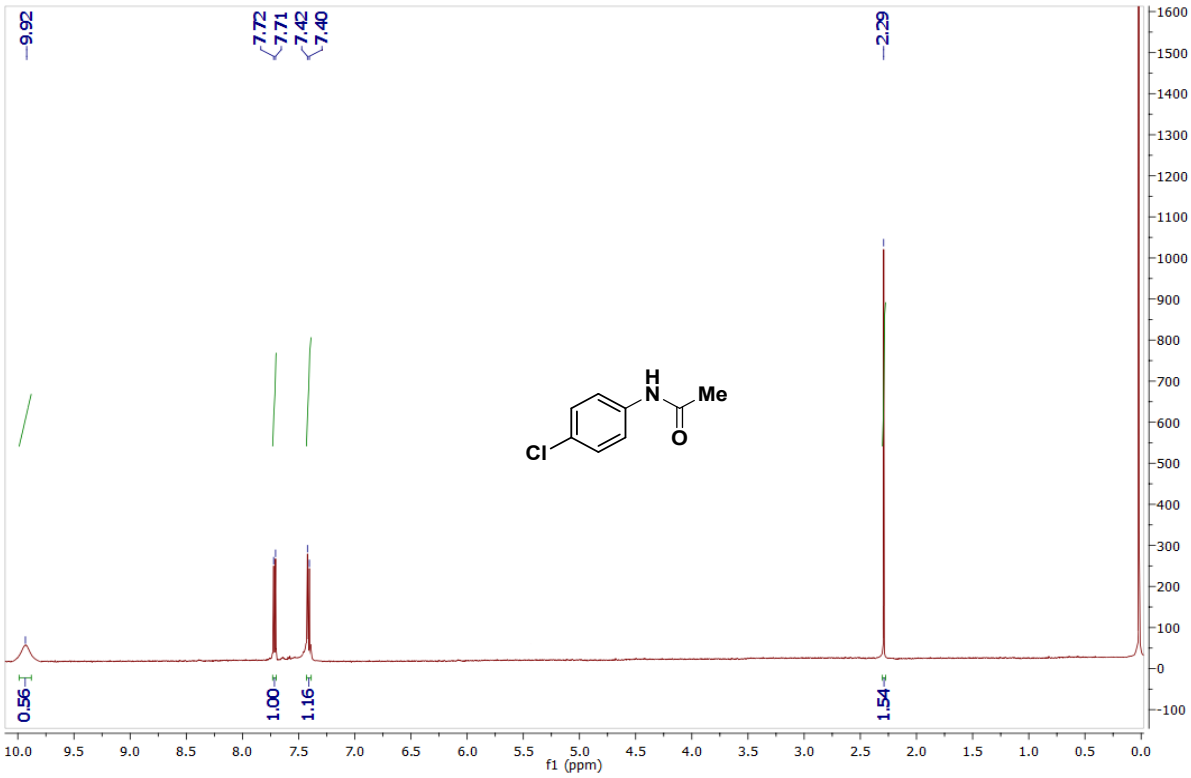

Fig. S77 ^{13}C NMR spectrum of derivative **7e** in $CDCl_3$

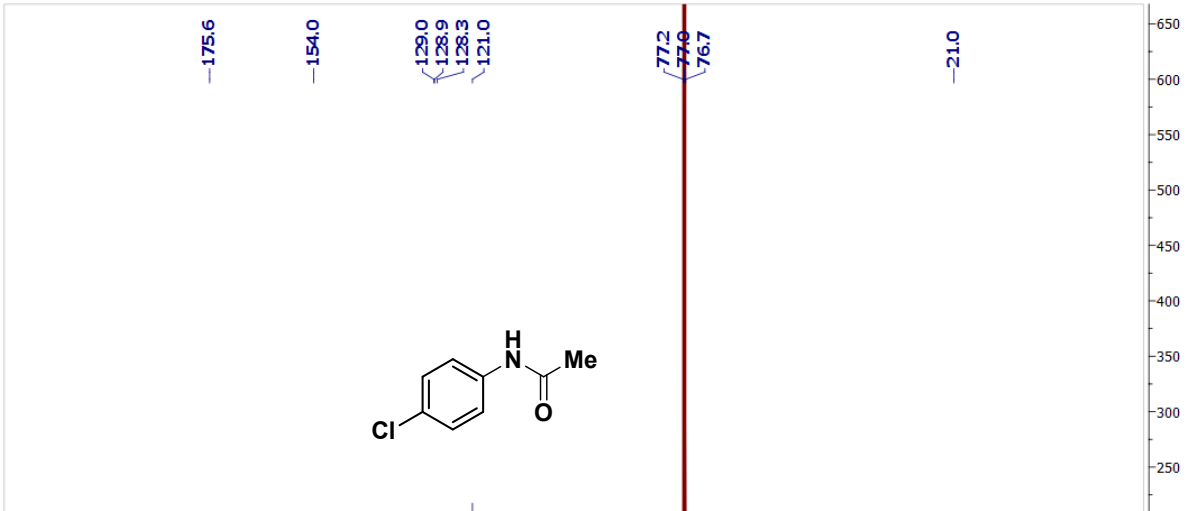

Fig. S78 ^{1}H NMR spectrum of derivative **6f** in $CDCl_3$

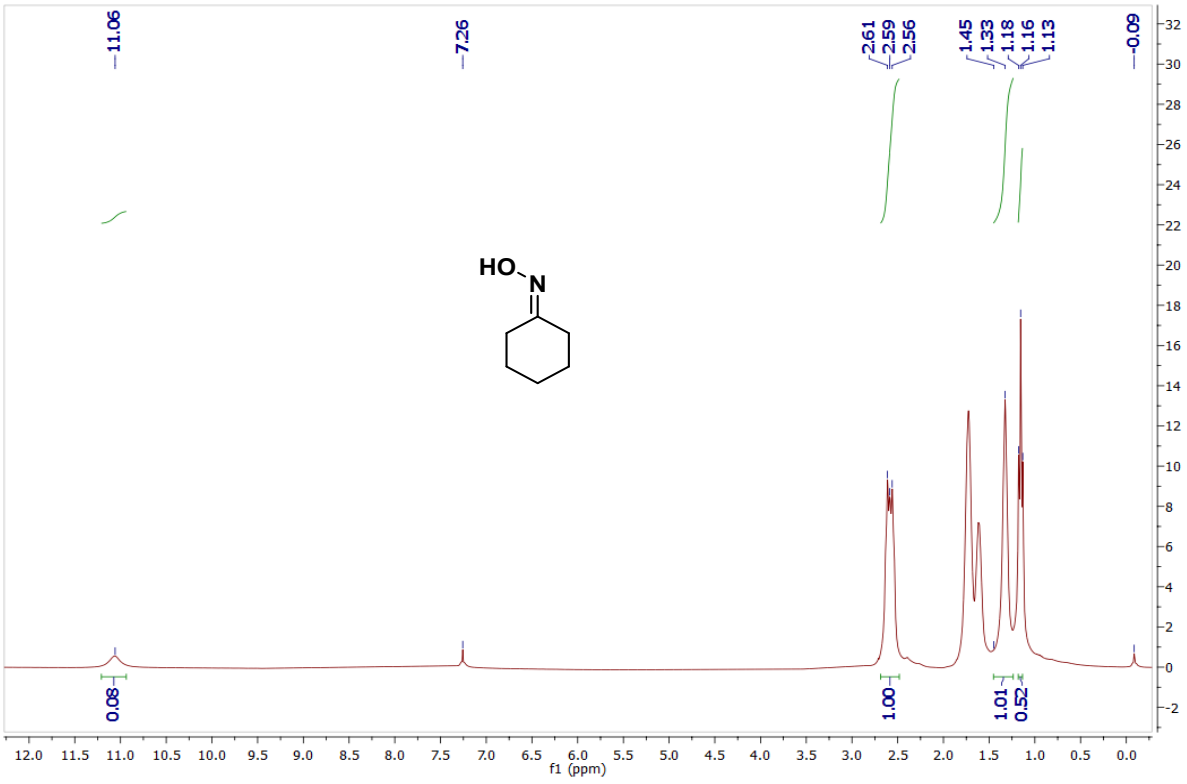

Fig. S79 ^{13}C NMR spectrum of derivative **6f** in $CDCl_3$

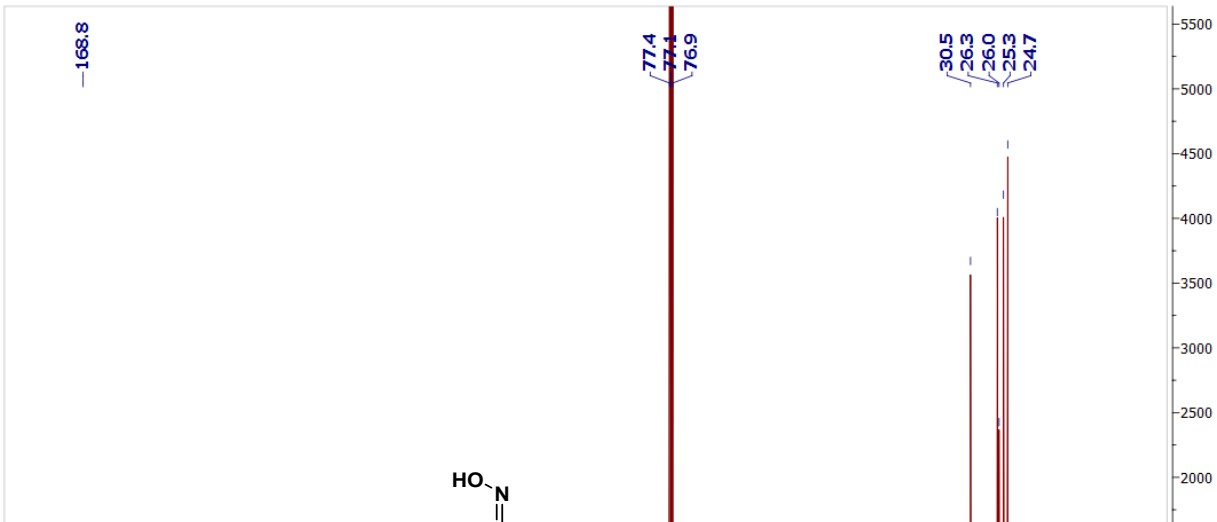

Fig. S80 ^{1}H NMR spectrum of derivative **7f** in $CDCl_3$

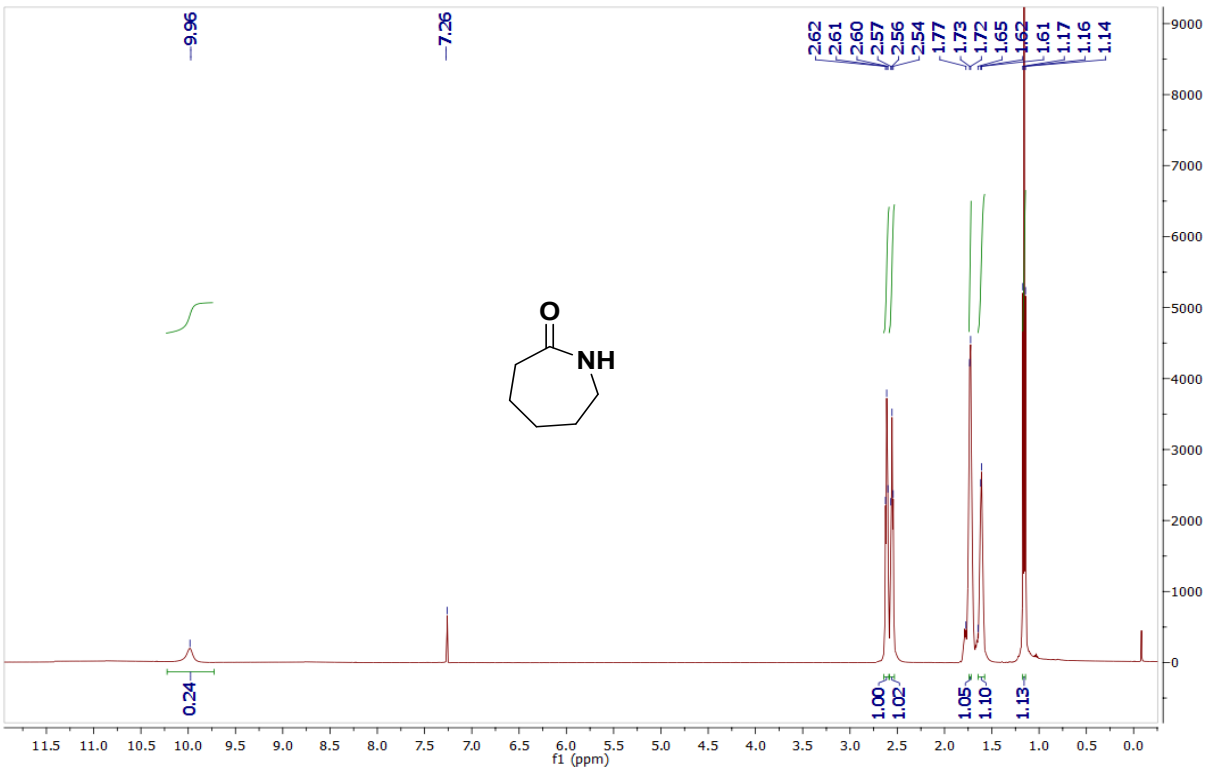

Fig. S81 ^{13}C NMR spectrum of derivative **7f** in $CDCl_3$

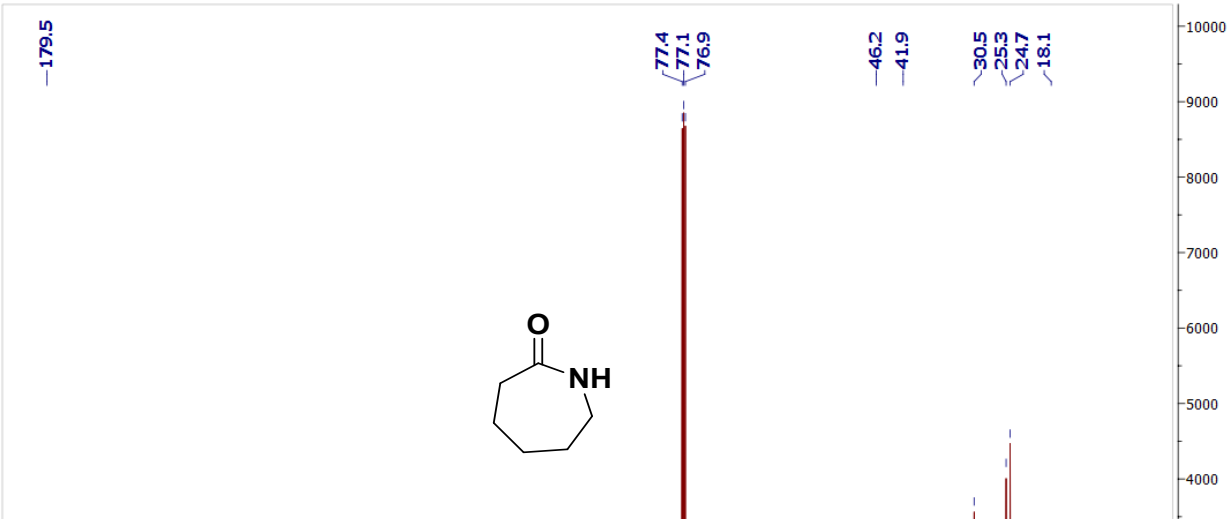

Fig. S82 ^{1}H NMR spectrum of derivative **6g** in $CDCl_3$

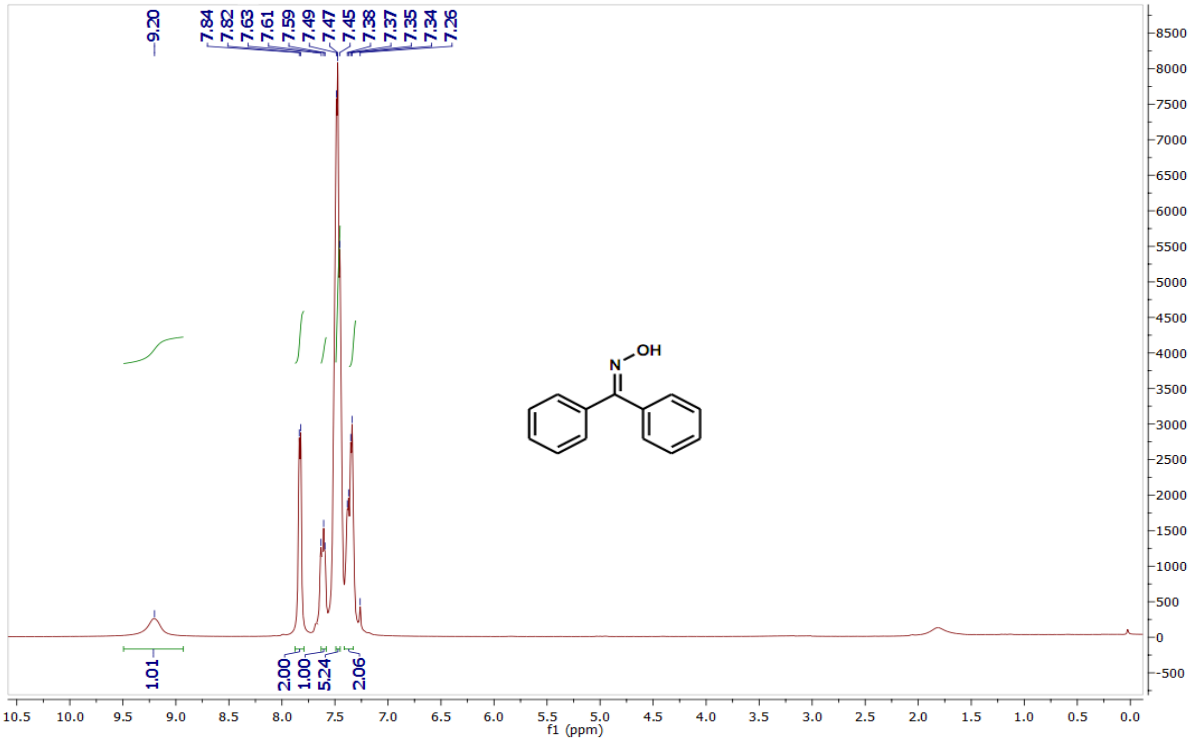

Fig. S83 ^{13}C NMR spectrum of derivative **6g** in $CDCl_3$

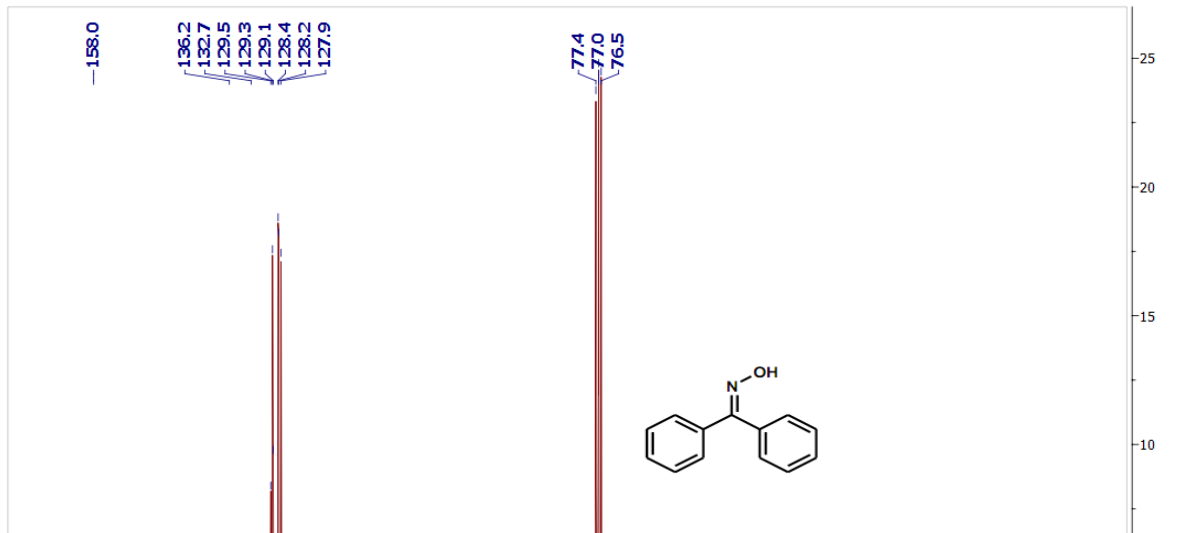

Fig. S84 ^{1}H NMR spectrum of derivative **7g** in $CDCl_3$

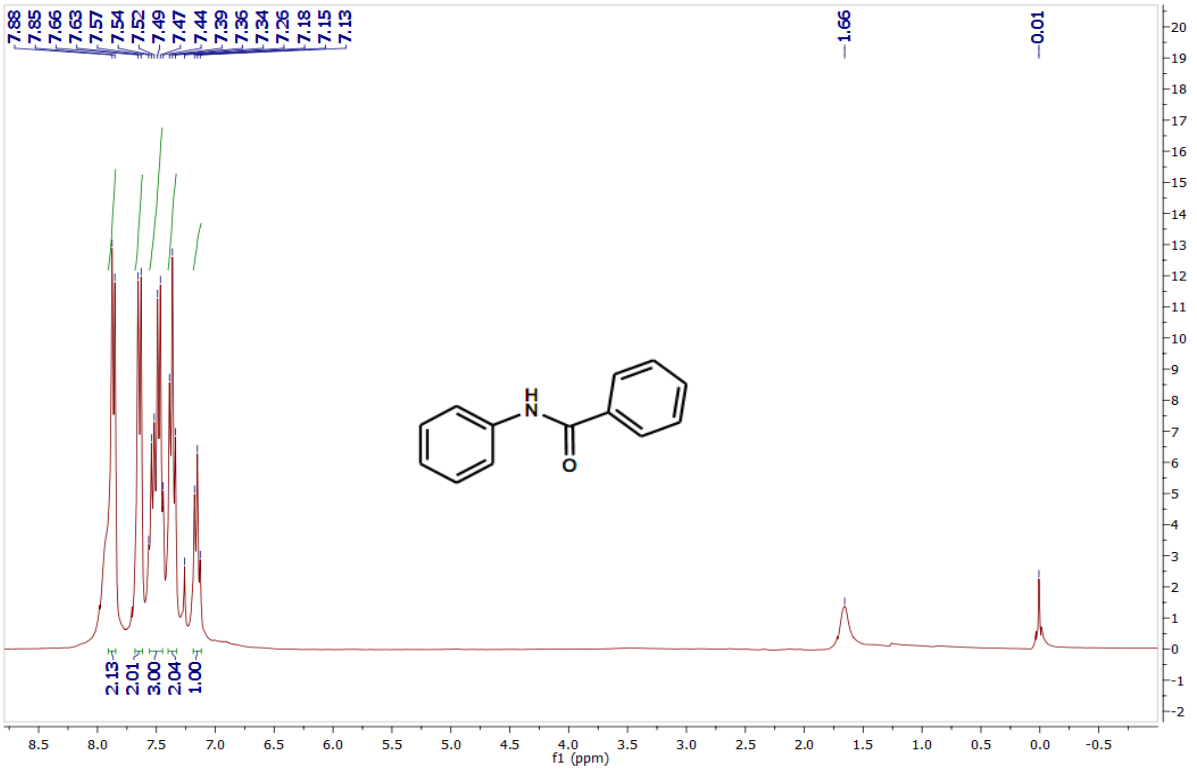

Fig. S85 ^{13}C NMR spectrum of derivative **7g** in $CDCl_3$

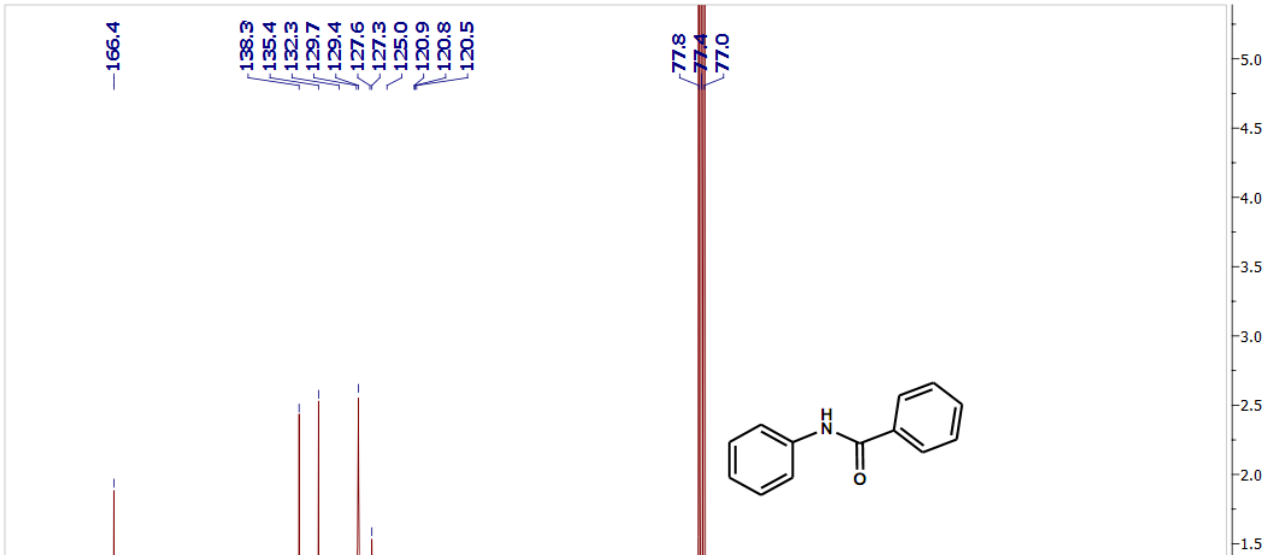

Fig. S86 ^{1}H NMR spectrum of derivative **8** in DMSO-d_6

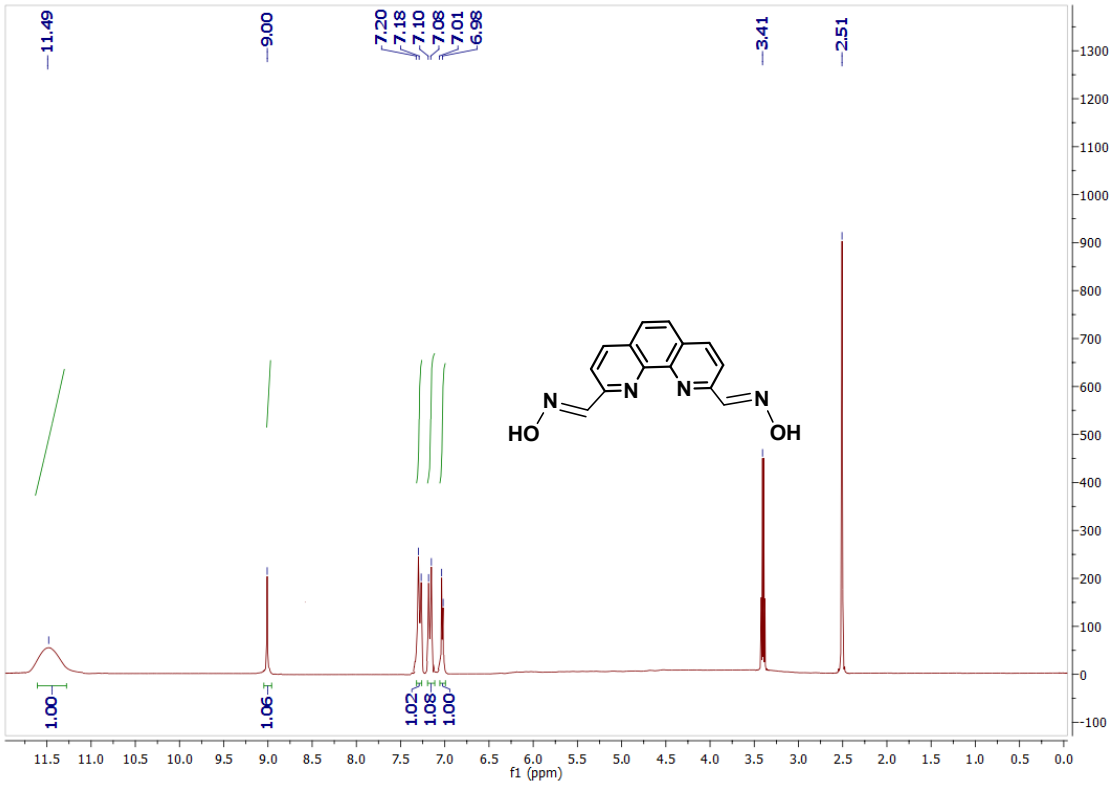

Fig. S87 ^{13}C NMR spectrum of derivative **8** in DMSO-d_6

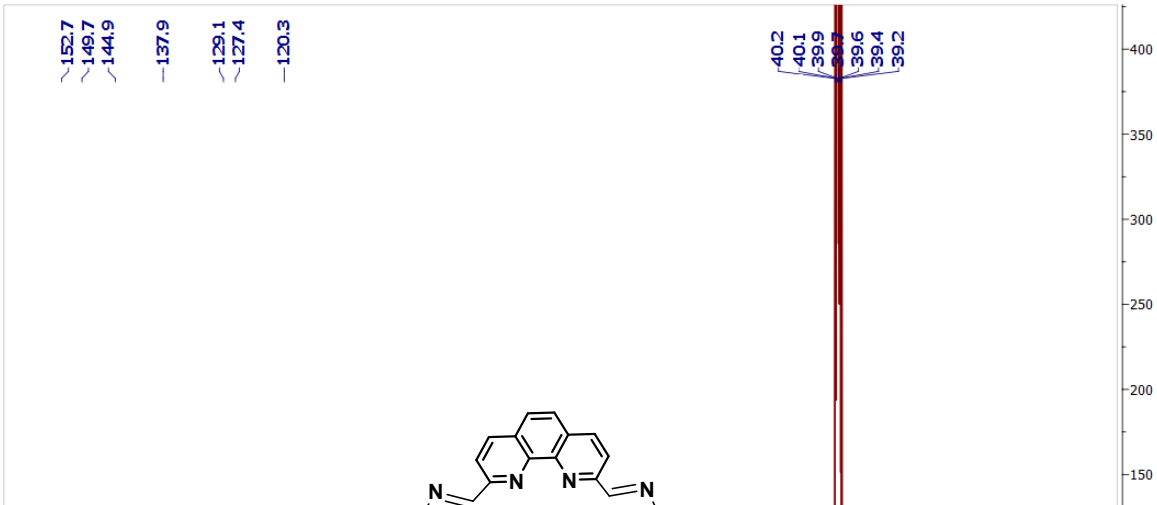

Fig. S88 ^{1}H NMR spectrum of derivative **9** in DMSO-d_6

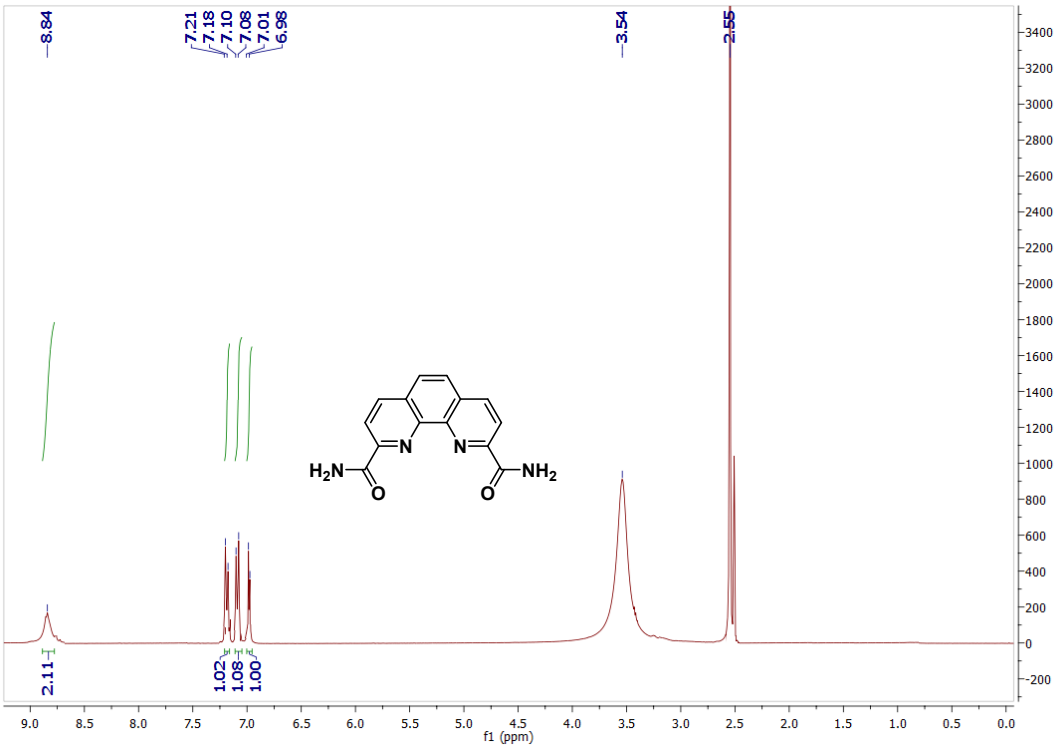

Fig. S89 ^{13}C NMR spectrum of derivative **9** in DMSO-d_6

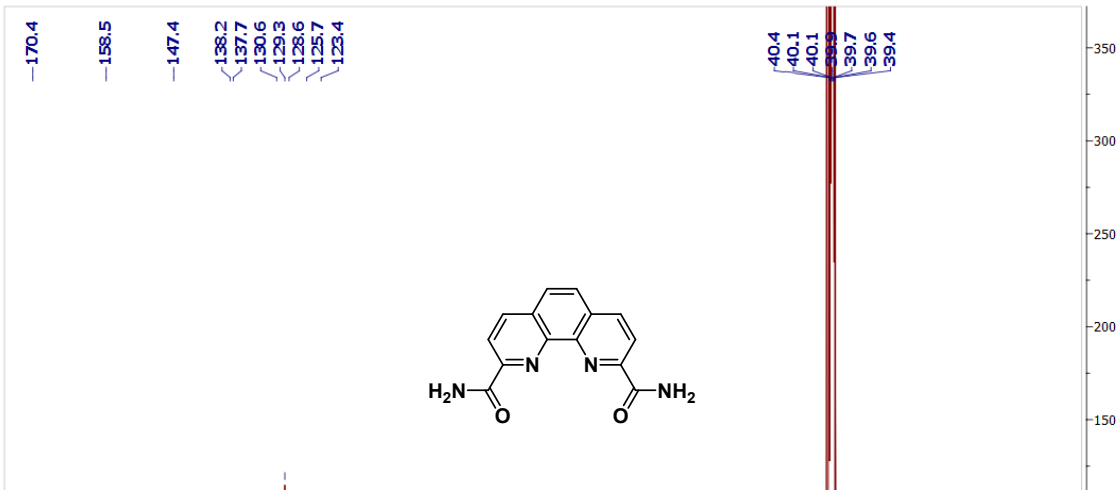

Fig. S90 ^{1}H NMR spectrum of derivative **10** in $CDCl_3$

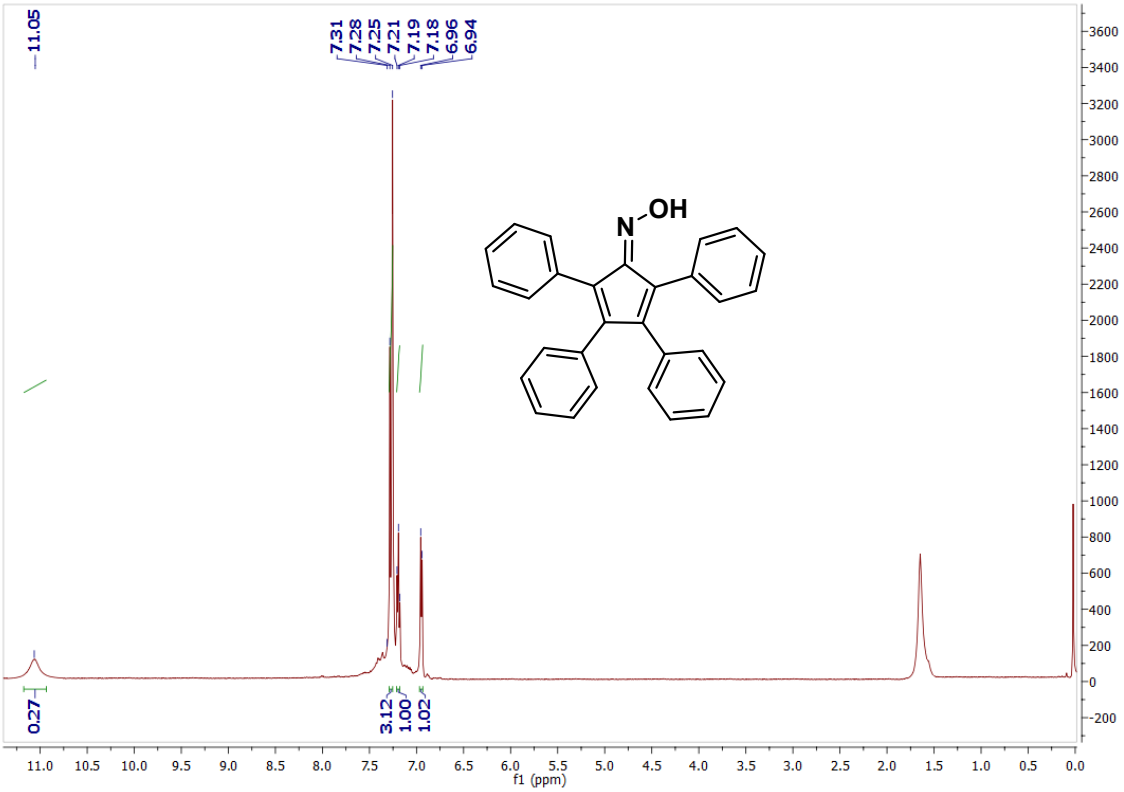

Fig. S91 ^{13}C NMR spectrum of derivative **10** in $CDCl_3$

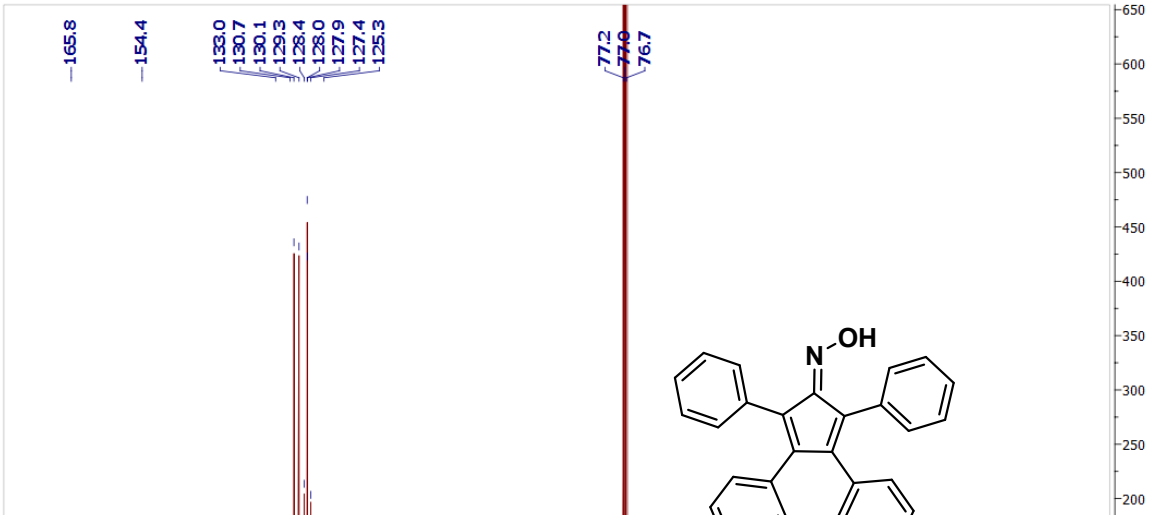

Fig. S92 ^{1}H NMR spectrum of derivative **11** in $CDCl_3$

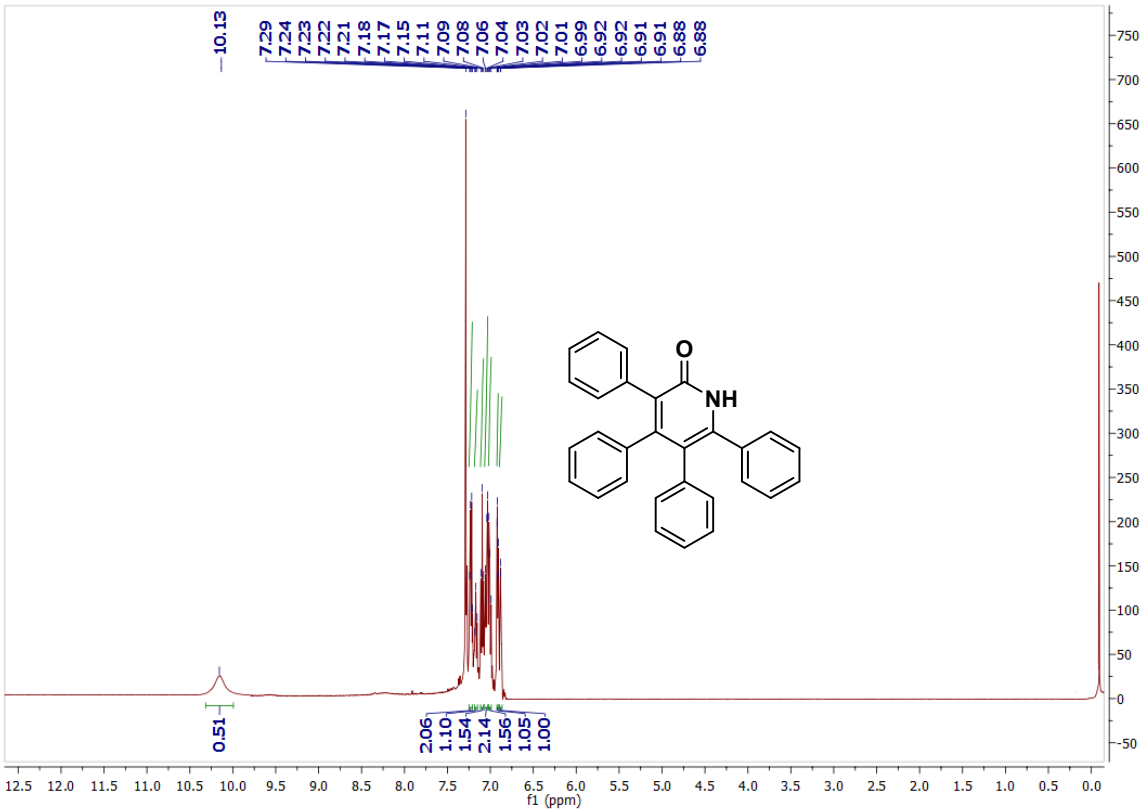

Fig. S93 ^{13}C NMR spectrum of derivative **11** in $CDCl_3$